HUMAN RNA METHYLTRANSFERASE METTL16 AFFECTS MULTIPLE CELL PROCESSES THROUGH DIFFERENTIAL FUNCTION OF ITS DOMAINS

By

Emily Satterwhite Talic

December, 2022

Director of Dissertation: Kyle Mansfield, PhD

Major Department: Biochemistry and Molecular Biology

ABSTRACT

In recent years, disease therapies have been developed to target specific RNA and protein expression changes in the affected cells/tissue. The RNA post-transcriptional modification, methyl-6-adenosine (m6A), has been implicated in a number of disease-states as a driver of aberrant RNA and protein expression. m6A is the reversible methylation of adenosine which is produced by enzymes known as m6A RNA methyltransferases. There are currently two known m6A RNA methyltransferases which methylate messenger RNA in humans: METTL3/14 complex, and METTL16. The METTL3/14 complex has been widely implicated and studied in cancer development and progression, while much of METTL16 has not been investigated. While a few studies have probed the biochemical details of METTL16, cancer studies have shown METTL16 protein expression level changes have been associated with a variety of cancer types. The research in this dissertation project was performed in an effort to determine the RNAs affected by and the cell-wide effects of METTL16's function. Using RNA immunoprecipitation, the studies here show that METTL16 binds a number of RNAs outside the 3 that are currently accepted as RNA targets. It was also discovered that METTL16 is localized to both the nucleus and cytoplasm, suggesting a role in addition to methylation in the cell. Mutation of key residues in METTL16

protein resulted in a large number of changes in RNA and protein expression levels determined with RNA sequencing, real-time PCR, and mass spectrometry proteomics. A majority of these RNAs and proteins are associated with cytoskeletal maintenance, calcium signaling, and cell cycle regulation, all of which have implications in distinct diseases including cancer. Of interest, only some of the METTL16 mutations seemed to affect cell cycle phase occupancy. Given the multiple changes seen among cells containing mutated METTL16, it is plausible that this protein could aid in presentation or progression of associated diseases and could therefore be a justified target for cell therapies.

HUMAN RNA METHYLTRANSFERASE METTL16 AFFECTS MULTIPLE CELL PROCESSES THROUGH DIFFERENTIAL FUNCTION OF ITS DOMAINS

A Dissertation

Presented to the Faculty of the Department of Biochemistry and Molecular Biology

East Carolina University

In Partial Fulfillment of the Requirements for the Degree

Doctor of Philosophy in Biochemistry and Molecular Biology

By

Emily Satterwhite Talic

December, 2022

HUMAN RNA METHYLTRANSFERASE METTL16 AFFECTS MULTIPLE CELL PROCESSES THROUGH DIFFERENTIAL FUNCTION OF ITS DOMAINS

By

Emily Satterwhite Talic

APPROVED BY:

DIRECTOR OF DISSERTATION: _____

Kyle Mansfield, PhD

COMMITTEE MEMBER: _____

Brett Keiper, PhD

COMMITTEE MEMBER: _____

Tonya Zeczycki, PhD

COMMITTEE MEMBER: _____

Jessica Ellis, PhD

CHAIR OF THE DEPARTMENT OF

Biochemistry and Molecular Biology: _____

John Cavanagh, PhD

INTERIM DEAN OF GRADUATE STUDIES: _____

Kathleen Cox, PhD

DEDICATION

To my husband: *venimus, vidimus, vicimus;*

To all the others: *bona fortuna!*

TABLE OF CONTENTS

LIST OF TABLES

LIST OF FIGURES

LIST OF SYMBOLS/ABBREVIATIONS

RNA	Ribonucleic Acid	2
mRNA	Messenger RNA	2
METTL	Methyltransferase-like	2
rRNA	Ribosomal RNA	2
tRNA	Transfer RNA	2
m6A	Methyl-6-adenosine	2
m5C	Methyl-5-cytosine	2
FTO	Fat mass and obesity-associated	2
ALKBH5	AlkB homolog	2
KIAA1429	Kazusa cDNA sequencing project entries	3
RBM	RNA Binding Motif	3
SAM	S-adenosylmethionine	3
ZCCHC4	Zinc finger CCHC-type	4
ncRNA	Non-coding RNA	4
miRNA	MicroRNA	4

Chapter 1

Introduction: Current Knowledge and Implications of METTL16 as an RNA-binding Protein

The majority of the work presented in this chapter was published as "RNA methyltransferase METTL16: Targets and function"

Emily R. Satterwhite[1], Kyle D. Mansfield[1]

Wiley Interdisciplinary Reviews: RNA, e1681 July 2021

[1]Biochemistry and Molecular Biology Department, Brody School of Medicine, East Carolina University, Greenville NC, 27834

Introduction

RNA modifications of messenger RNA (mRNA) play an important role in posttranscriptional and translational regulation [1–5]. As such, interest in RNA-modifying enzymes such as METTL16 has dramatically increased in recent years. There are over 100 known RNA modifications, and it is well established that ribosomal RNA (rRNA) and transfer RNA (tRNA) are rife with modifications [6–8]. In fact, the most prevalent RNA modification, pseudouridine, is found mostly in rRNA and tRNA [9,10]. It is for this reason that modifications in these RNAs have been well studied. Many of these studied modifications in tRNA and rRNA have been revealed to fine-tune their functions in translational efficiency[11–14]. To date, eukaryotic mRNA has been found to contain at least 13 modifications, including N6-methyladenosine (m6A), 5-methylcytidine (m5C), and 7-methylguanosine, but the functions of these modifications are just beginning to be elucidated [15,16]. Interest in understanding the role of RNA modification in regulating mRNA has exploded over the last few years, fueled largely by the identification of the RNA binding proteins responsible for writing, reading, and erasing some of these modifications[17–19]. Of these, methylation of the nitrogen at the sixth carbon residue on adenosine, otherwise known as m6A has arguably received the most attention to date [20]. One reason for this is that both m6A "writers" (including METTL16 and METTL3/METTL14) and m6A "erasers" (FTO and ALKBH5) acting on mRNA have been identified, suggesting that the presence of the modification (and hence the fate of the affected mRNA) may be regulated in some manner [18,19].

N6-Methyladenosine (m6A) Modification

The m6A modification, found in most eukaryotes, is the most abundant modification in mRNA [21], with estimates of approximately three m6As per mRNA[22]. This modification has been

shown to be important for the stability and translational efficiency of a number of mRNAs[23–27], and is involved in many different physiological processes including embryonic development[28–30], circadian rhythm[31,32], and many types of cancer [17,33]. In addition to METTL16, which is the focus of this review, there are a number of other m6A methyltransferases that have been identified (Table 1.1).

METTL3/METTL14/WTAP Complex

Interest in the m6A modification has recently grown in part due to the identification of a methyltransferase complex responsible for m6A-methylating nascent pre-mRNA within the nucleus. The core complex consists of METTL3 and METTL14, as well as Wilms' tumor associating protein [34–38]. Other proteins including KIAA1429, RBM15, and RBM15B have also been shown to function with the core methyltransferase complex as loss of these proteins decreases cellular m6A levels [39,40]. METTL3 contains a Rossmann-like fold domain typical of other class I methyltransferases, and utilizes S-adenosylmethionine (SAM) as a substrate to methylate adenosines within a DRACH consensus sequence (modified adenosine underlined), often found in 30 UTR's and around both start and stop codons of mRNA[35,41–44]. METTL3 also contains two CCCH-type zinc fingers outside of the methyltransferase domain that are required for RNA binding and hence methylation[45,46]. METTL14 lacks a SAM binding site and catalytic activity but does participate in mRNA binding/targeting[45,47,48]. Although predominantly found in the nucleus, the methyltransferase complex and its activity has been found within the cytoplasm as well and is thought to be responsible for the bulk of cellular m6A mRNA modification[37,49–52].

Table 1.1

m6A Methyltransferase	Validated RNA Methylome
METTL3/METTL14	mRNAs, ncRNAs, microRNAs, circRNAs
METTL16	*U6* snRNA, *MAT2A* pre-mRNA
METTL5	*18S* rRNA
ZCCHC4	*28S* rRNA

Table 1.1. Human m6A RNA methyltransferases and their identified methylated RNAs.

METTL16

More recently, another m6A methyltransferase, METTL16, has been identified although its targets appear to be more limited in number[53–58]. Like METTL3, METTL16 contains the Rossmann-like fold of class I methyltransferases and uses SAM as the methyl donor but appears to have additional regulatory and RNA binding domains which we will discuss below. The two verified targets of METTL16 share a consensus sequence (UACAGARAA) that is different from METTL3/14's consensus and the RNA methylation sites of the known METTL16 targets also harbor structural elements shown to be important for methylation[56,59,60]. Like METTL3, METTL16 contains additional regions outside of its methyltransferase domain that also interact with RNA substrates and presumably provide specificity[60,61]. Interestingly, in global mRNA binding protein identification studies in which polyadenylated mRNA is isolated along with endogenous interacting proteins, METTL16 is frequently captured, while components of the METTL3/14 complex are not[62–66]. In addition, while many METTL16 RNA interactors have been identified, only two have been verified as methylation substrates, perhaps suggesting additional roles for METTL16 beyond its catalytic activity.

Non-Coding RNA m6A Methyltransferase

Even though m6A is prevalent in mRNA, it is also found in other types of RNAs including rRNA, long noncoding RNA (lncRNA), microRNA, and small nuclear RNA (snRNA) [67–70]. Due to its homology with the *Escherichia coli* 23S rRNA m6A methyltransferase, ybiN/ rlmF, METTL16 was originally predicted to mediate eukaryotic rRNA m6A methylations. However, METTL5 has recently been shown to methylate 18S rRNA and ZCCHC4 has been identified as the eukaryotic 28S m6A methyltransferase[71–74]. Interestingly, both enzymes appear to be very

specific to their rRNA substrates although other RNA interactors have been preliminarily identified. While the function of these rRNA modifications is not yet known, structure predictions suggest that the m6A sites are located in areas important for translational fidelity[75–77]. Thus, while METTL16's role in rRNA methylation is still unclear, substantial progress into its structure, function, and preferred RNA substrates have been made in recent years.

METTL16 Domains and Their Functions

There are two known m6A RNA methyltransferases with verified mRNA targets in humans: the METTL3/14 complex, and METTL16. While there is a large overlap of structural similarity between these two enzymes[59,61] there are differences that suggest they have unique responsibilities in the cell. METTL3/14 has been extensively researched and many RNA interactors and methylation targets have been identified (a review of METTL3/14 can be found in [78]). METTL16 has been investigated much less and therefore has only a few known interactors. METTL16 is a conserved protein, with homologs found from vertebrates to yeast and bacteria[53,56,60]. A phylogenetic tree showing a few of these homologs with respective protein diagrams is shown in Figure 1.1. From this analysis, it is clear the protein has evolved, adding an additional domain in vertebrates. METTL16's protein domains have been investigated and, for the human protein, are categorized as an N-terminal RNA-binding, methyltransferase, and vertebrate conserved region (VCR) domains (Figure 1.2). Although METTL16 has never been crystallized in its full form, four groups have published fragment structures of METTL16[53,59–61]; there is also one unpublished structure listed as 2h00 in PDB (an excellent review of METTL16 structure can be found in Ruszkowska, 2021). Here we briefly discuss each domain, their responsibilities, and the

implications in RNA interaction. We also discuss the region predicted to contain a nuclear localization sequence.

N-terminal RNA-Binding Region

The N-terminus of METTL16 contains a group of polar and positive-charged amino acids that form a groove large enough to accommodate double-stranded RNA[60,61] (see Figure 1.2). Among vertebrates it is highly conserved (Mendel et al., 2018; Ruszkowska et al., 2018) with lesser but still significant conservation in lower organisms (see Figure 1.1). This region is sometimes grouped with the methyltransferase domain as it was not distinguished from the methyltransferase domain until 2018 by Ruszkowska et al. who identified this region as one unique from other RNA methyltransferases[61]. A few months later, Mendel et al. showed that mutations to charged residues (the first five arginines and lysines) in this region abolished RNA binding, and subsequently, methylation of RNAs [60]. Therefore, while the methyltransferase domain forms a groove to accommodate RNA during methylation, it is unable to secure the RNA for catalysis without the N-terminal binding domain. While only five amino acids in this region have been shown to be responsible for RNA binding, the first 40 N-terminal amino acids have been classified as an RNA binding domain, even though it does not follow "canonical" RNA-binding motifs. This domain forms a projection from the methyltransferase domain of the protein and is thought to act as a "claw" to further stabilize the RNA in the methyltransferase RNA groove[61]. Interestingly, in the co-crystal structure, these residues do not appear to contact RNA [59], however, functionally they clearly play a role in RNA binding [60]. This domain is one of those unique to METTL16, potentially dictating the group of RNAs with which it can interact.

Figure 1.1

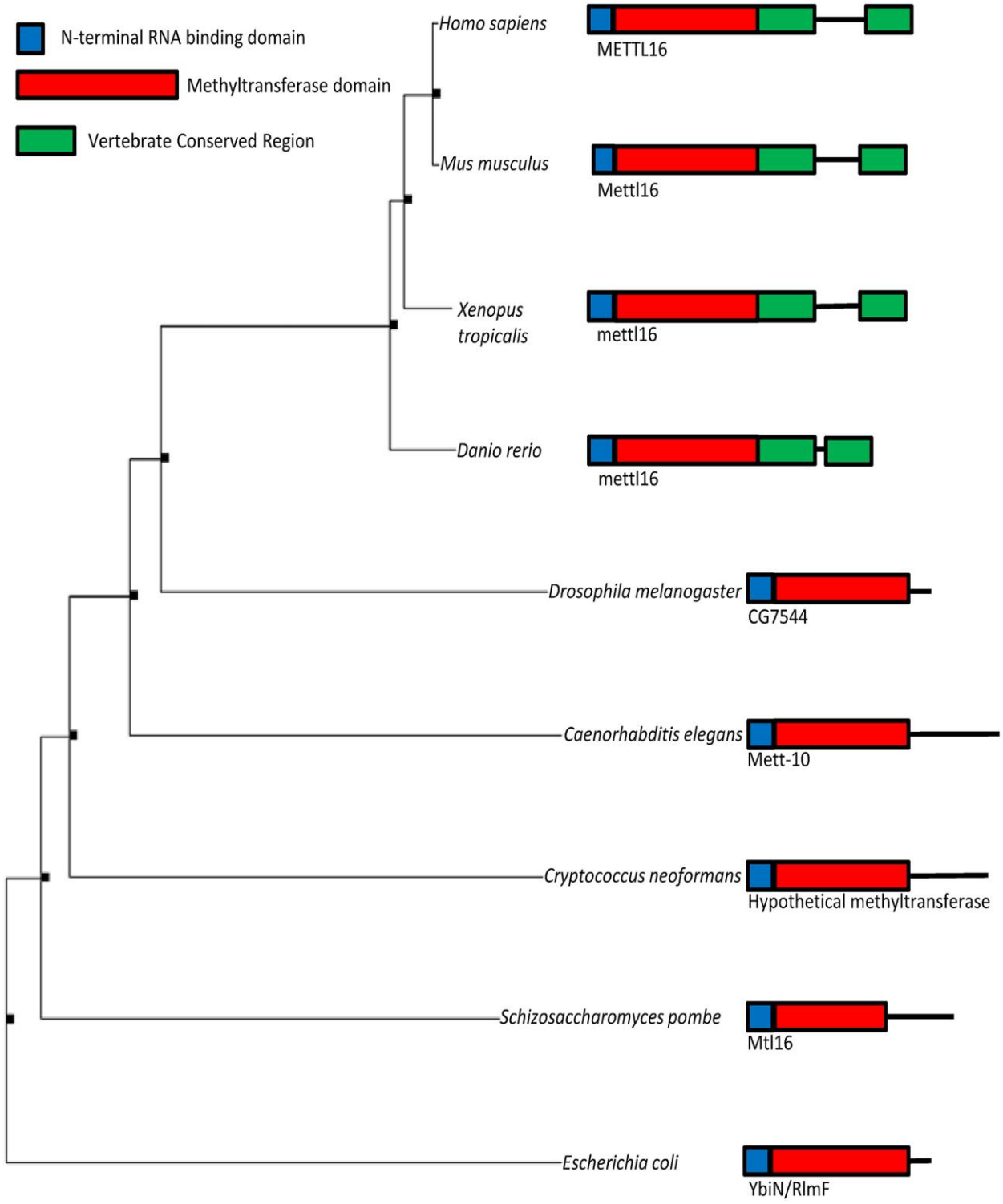
N-terminal RNA binding domain
Methyltransferase domain
Vertebrate Conserved Region
Homo sapiens
METTL16
Mus musculus
Mettl16
Xenopus tropicalis
mettl16
Danio rerio
mettl16
Drosophila melanogaster
CG7544
Caenorhabditis elegans
Mett-10
Cryptococcus neoformans
Hypothetical methyltransferase
Schizosaccharomyces pombe
Mtl16
Escherichia coli
YbiN/RlmF

Figure 1.1: Phylogenetic tree of METTL16 and homologs. Simple protein diagram of each organism's homolog and the protein name is located next to each respective species. Tree was generated using Seaview using distance methods under standard parameters [79]. Sizes of protein diagrams are approximate and not to scale.

Figure 1.2

Figure 1.2: Schematic of human METTL16 protein. Numbers indicate amino acids from N to C terminals. RBD, N-terminal RNA binding domain; VCR1, vertebrate conserved region 1; VCR2, vertebrate conserved region 2.

Methyltransferase Domain

The methyltransferase domain of METTL16 is highly conserved through vertebrates [53,61], with lower conservation still identified through E. coli[80,81] (see Figure 1.1). As mentioned above, approximately the first half of the protein was termed the methyltransferase domain until 2018, whereas it is now considered to be comprised of amino acids 40–288 (see Figure 1.2). The methyltransferase domain has the conserved Rossmann-like fold of class I methyltransferases containing the amino acids needed for several actions which are almost identical to METTL3 [61]. A hydrophobic pocket and several hydrogen bonds are required for the proper placement of the adenosine portion of SAM while the canonical "NPPF" amino acid sequence stabilizes the methionine region in SAM [59]. This "NPPF" region is also needed for destabilization of the sixth nitrogen on the RNA adenosine for transfer of the methyl group [59]. The methyltransferase domain also provides additional support to the N-terminal RNA-binding domain with positive-charged amino acids that line the internal groove [60,61]. As mentioned above, ridding METTL16 of the N-terminal RNA binding domain abrogates RNA binding [60]. Even though the methyltransferase domain contains a groove lined with amino acids that can attract the negative-charged RNA backbone, it alone does not appear to be strong enough to retain the RNA in the groove. Intriguingly, this RNA accommodating region is not an open-ended groove like METTL14, which is needed to bind single-stranded RNA at an internal site, rather it is a closed groove [48,60]. It is therefore suggested that the RNA interaction here must either be at the end of the strand or in a hairpin secondary structure. One unique aspect of METTL16's methyltransferase domain is the "auto-regulatory K-loop" (amino acids 163–167) which lowers methylation efficiency by obstructing the SAM binding pocket [59]. Lowered methylation efficiency is suggested to attenuate the overall activity of METTL16 in the cell [59] and could perhaps contribute to its role as a methyl

sensor. It is therefore plausible that mutations in this region, which have been shown to produce a hyperactive methyltransferase, could result in dysregulation [59]. A more detailed account of the biochemical mechanics of METTL16's RNA methylation can be found here[82].

Vertebrate Conserved Region Domain

The VCR domain is located at the C-terminus of METTL16 from amino acids 310–562 (see Figure 1.2). The domain contains two regions (VCRs) conserved among vertebrates[53,56,61] (see Figure 1.1). Amino acids 289–400 are classified as VCR1, 514–562 are classified as VCR2, and 401–513 are considered a linker region between these two [53]. The domain was first discussed in 2017 as a potential splicing director for MAT2A RNA when cellular SAM levels were below a critical level [56]. Due to its highly dynamic nature, the crystal structure of this region was not determined until 2020 [53]. Crystallization was achieved by removing the unstructured linker region between the two VCRs [53]. Because of the presumed motion of this domain, it is believed to bind near the target adenosine (in a double-stranded region) to bend the RNA and allow better access of the adenosine to the core methyltransferase domain [53].

Interestingly, the VCR domain is structurally homologous (although not in sequence) with the kinase-associated 1 (KA1) domain of TUT1, a U6 snRNA-specific terminal uridylyl transferase [53]. As in TUT1's KA1 domain, the VCR domain of METTL16 acts as a clamp that binds double-stranded RNA. The KA1 domain in TUT1 is known to aid U6 snRNA binding for polyuridylation [83], however the KA1 domain is also found in other proteins such as serine/ threonine kinases [84]. The proposed functions of the domain in these kinases include autoinhibition and targeting the protein for anionic membranes [85,86]. It has been noted that these domains are observed to show low sequence conservation while maintaining high structural homology [84]. With

these similarities between the VCR and KA1 domains, it is possible that METTL16 has roles outside those currently known and solidifies U6 snRNA as one of the main METTL16 interactors. Because the VCR domain of METTL16 has only recently been identified, the next few years of investigation into this region will be exciting.

Potential Nuclear Localization Sequence

Located in the region between the end of the methyltransferase domain and the beginning of the VCR domain, a vertebrate-conserved sequence of amino acids has a computationally predicted (yet unverified) nuclear localization sequence (SKRRKLEKPRK, amino acids 300–310; [87]). The *Caenorhabditis elegans* homolog of METTL16, METT-10, which contains a verified nuclear localization sequence in a non-conserved region, is transported to the nucleus by dynein light chain during mitosis[88]. Originally thought to be predominantly nuclear in human cells as well, our recent study using biochemical fractionation of several cell types suggests METTL16 is present in both the nucleus and cytoplasm [55]. In addition, when METTL16 was overexpressed, more was observed in the cytoplasmic fraction. Therefore, it may be that METTL16's main cellular compartment is the nucleus, with accumulated excess located in the cytoplasm.

METTL16 RNA Interactors

To date, three RNAs have been established as bona fide interactors of METTL16: MAT2A mRNA, U6 snRNA, and MALAT1 lncRNA. While MALAT1's methylation via METTL16 has not been proven, both MAT2A and U6 are definitively m6A methylated by METTL16. Similarity in the methylated region of these two RNAs led to the identification of a consensus nonamer sequence “UACAGARAA,” where the fourth base (underlined) is modified. While it is unlikely

this consensus is a mere coincidence, it does not exclude the possibility of additional sequence determinants. For example, studies have found that this nonamer sequence, which is found in thousands of other human mRNAs, is not widely methylated [56]. Furthermore, in the METTL16 knockout mouse embryo, expression level of RNAs with the consensus nonamer sequence was not affected by decreased METTL16 levels [60]. These and other observations suggest that while potentially necessary for methylation, perhaps this nonamer sequence alone is not sufficient for METTL16 methylation. Indeed, current data suggests that the nonamer sequence needs to be in a specific secondary structure for methylation to occur [59]. However, since the consensus sequence is based on only a few known interactors, this may also suggest the need to expand the RNAs considered for METTL16 binding and/or methylation. In this section, we review the three well-established RNAs and their interactions with METTL16. We also discuss other potential RNA interactors and the resulting implications.

MALAT1 LncRNA

Metastasis-associated lung adenocarcinoma transcript 1 (MALAT1), also known as NEAT2 (nuclear-enriched abundant transcript 2), is a common and conserved mammalian lncRNA known for its widespread role in transcriptional regulation, alternative splicing, and sequestering miRNAs [89,90]. MALAT1 lncRNA is ~8000 bases, with the last ~100 bases folded in a triple helix structure, as shown in Figure 1.3. Most notably, MALAT1 expression has multiple implications in cancer progression (reviews of MALAT1 can be found in[89,91]). It was also the first RNA discovered to associate with METTL16 through the use of electrophoretic mobility assays and UV crosslinking in HeLa cells [54]. Up until this time, METTL16 was predicted to be a putative rRNA methyltransferase. The specific interaction region of MALAT1 with METTL16 was identified

using RNA-proximity ligation assays[54] and shown to include the element for nuclear expression. Moreover, the ligation did not occur without the VCR domain of METTL16, providing evidence that this was the region of MALAT1 binding. Interestingly, an m6A-modified adenosine has been identified in MALAT1 at adenosine 8290 near the location of METTL16-MALAT1 interaction site[92,93], but it does not appear to be deposited by METTL16. Instead, the sequence with the m6A modification overlaps with the "RRACH" consensus sequence favored by the METTL3/14 complex (R = purine and H = A, C, or U) [35] and has been shown to increase with METTL3 overexpression, suggesting that it is deposited by METTL3/14 [92]. The purpose of METTL16 binding to MALAT1 is currently unknown. If methylation does not occur, it may a way to sequester MALAT1 or target it for interaction with an unidentified METTL16 protein cofactor. The triple helix of MALAT1 has been shown to stabilize and delay degradation of the RNA[94] but the role of METTL16 in this process has not been explored. This RNA–protein interaction is intriguing not only because methylation does not seem to occur, but also because METTL16 does not have any other identified RNA interactors in the triple helical form. Whether MALAT1 is unique in its status of being bound but not methylated by METTL16 remains to be determined. It is possible that this is another way METTL16 regulates its RNA interactors.

MAT2A mRNA

MAT2A is an mRNA that encodes the "A" (or alpha) subunit of methionine adenosyltransferase 2 (MAT2), which is the catalytic subunit of this enzyme. MAT2, as the name suggests, is responsible for fusing a methionine to adenosine to produce S-adenosyl methionine [95]. This resulting molecule, known also as AdoMet or SAM, is responsible for most methyl donation reactions in the cell, whether it be for DNA, RNA, protein, or other molecules[96]. This reaction is

Figure 1.3

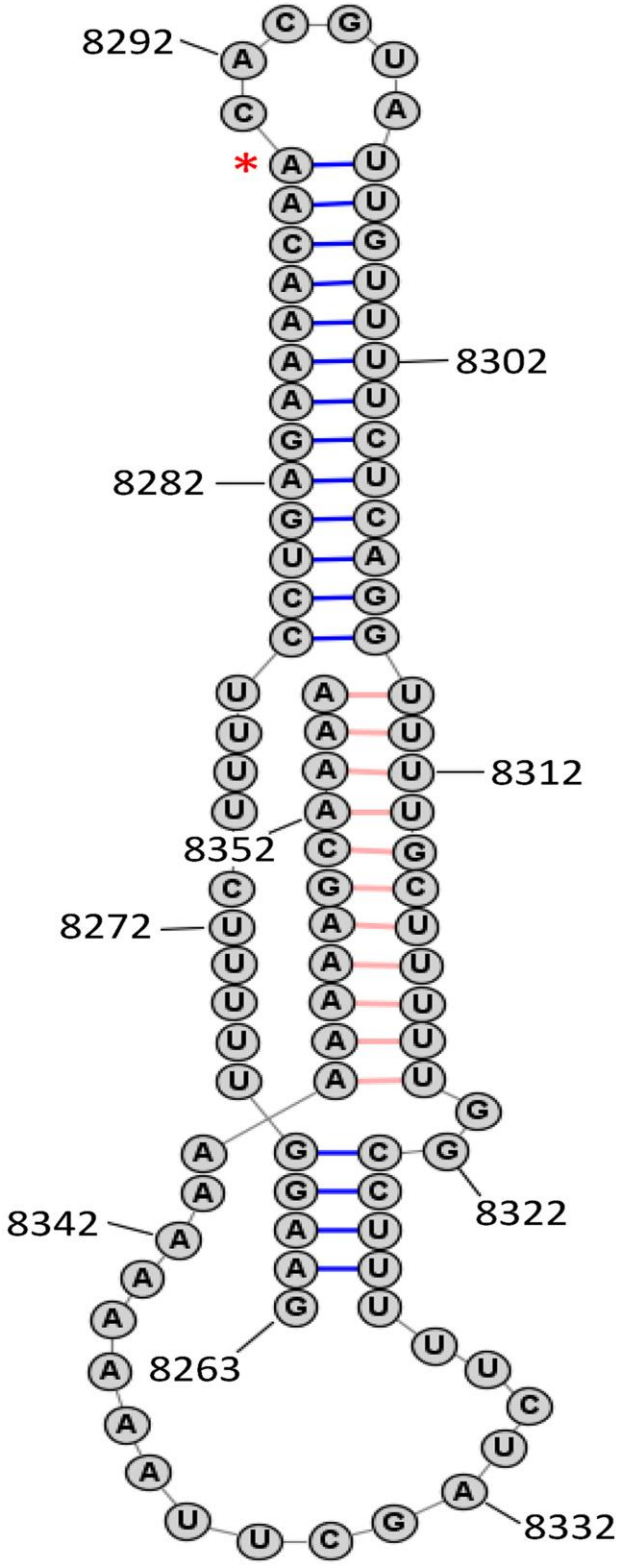

Figure 1.3: Partial RNA structure of human lncRNA MALAT1 predicted to bind METTL16. Structure shows triple helix region where METTL16 is reported to interact. Asterisk indicates predicted m6A site. Adapted from Brown et al. (2012).

energetically expensive, costing the cell one ATP molecule per SAM molecule produced [95]. As such, production of SAM is highly regulated to control the amount of methylation reactions that occur. SAM regulation varies among kingdoms of life and it seems mammals have evolved post-transcriptional regulation of MAT2A as one way to achieve this (there is also evidence of two miRNAs targeting both MAT2A and MAT2B; [97,98], not discussed here). A 2017 study demonstrated METTL16-regulated differential splicing of MAT2A RNA in response to SAM levels in human embryonic kidney cells [56]. When SAM levels are adequate, METTL16 binds and methylates adenosines in several hairpin loops located in the MAT2A 3` UTR (Figure 1.4). This impairs splicing of the terminal intron, leading to intron retention and degradation of the mRNA. However, when methionine levels in the media drop below a certain level (11–33 μM), METTL16 binds but is unable to complete the methylation reaction and remains bound to the hairpins. METTL16 then recruits splicing machinery to the last intron allowing for expression of a full-length mature mRNA and proper translation of the MAT2A protein[99]. Thus, through the sensing of SAM levels via its catalytic activity, METTL16 is able to maintain adequate SAM levels for all cellular methylation reactions. It should be noted that the MAT2A hairpins in Figure 4 are displayed as their stable structure when unbound by METTL16[100]. It has been shown that when bound to METTL16 (at least for hairpins 1 and 6), the structure changes (this structure can be found here[59]).

Previous studies have also shown that MAT2A's mRNA stability is also dependent on SAM levels[101] and recently METTL16 has been confirmed to bind several regions of the 3` UTR of MAT2A mRNA [58]. Furthermore, upon m6A methylation of the 3` UTR hairpins, MAT2A reporter mRNA is bound by the m6A reader YTHDC1 and targeted for degradation in HeLa cells [81]. All six MAT2A 3` UTR hairpins were found to be m6A modified (and also had lower levels of

Figure 1.4

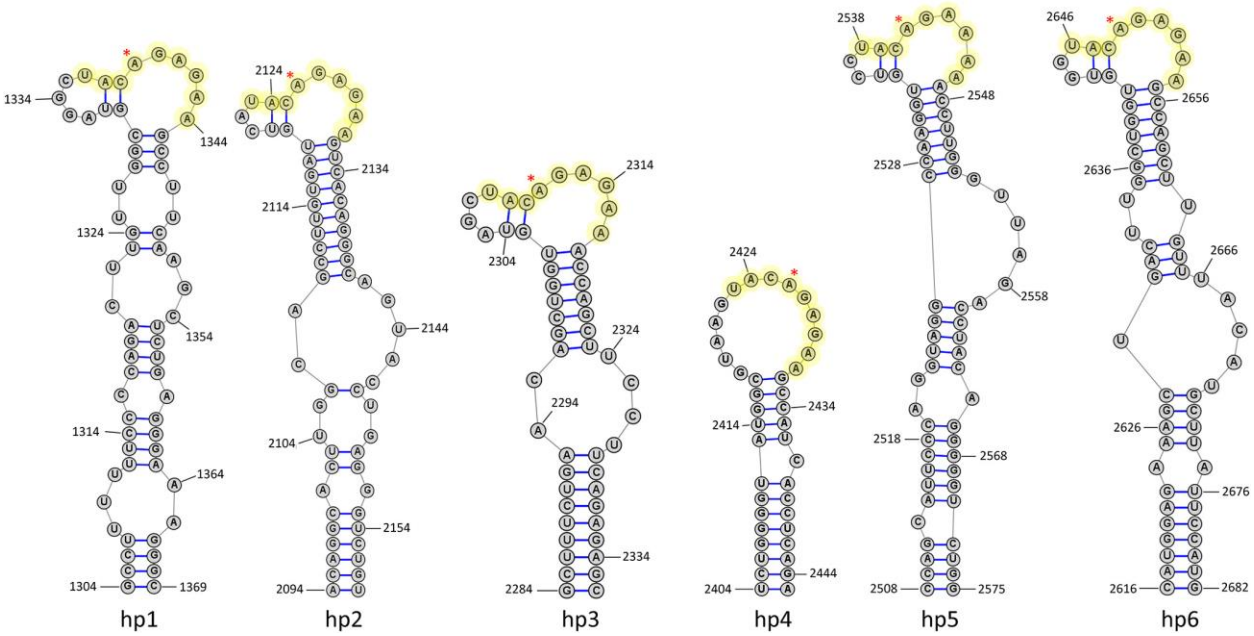
1334
1344
1324
1354
1314
1364
1304
1369
hp1
2124
2134
2114
2144
2104
2154
2094
hp2
2314
2304
2324
2294
2334
2284
hp3
2424
2434
2414
2444
2404
hp4
2538
2548
2528
2558
2518
2568
2508
2575
hp5
2646
2656
2636
2666
2626
2676
2616
2682
hp6

Figure 1.4: Partial RNA structures of human mRNA MAT2A 3′ UTR. The six hairpins are labeled relative to 5′ to 3′ direction. Nonamer sequence is highlighted, and asterisk indicates predicted m6A sites. Structures shown are when unbound to METTL16. Adapted from Parker et al. (2011).

modification after METTL16 knockdown), a finding supported by a single-base-resolution m6A study as well[102]. Ridding the MAT2A mRNA reporter of only the fifth and sixth hairpins impaired the mRNA stability response to low SAM levels, however, to fully interrupt this response, at least four hairpins had to be mutated. Interestingly, both studies [56,81] showed increased MAT2A mRNA in response to treatment with cycloleucine, a competitive inhibitor of the MAT2A enzyme, although Pendleton et al. showed higher levels of the intron-retained nuclear isoform compared to Shima et al. Thus, while there may be small differences due to cell type, growth conditions, media, detection methods, and so on, in both cases MAT2A mRNA was posttranscriptionally responsive to SAM levels in a METTL16-dependent manner. Shima et al. noted two further observations. Downregulation of FTO, a m6A demethylase, resulted in lower expression of MAT2A reporter mRNA suggesting that demethylation may play a role in maintaining basal MAT2A mRNA levels even in the presence of sufficient SAM. Also, despite showing clear regulation of a MAT2A reporter RNA, YTHDC1 knockdown showed no effect on endogenous MAT2A RNA expression [81]. It may be that the 5` UTR is regulated in a way that is redundant with YTHDC1 interaction (since this would be present on the endogenous mRNA but not included in the reporter RNA), however this is speculative. It is also possible that this is an artifact of using a reporter RNA, but again that possibility would need to be explored further. Still, it is clear that methylation via METTL16 regulates MAT2A mRNA stability.

Overall, these two studies consistently demonstrate that when cellular SAM levels are adequate, MAT2A mRNA is targeted for degradation both in the nucleus (through aberrant splicing and subsequent degradation) and the cytoplasm (through increased degradation) via METTL16 activity. Conversely, when cellular SAM levels decrease and MAT2A is needed, increased splicing, along with increased mRNA half-life ensure the cell can increase its SAM

synthesis to meet demands. This redundancy may be a fail-safe mechanism because if METTL16 levels were depleted for some reason, intron retention would reduce the production of new mature mRNA, however reduced m6A methylation would also lead to increased half-life of the mature mRNA. It is very possible that all mechanisms mentioned, and potentially others not yet known, can contribute to an elaborate posttranscriptional regulation process of intracellular SAM levels. Currently, only MAT2A hairpins 1 and 6 have been crystallized in complex with the N-terminal and methyltransferase domains of METTL16 (amino acids 1–291) [59]. These structures were acquired through stabilization of the RNA by removing the mismatches normally found in the wild-type MAT2A hairpin stems. Using hairpin 1, Aoyama et al. determined methylation by full-length METTL16 occurred at Km = 0.027 μM and had a Kd = 0.042 μM [53]. Interestingly, when using only the first two domains of METTL16 (amino acids 1–300, lacking the VCR domain), methylation was much lower at Km = 0.76 μM. Of note, several previous studies have used this truncated version of the METTL16 protein to obtain their results as well [56,59,61] so variations between publications are likely dependent on the exact nature of the METTL16 construct used.
Because of the numerous implications of SAM regulation through MAT2A levels, other studies have investigated METTL16's role in this process. An attempt to knockout METTL16 in mice revealed viable embryos up to the implantation stage where it is known a large DNA methylation event (following massive demethylation) occurs to radically change RNA expression [60]. Even though this group did not observe a large change in the 3` intronic region of MAT2A (the region of METTL16-directed alternative splicing), aberrant splicing was reported, and it was concluded the embryo cannot recover from the demethylation event without METTL16's involvement.

There are several papers that focus on correlating RNA expression with survival rates of specific cancers that have shown anomalous METTL16 levels to be consistently related to poor

outlook[103–109]. Although it has not been proven, it may be that dysregulation of MAT2A is the main cause for this relation, given that unregulated methylation events in the cell can lead to a plethora of overexpressed protooncogenes/oncogenes or under-expressed tumor suppressors through epigenetic mechanisms[78,104,110]. This is speculative since it has not been shown that METTL16 is directly responsible. There is even a study relating the lack of a typical microbiome with MAT2A hypomethylation and subsequent lower expression (due to downregulation of METTL16) in mice intestine, colon, and brain cells[111]. Whether METTL16's influence on MAT2A is the sole cause of these observations or there are influences left to be discovered, it is certain that METTL16 is a key component in overall cellular processes.

U6 snRNA

snRNA U6 directs intron splicing by associating with and destabilizing the 5` splice site, as well as serving as the catalytic subunit of the splicing machinery. About 40 years ago, human U6 snRNA was determined to have an m6A at A43[112], located in a stem bulge of the major hairpin structure (Figure 1.5). However, it was not until a few years ago that METTL16 was identified as the responsible m6A methyltransferase in vitro for A43 [56]. Interestingly, while METTL16 homologs have been identified in most species, the m6A status of U6 snRNA in species other than human and yeast has not been investigated. More research is needed to determine the methylation status of these snRNA homologs and, if present, whether it is due to the respective METTL16 homolog.

Human U6 is methylated by METTL16 with a Km = 0.025 μM and a Kd = 0.016 μM when using full length METTL16 [53]. These values are comparable to those of MAT2A methylation and binding, but surprisingly, removing the METTL16 VCR domain increases the Km to more than 4

μM for U6. For comparison, the Km for MAT2A using the same truncated METTL16 was 0.76 μM. The authors suggest the structural differences surrounding the methylation sites in each RNA explain this, with U6 snRNA showing more flexibility than the MAT2A mRNA [53]. Thus, it is proposed that without the stabilization of the RNA via the VCR domain, METTL16 cannot easily keep U6 in the binding pocket long enough for methylation to occur. Furthermore, it is suggested that the VCR domain binds and bends U6 so the adenosine to be modified is more accessible to the pocket where methyl transfer occurs. Thus, through U6-METTL16 kinetics, the importance of the VCR domain is highlighted.

It should be noted that while the region surrounding the m6A methylation site of U6 is necessary for properly directing splicing, it has not been proven (although it has been speculated) that an unmethylated adenosine in this position could not perform the same function. Warda et al. deeply explored the U6-METTL16 interaction and determined modification of A43 occurs after the 5` capping of U6 but before association of U6 with the rest of the spliceosome complex [58]. They speculated that, because U6 associates with pre-mRNA via weak interactions, the m6A thermodynamically "fine-tunes" this interaction. It is known that double-stranded RNA is stabilized by an m6A near but not in the duplex, whereas it is destabilizing if located in the duplex[113]. Therefore, the m6A at A43 in U6 may further weaken binding with the pre-mRNA for proper splicing and dissociation after splicing is complete.

Interestingly, knockdown of METTL16 in HEK293 cells resulted in no change in overall U6 levels but ~50% reduction in U6 containing an m6A [58]. However, because there is an additional m6A at A76 in U6 RNA, this may be expected if the second m6A is not deposited by METTL16 [58]. Embryonic knockout of METTL16 in mice showed no global changes in splicing in the transcriptome, suggesting this U6 methylation may not be necessary for splicing in mammals [60].

Figure 1.5

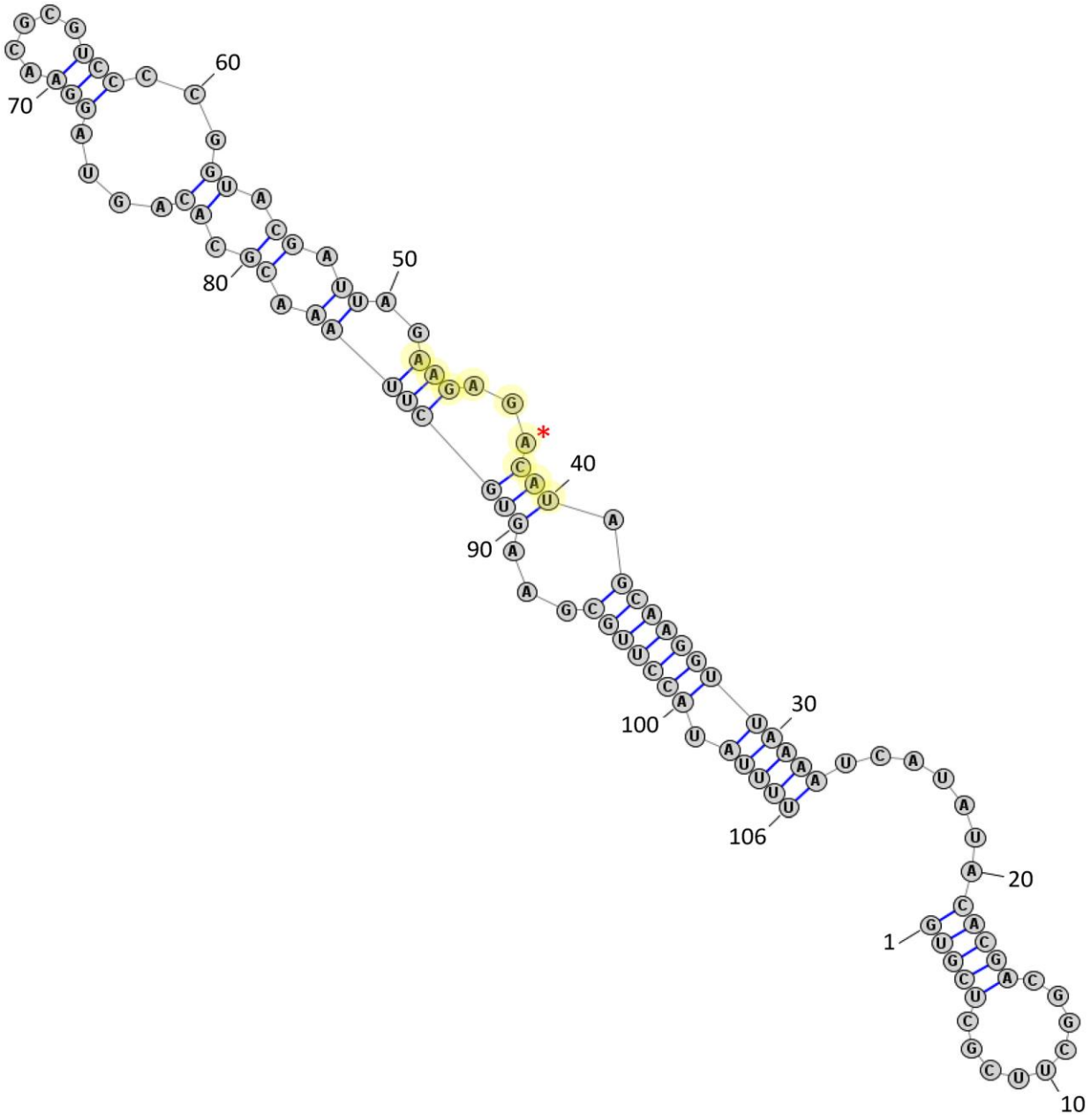

Figure 1.5: Full RNA structure of human snRNA U6 predicted to bind METTL16. Numbered bases indicate 5′ to 3′ direction. Nonamer sequence is highlighted, and asterisk indicates m6A site (A43). Adapted from Aoyama et al. (2020).

Regardless, U6 is a reliable RNA of the human METTL16 interactome and methylome, although the exact function of the m6A modification remains a mystery.

Other RNA Interactors

18S and 28S rRNA

MAT2A, U6, and MALAT1 are the most widely accepted RNA interactors of METTL16. However, several other types of RNAs have been implicated as potential interactors. It is well established that rRNAs contain modified nucleotides including m6A[6,8]. Immunoprecipitations (IPs) of both endogenous and exogenous METTL16 and identification of associated RNAs have revealed several rRNAs as potential interactors [54,55,58], although this could be attributed to non-specific crosslinking (due to proximity) or interactions (due to the large amount of rRNAs in total cellular RNA). The closest related METTL16 homolog in *E. coli*, ybiN/rlmF (~31% sequence homology), is the methyltransferase responsible for depositing an m6A on the 23S rRNA [80]. Additionally, a probable 28S rRNA m5C methyltransferase, NOP2, has been identified in complex with METTL16 [60]. Therefore, it is plausible that METTL16 binds and/or methylates rRNA. While rRNA m6A levels have not been investigated, knockdown of METTL16 does not result in differences in overall expression of rRNAs but this is not surprising due to the shear amount and half-life of this class of RNA. However, as mentioned previously, there are two other identified rRNA m6A methyltransferases in vertebrates (METTL5, ZCCHC4), so it is possible that through evolution one or both of those methyltransferases took on this responsibility and METTL16 no longer methylates rRNA in human cells.

DNA Damage-Associated Small RNAs

Recently, a study investigating DNA damage via ultraviolet radiation observed the recruitment of METTL16 to the region of damage and association with small RNAs in the vicinity [114]. While recruitment of m6A modified RNAs to the region of UV-induced DNA damage has been shown, a previous study identified recruitment of METTL3/14 to the damaged region[115]. The more recent study showed a small percentage of irradiated cells demonstrating higher localized METTL16 levels during subsequent repair. While this finding awaits further verification, it is an interesting development that expands upon the RNAs expected to interact with METTL16.

Other mRNAs

Identifying additional METTL16 RNA interactors has been more difficult. There are multiple deep sequencing datasets of RNA resulting from immunoprecipitations of exogenous METTL16 and knockdown studies of endogenous METTL16. However, there is little consensus among these sets other than the three established RNA interactors (MAT2A, U6, and MALAT1) already described. We caution that some that the immunoprecipitations and RNA expressions could result from non-specific pulldowns or secondary effects due to dysregulation of MAT2A (and therefore cellular SAM and m6A levels; [102,116]. Many of the potential RNA interactors were identified using an RNA–protein crosslinking method. Because METTL16 has multiple RNA binding domains (one of which seems highly dynamic and could potentially bind generic double-stranded RNA), it is possible many of these "interactors" are simply RNAs that were briefly in contact with METTL16 but not truly bound by the protein [117–120]. One must also consider the proteins found to interact with METTL16: if these proteins bring RNA near METTL16, it could again become crosslinked with METTL16 without being a true interactor. It is therefore imperative to use other methods and evidence to verify these as bona fide METTL16 interactors.

Using m6A immunoprecipitation datasets published by Pendleton et al. and others, one group produced a bioinformatics-based approach to determine the overall cellular processes affected by several m6A methyltransferases [121]. These datasets revealed the RNAs that were hypomethylated after METTL16 knockdown in HEK293 cells [56]. They categorized the resulting high-scoring RNAs and highlighted the top 10 processes with the most RNAs in each group. The highest scored groups were: “endoplasmic reticulum-associated misfolded protein catabolic process,” “regulation of cell cycle,” “actin cytoskeleton organization,” “positive regulation of apoptotic process,” and “protein ubiquitination.” To avoid potential overlap, they excluded genes that were shown to be reliant on more than one methyltransferase. This may have eliminated processes that are affected by multiple methyltransferases from the higher scoring processes. They also warned that, as only one dataset was available for the METTL16 methylome at the time of publication, future datasets are needed to solidify these findings, but will also likely skew the current readout. While they provided an in-depth library of genomic features to determine likely types of and regions on methylated RNAs, they warn it is not completely extensive. Even given these caveats, this is still one of the publications that fills a hole in the much-needed knowledge of METTL16's responsibilities, and the addition of more datasets is eagerly awaited.

A more recent publication using synthetic reactive SAM, which is added to RNA by its corresponding methyltransferase, revealed ~70% overlap with previous antibody-based datasets for METTL16 interactors [116]. The overlap was identified in MOLM-13 cells which stably expressed a short hairpin RNA targeting METTL16 and confirmed with m6A IP. The identified RNAs strongly aligned with a “UACAG” consensus, shortened from the “UACAGARAA” consensus sequence found in MAT2A and U6. This is an exciting addition to METTL16 investigation by giving verification to the somewhat fickle datasets produced through

immunoprecipitation alone. Within this group of RNAs, ~7600 are mRNA and ~900 are lncRNA. However, as with other studies, there was concern about the potential of a secondary effect due to METTL16's influence on MAT2A and hence cellular SAM levels. As a solution, RNA from the METTL16 set was compared to RNA identified as METTL3-methylated. If an RNA showed dependence on both methyltransferases, it was assumed to most likely be a METTL3 target with a secondary effect from METTL16. Similarly, a study from 2019 used an approach similar to an m6A IP (m6A-crosslinking-exonuclease- sequencing [m6ACE-seq]) coupled with knockdown of the respective methyltransferase in HEK293T cells to identify METTL3 and METTL16 RNA interactors. They suggested that a large portion of RNAs identified as METTL16-dependent were actually the result of indirect dependency due to SAM regulation [102]. The Mikutis study also discovered a striking similarity between the METTL16-dependent lncRNAs m6A region and intronic polyadenylated sites suggesting that METTL16 may have a role in intronic polyadenylation which could direct splicing and contribute to cancer progression [116]. As mentioned previously, the VCR domain of METTL16 is structurally homologous to the KA1 domain of TUT1 [53]. In TUT1, the KA1 domain binds double-stranded RNA for polyuridylation to occur [83]. This suggests the VCR domain could act in a similar fashion and therefore adds to the theory of METTL16's involvement in intronic polyadenylation.

Our recent publication using endogenous METTL16 immunoprecipitation without crosslinking identified several RNAs bound to METTL16: NT5DC2, MYC, HIF1A, β2M, and STUB1 [55]. Knockdown of METTL16 in vitro shows differential expression in some but not all these identified RNAs. Interestingly, these RNAs have been identified in some of the previously published exogenous METTL16 immunoprecipitation and endogenous knockdown datasets as well [56,58,102]. Reoccurring identification of these RNAs in multiple datasets obtained via different

methods argues against non-specific pulldowns but could suggest they may simply be weaker interactors with METTL16 which will require more evidence to confirm binding and methylation and determine the role of each.

METTL16 in Model Organisms

Caenorhabditis elegans

There are two groups who have studied the *C. elegans* METTL16 homolog, METT-10. The first group published two papers in 2009 after METT-10 was identified in a screen for effectors of cell proliferation and differentiation [88,122]. Worm lines with genetic variations in METT-10 showed that it promotes cell cycle progression and potentially meiotic entry. Nuclear accumulation of METT-10 was observed during meiosis, whereas METT-10 knockout promoted mitotic entry. METT-10 had previously been identified as a dynein light chain 1 (DLC-1) interactor from a genome-wide yeast two-hybrid study [123]. Interestingly, knockdown of dlc-1 caused a decrease in nuclear METT-10 protein in both germ and somatic cells using fluorescent microscopy. However, overall METT-10 protein levels were also reduced, prompting further investigation. With the dlc-1 RNA knockdown, they showed mett-10 RNA was also reduced, although the mechanism was not investigated. It was also determined that METT-10 exists as an oligomer. With mutated METT-10 studies, they determined that METT-10's catalytic activity is essential for proper cell cycle progression, although it seems when nuclear localization was disrupted, cytoplasmic METT-10 could still modify RNAs before they entered the nucleus and not disrupt cell cycle progression.

More recently, another group produced a METT-10 knockout line of *C. elegans* and report, with both m6A-RIP-Seq and SCARLET methods, that m6A was undetectable in both U6 snRNA and sams-3, sams-4, and sams-5 (the SAM synthetase mRNAs) [124]. The SAM synthetase RNAs'

splicing was inhibited upon m6A modification by METT-10, leading to RNA degradation and no functional protein produced. To investigate the similarity of METT-10 function to human METTL16, a sams-3 mRNA reporter was introduced into human HeLa cell extracts. Splicing of the reporter RNA was inhibited in the same manner as in worm extracts suggesting human METTL16 could carry out the reaction. Furthermore, the U2 auxiliary factor 35 (U2AF35) was unable to bind to the m6A-modified sams fragment, which ultimately blocked splicing in this area. Interestingly, U2AF35 was not needed if the pre-mRNA had a strong polypyrimidine tract adjacent to the 3` splice site, in which case only U2AF65 was needed. While C. elegans do not show these strong polypyrimidine tracts, it may be that other organisms use this method to regulate splicing only in certain RNAs. Interestingly, no global splicing changes were observed upon loss of U6 methylation. METT-10 knockout in *C. elegans* did show a strong fertility defect suggesting METT-10 may contribute to fertility in ways other than those discussed. These results suggest that METT-10 can inhibit splicing through 3` splice site m6A modification, however most predicted METTL16 m6A sites in human cells are not at 3` splice sites. Furthermore, there is currently no evidence that the m6A deposited by METT-10 in human extracts specifically inhibits splicing or activates alternative splicing.

Mus musculus

To date, the only in vivo knockout of METTL16 in mice was accomplished by insertion of a triple-stop codon into the Mettl16 gene [60]. Unable to obtain viable homozygous mice, heterozygous mice were used to produce knockout mouse zygotes and embryonic development tracked. At embryonic day 2.5, the METTL16 null mice were present in normal Mendelian ratios and showed only ~20 RNAs differentially expressed, including MAT2A, compared to the

heterozygous and wild-type Mettl16 mice embryos. At embryonic day 3.5, normal Mendelian ratios were also obtained, however there were ~5000 differentially expressed RNAs. By embryonic day 6.5, the METTL16 knockout mice were only 2% of the population and at embryonic day 8.5, no knockout embryos were detected. It was theorized that the large DNA methylation and demethylation that occurs around this time of development was unable to occur without proper MAT2A regulation by Mettl16 leading to loss of viability. While the RNAs identified in this paper are not human, they can be compared to the human homologs to determine the RNAs most likely regulated by Mettl16 during development. This group has also produced a conditional knockout of Mettl16, which was induced once the mice were adults [124]. The males, which show the highest level of Mettl16 tissue expression in the testes, were infertile due to lack of germ cell development. While they did not investigate this further, they determined that Mettl16 has important roles beyond that in embryonic development.

Concluding Perspectives

Here we have discussed the individual domains of the METTL16 protein, their proposed functions, and known and predicted RNA interactors of the enzyme. The amount of published work on METTL16 is impressive, given that the first study citing function was only published in 2016. Even so, there is quite a bit still unknown. METTL16 has been shown by several CRISPR screens to be essential for life, and all reported attempts to remove METTL16 via CRISPR-Cas9 from normal and cancerous cells have been unsuccessful[60,125–127]. While there has been speculation, it is not yet proven what METTL16 does that makes it indispensable. Two main theories are currently discussed: regulation of MAT2A mRNA or regulation of U6 snRNA. It

should be noted that neither has been proven and there is still the possibility that one, neither, or both are the reason for METTL16's essentiality.

MAT2A transcription and mRNA half-life are regulated by multiple pathways in addition to METTL16[96,128,129]. As previously mentioned, MAT2A is the enzymatic subunit of methionine adenosyltransferase 2, responsible for producing SAM, which acts as a methyl group donor for most cellular needs. This is just one part of the methionine cycle in the cell, where several enzymes work together to keep methionine readily available for methylation and other reactions, such as protein synthesis and the glutathione pathway. Because humans do not synthesize methionine, it is critical for the cell to tightly regulate its usage. Moreover, excessive methyl-donating molecules in the cell can lead to hypermethylation of chromatin, RNA, and others, resulting in aberrant cell functions. At the same time, under-production of the methyl-donators would lead to hypomethylation, again skewing cell functions. Therefore, it is plausible that loss of interaction with METTL16 would be enough to permanently injure SAM production and cause lethality. In our previous studies, transient knockdown of METTL16 did not result in a change in MAT2A protein expression [55]. However, upon both METTL16 knockdown and cycloleucine treatment, others have reported decreased MAT2A protein levels [56,81]. A potential solution to understanding the role of SAM in METTL16's essentiality would be to overexpress MAT2A before removing METTL16 from the genome. Supplementing the culture media with extra methionine could ensure enough substrate for optimal methionine adenosyltransferase performance, avoiding a potential complication. In addition, deeper investigation into the specific in vivo interaction between METTL16 and MAT2A could be accomplished by inactivating a particular METTL16 functional domain (methyltransferase, N-terminal RNA binding, etc.) and observe the effect, if any, on MAT2A mRNA stability and modification.

The other major METTL16 interactor is U6 snRNA, a spliceosome RNA. This RNA binds a pre-mRNA at the 5` splice site, helping to destabilize this region, so when the 3` splice site is brought into proximity, transesterification can occur. It is unknown whether the m6A modification is needed for proper function of U6. The modification of U6 was shown to be inefficient without the VCR domain of METTL16 [53]. As mentioned earlier, the VCR domain is unique to vertebrates. However, because the m6A in U6 is highly conserved from vertebrates to yeast[130], either the m6A is deposited another way outside of the vertebrate classification, or the methylation may not be necessary for proper function. It could also be that methylation is necessary for some but not all species. A METTL16 homolog has not been reported in *Saccharomyces cerevisiae*, however, fission yeast such as *Schizosaccharomyces pombe* do have a METTL16 homolog (Mtl16; see Figure 1.1) and their U6 snRNA is m6A modified. Removal of the Mtl16 homolog is not lethal, although it does result in slower growth rates [131]. A more recent study in *S. pombe* found that without U6 snRNA m6A modification, splicing of some RNAs were affected. Pre-mRNAs that contained an AAG sequence at the 5` splice site were unaffected by the m6A status of U6, however those that contain a BBH sequence required the m6A in U6 for proper splicing to occur [132].

One of the largest obstacles in the RNA modification field today is detection. Several studies have attempted to produce new protocols to isolate and correctly identify m6A in modified RNAs[102,116,133–136]. Because METTL3/14 has many known targets, it is often used in these studies with METTL16 often being included experimentally (as there are few verified interactors). This does come with some issues. First, it is generally regarded that METTL3/14 and METTL16 have different consensus sequences[56,59,60,81]. Therefore, some m6As that are in close proximity may be assigned to only one methyltransferase. Also, these studies tend to use polyadenylated RNA selection for more efficient sequencing, however this is very likely to exclude some interactors,

since it is known that METTL16 interacts with RNAs other than mRNA. Furthermore, some studies show results as dependence of methylation on a certain methyltransferase. If an RNA shows dependence on both METTL3/14 and METTL16, it seems it is considered a "true" METTL3/14 target while showing secondary dependence on METTL16 due to the indirect effect of MAT2A [102,121]. Looking to refine a consensus motif among these results will exclude potential interactors and could be why there are differences among published results. Lastly, if MAT2A function is crucially dependent on METTL16, the knockdown of METTL16 (which is used to compare RNAs subsequently hypomethylated) could lower the cellular concentration of SAM. This is the basis of the argument of secondary dependence mentioned before. However, demethylases could also be responsive to the induced lower level of m6A-modified RNA and demethylate further for SAM recycling, which could result in RNAs appearing dependent on the methyltransferase knocked-down. These speculations are not verifiable until more information is known about the innerworkings of methyltransferases, demethylases, and their regulation on/by the methionine cycle.

In this chapter, we have discussed the current state of METTL16 understanding, predictions, and speculations. Even though there is little information that is considered to be confirmed about this protein, it is evident that it has a significant and intriguing influence in humans. The goal of this publication is to combine the results and implications of studies on this protein to educate and guide the m6A community to what is and is not yet known about METTL16.

Chapter 2:

Characterization of METTL16 as a cytoplasmic RNA binding protein

The work presented in this chapter was published as

"Characterization of METTL16 as a cytoplasmic RNA binding protein"

PLoS ONE 15(1): e0227647; January 2020

Daniel J. Nance*, Emily R. Satterwhite, Brinda Bhaskar**, Sway Misra***, Kristen R. Carraway, Kyle D. Mansfield

Biochemistry and Molecular Biology Department, Brody School of Medicine, East Carolina University, Greenville NC, 27834

*Current address: University of North Carolina at Chapel Hill School of Medicine, Chapel Hill NC, 27516

**Current address: Wake Forest School of Medicine, Winston Salem NC, 27101

***Current address: University of Georgia, Athens GA, 30602

Abstract

mRNA modification by N6-methyladenosine (m6A) is involved in many post-transcriptional regulation processes including mRNA stability, splicing and promotion of translation. Accordingly, the recently identified mRNA methylation complex containing METTL3, METTL14, and WTAP has been the subject of intense study. However, METTL16 (METT10D) has also been identified as an RNA m6A methyltransferase that can methylate both coding and noncoding RNAs, but its biological role remains unclear. While global studies have identified many potential RNA targets of METTL16, only a handful, including the long noncoding RNA MALAT1, the snRNA U6, as well as the mRNA MAT2A have been verified and/or studied to any great extent. In this study we identified/verified METTL16 targets by immunoprecipitation of both endogenous as well as exogenous FLAG-tagged protein. Interestingly, exogenously overexpressed METTL16 differed from the endogenous protein in its relative affinity for RNA targets which prompted us to investigate METTL16's localization within the cell. Surprisingly, biochemical fractionation revealed that a majority of METTL16 protein resides in the cytoplasm of a number of cells. Furthermore, siRNA knockdown of METTL16 resulted in expression changes of a few mRNA targets suggesting that METTL16 may play a role in regulating gene expression. Thus, while METTL16 has been reported to be a nuclear protein, our findings suggest that METTL16 is also a cytoplasmic methyltransferase that may alter its RNA binding preferences depending on its cellular localization. Future studies will seek to confirm differences between cytoplasmic and nuclear RNA targets in addition to exploring the physiological role of METTL16 through long-term knockdown.

Introduction

Methylation on the sixth position of the base moiety of adenosine (m6A) is one of the most common mRNA modifications in eukaryotes, and it has been shown to affect all aspects of post-transcriptional regulation including mRNA splicing, stability, and translation[4,5,23,24,27,137–140]. Methyltransferase like -3 and -14 (METTL3 and METTL14) and Wilms' tumor associating protein (WTAP) in addition to KIAA1429 are all components of the mRNA m6A methyltransferase complex, which uses a S-adenosyl methionine (SAM) binding domain on METTL3 to methylate specific mRNAs for methylation with a RRACH m6A consensus sequence[37,39,40,42,141]. Many RNA binding proteins (RBPs) including the YTH family of proteins modulate the effects of m6A through specific binding to the methylated RNA. For example, YTHDF1 has been shown to increase translation of m6A containing mRNA, while YTHDF2 appears to direct mRNA degradation and YTHDF3 appears to play roles in both processes[22,23,26,27,138,139]. m6A has been shown to play a role in a number of physiological processes including embryonic stem cell differentiation, circadian rhythms, response to hypoxia and other stressors, and is implicated in many different aspects of cancer[4,22,24,30,52,142–149].

METTL16 has also been identified as an RNA m6A methyltransferase that methylates both coding and noncoding RNAs. Primarily, METTL16 has been shown to methylate the U6 snRNA [56,58]. It can also bind and methylate the long noncoding RNAs MALAT1 and XIST [54,58]. In addition, METTL16 has been shown to bind and methylate mRNAs, including MAT2A, which can regulate its alternative splicing in response to cellular SAM levels [56,60,81]. Furthermore, global analysis suggests that many other mRNAs including RBM3 and STUB1 may also be METTL16 targets [58].

Perhaps the most intriguing aspect of the METTL16 methyltransferase is the importance of structure when binding targets, not just sequence like the METTL3/METTL14/WTAP complex. METTL16 m6A methylation of MAT2A is reliant upon a conserved hairpin (hp1) for binding and a similar sequence and structure is required for U6 methylation as well, but interestingly, is not readily apparent in other METTL16 targets [56]. In *in vitro* methylation studies, METTL16 appears to prefer stem loop structures with the methylated adenosine being unpaired in a single stranded loop or bulge [59,61].

At a molecular level, the effects of METTL16 m6A activity are best understood in the context of cellular S-adenosylmethionine (SAM) levels and intron retention of MAT2A pre-mRNA. SAM is a methyl donor for most cellular methylation reactions and is created using SAM synthetases that convert methionine and ATP into SAM [56]. In human cells, the SAM synthetase is encoded by the MAT2A gene and is expressed in all cell types except liver cells. Methionine depletion stabilizes MAT2A mRNA, which has six hairpin structures (hp1-6) in its 3' UTR that serve as binding sites for METTL16. When intracellular SAM levels are high, METTL16 binds the hp1 of MAT2A RNA, methylates it, and quickly dissociates to support intron retention. Intron retention targets the MAT2A mRNA for nuclear degradation. Low intracellular levels of SAM do not allow for efficient methylation by METTL16, increasing METTL16 occupancy on the mRNA which results in increased splicing of the retained intron. This increases stabilization and translation of the MAT2A mRNA and production of SAM synthetase which increases SAM levels in the cell. Additionally, the YTHDC1 m6A "reader" protein may play a role in processing the mature MAT2A mRNA and monitoring intracellular SAM levels [81].

Other than regulating MAT2A in response to SAM levels, the physiological significance of METTL16 is largely unknown at this point. METTL16 does appear to be vital for the

proliferation/ survival of a number of cancer cells [125] and has been identified in a number of screens for essential genes[127,150–153]. Interestingly, whole mouse METTL16 knockout results in blastocysts that are unfit to develop further and abort, although the reason for this is not definitively known, but may also be due to regulation of MAT2A expression [60]. Thus, METTL16 appears to be essential for mammalian life, even though its physiological role has not been fully characterized. In this study, we have confirmed that METTL16 binds a number of coding and noncoding RNAs and identify a number of novel METTL16 targets. In addition, we show that overexpression of METTL16 can affect both its cellular location as well as its RNA binding preferences.

Our results suggest that the majority of METTL16 protein resides in the cytoplasm of a number of cell types, and that knockdown of METTL16 protein can affect the expression of a few of its mRNA binding targets. These results suggest that METTL16 may have additional roles in the cell that could contribute to its essentiality.

Results

Identification of METTL16 binding targets

To identify potential METTL16 RNA targets as well as verify reported literature targets, HEK293T cells were transiently transfected with either FLAG-GFP or FLAG-METTL16 overexpression constructs. Cell extracts were then subjected to Ribonucleoprotein Immunoprecipitation (IP) using FLAG magnetic beads. Western blotting was used to confirm successful immunoprecipitation as evidenced by depletion of the expected band in the supernatant and enrichment in the IP (Figure 2.1A). RNA was also extracted, and real-time PCR was used to measure enrichment of METTL16 targets. Two methods were used to calculate enrichment. In the

first analysis, the amount of the RNA target in the GFP or METTL16 IP was compared to the input levels from 50% of the sample to generate a relative enrichment (Figure 2.1B, left panels). Specifically, the value is a fold enrichment in the IP relative to the Input and is calculated by raising two to the power of the Cq value of the IP subtracted from the Cq value of the Input. In the second analysis, fold enrichment of the RNA target in the METTL16 IP compared to the GFP IP was calculated (Figure 2.1B, right panels) by dividing the METTL16 relative enrichment (as described above) by the GFP relative enrichment value. By comparing enrichment to both the input as well as a negative IP we can get a better sense of the nature of the binding and have greater confidence in identifying METTL16 binding targets. As shown in Figure 2.1B, U6 snRNA appears to be the primary binding target of METTL16 by either analysis. Importantly, U1 and U2 snRNA, which are not known to harbor an m6A, served as negative controls and exhibited very little enrichment in the METTL16 IP. It does appear that 18S rRNA is also a target, showing an almost 1,000-fold enrichment in the METTL16 IP over the GFP IP. Interestingly, in addition to MAT2A, a number of mRNA's including β2M, MYC, and NT5DC2 also appeared to be FLAG-METTL16 targets, while the long noncoding RNA (lncRNA) MALAT1 did not appear to be bound by FLAG-METTL16.

To determine if these targets were the same for endogenous METTL16, we repeated the immunoprecipitation in HEK293T extracts using either METTL16 antibody or normal rabbit serum (NRS) coated magnetic beads. Western blotting confirmed that the IP was successful with METTL16 protein remaining in the supernatant of the negative IP while appearing in the IP lane of the METTL16 antibody (Figure 2.2A). Real-Time PCR was again used to measure RNA enrichment of targets either compared to the input levels (Figure 2.2B, left panels) or in relation to the negative IP after normalizing for input levels (Figure 2.2B, right panels). Interestingly, in

Figure 2.1

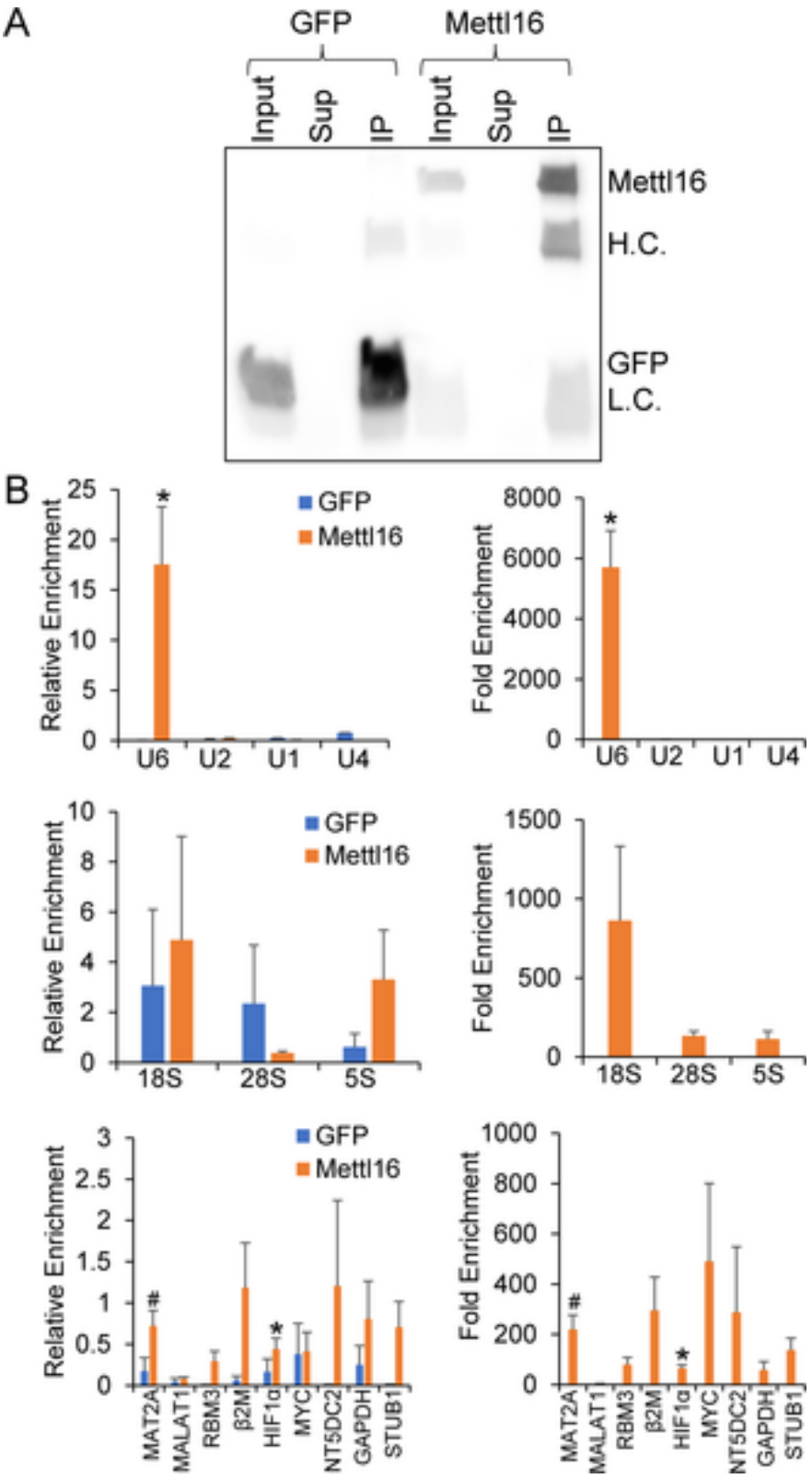
A
GFP
Mettl16
Input
Sup
IP
Input
Sup
IP
Mettl16
H.C.
GFP
L.C.
B
Relative Enrichment
GFP
Mettl16
U6
U2
U1
U4
Fold Enrichment
18S
28S
5S
MAT2A
MALAT1
RBM3
β2M
HIF1α
MYC
NT5DC2
GAPDH
STUB1

Figure 2.1: Identification of FLAG-METTL16 targets. FLAG-METTL16 or FLAG-GFP protein was overexpressed and immunoprecipitated from HEK293T cells. (A) Input, Supernatant (Sup), and Immunoprecipitated (IP) protein were subjected to Western blotting to confirm successful immunoprecipitation (Antibody Heavy Chain (H.C.) and Light Chain (L.C) are indicated). (B) Associated RNAs were isolated via Trizol and real-time PCR was used to determine enrichment. The left panel depicts data as relative enrichment compared to the input, while the right panel shows enrichment in the METTL16 relative to the FLAG-GFP control immunoprecipitation. (*) $P \leq 0.05$, (#) $P \leq 0.1$ by paired Student's t-test. Error bars represent SEM of four to seven experiments. The experiments in this figure were performed by Daniel Nance.

Figure 2.2

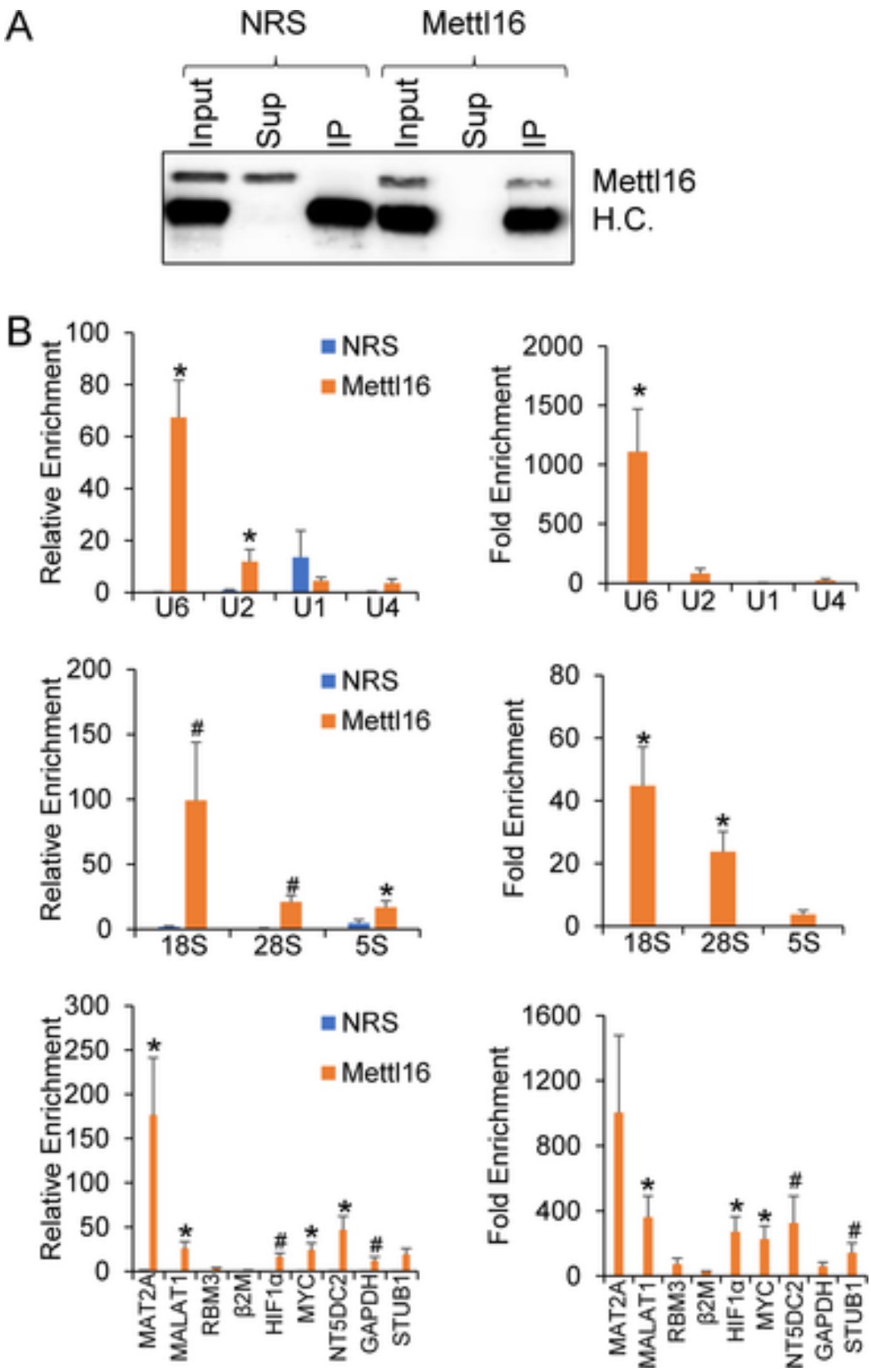
A
NRS
Mettl16
Input
Sup
IP
Input
Sup
IP
Mettl16
H.C.
B
Relative Enrichment
NRS
Mettl16
U6
U2
U1
U4
Fold Enrichment
18S
28S
5S
MAT2A
MALAT1
RBM3
β2M
HIF1α
MYC
NT5DC2
GAPDH
STUB1

Figure 2.2: Identification of endogenous METTL16 targets. HEK293T extracts were immunoprecipitated with either METTL16 antibody or normal rabbit serum (NRS) as a negative control. (A) Input, Supernatant (Sup), and Immunoprecipitated (IP) protein were subjected to Western blotting to confirm successful immunoprecipitation (Antibody Heavy Chain (H.C.) is indicated). (B) Associated RNAs were isolated via Trizol and real-time PCR was used to determine enrichment. The left panel depicts data as relative enrichment compared to the input, while the right panel shows enrichment in the METTL16 relative to the FLAG-GFP control immunoprecipitation. (*) $P \leq 0.05$, (#) $P \leq 0.1$ by paired Student's t-test. Error bars represent SEM of six experiments.

contrast to the FLAG-METTL16 immunoprecipitation, MAT2A mRNA appeared to be the primary target of endogenous METTL16, although U6 snRNA was still a significant target. Additional mRNAs such as HIF-1α, MYC, and NT5DC2 were also identified as potential METTL16 targets while 5S rRNA and U1 and U2 snRNA appear to not be bound by METTL16, which is expected given that they are not known to be m6A methylated. In contrast to the FLAG-IP, the lncRNA MALAT1 did appear to be a binding target of the endogenous METTL16.

Investigation of METTL16 cellular localization

Based on the differences in targets between exogenous FLAG-tagged and endogenous METTL16, we theorized that METTL16 localization may change based on expression levels and that this may impact target selection. Biochemical fractionation of FLAG-METTL16 overexpressing HEK293T cells revealed that exogenously expressed METTL16 protein was found in both the cytoplasmic and nuclear fractions (55% in cytoplasm; 45% in nucleus) (Figure 2.3A). Lactate Dehydrogenase (LDH) served as a marker for the cytoplasmic fractions, while the nuclear matrix protein Lamin B and the transcription factor Specificity Protein 1 (SP1) served as markers for the insoluble and soluble nuclear fractions respectively and confirm successful fractionation. To investigate whether overexpression affected METTL16 cellular localization we also analyzed endogenous METTL16's localization in HEK293T cells using biochemical fractionation (Figure 2.3B). Compared to the FLAG-overexpressed METTL16, slightly more endogenous METTL16 was found in the cytoplasm (60%) relative to the nucleus (40%). These results suggest that overexpression of METTL16 may affect its cellular localization and that this may impact the RNA targets identified in the immunoprecipitations.

Previously, METTL16 has been reported to be a predominantly nuclear protein[54,56,58,88].

Figure 2.3

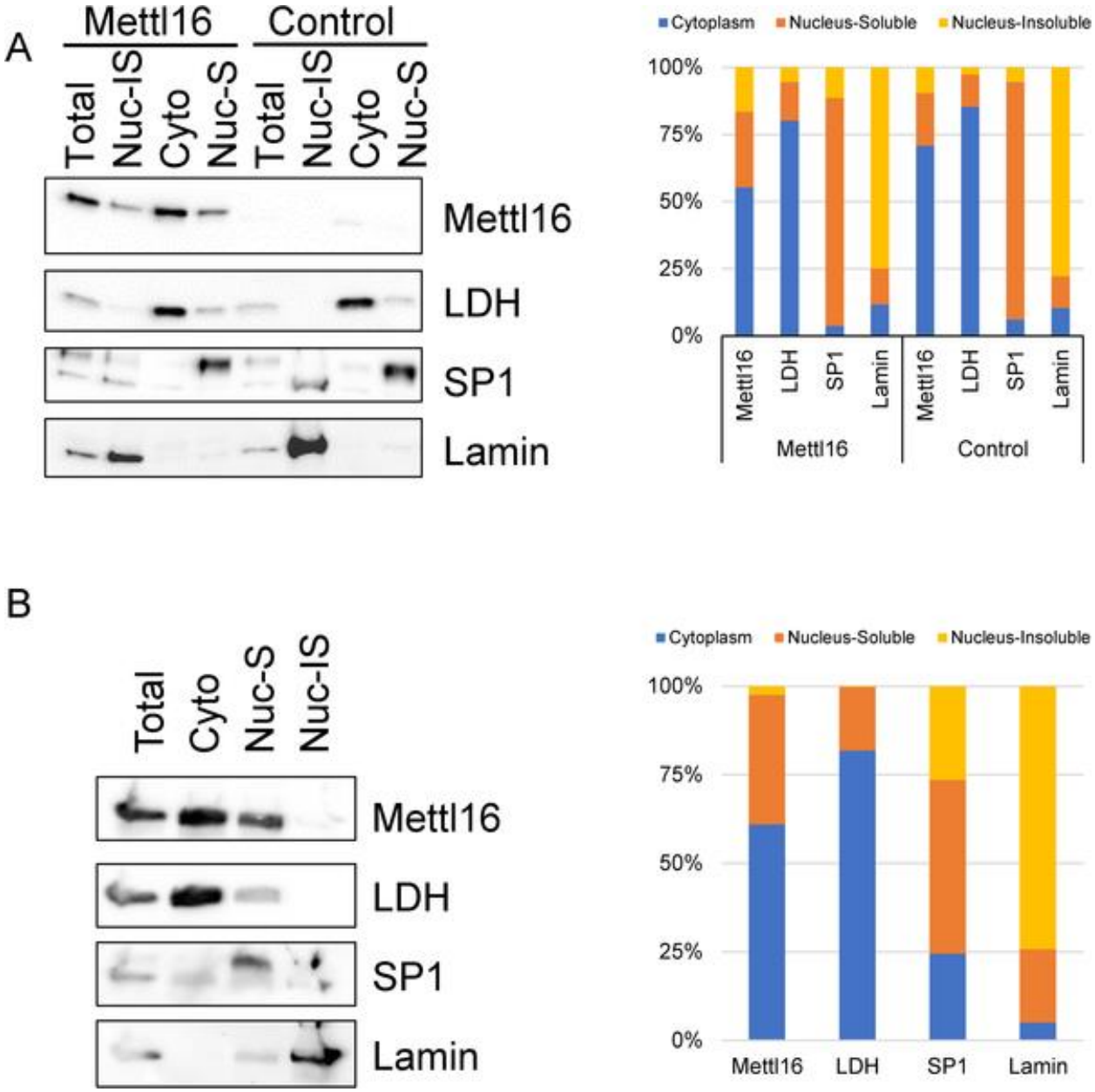
A
Mettl16
Control
Total
Nuc-IS
Cyto
Nuc-S
Total
Nuc-IS
Cyto
Nuc-S
Mettl16
LDH
SP1
Lamin
Cytoplasm
Nucleus-Soluble
Nucleus-Insoluble
100%
75%
50%
25%
0%
Mettl16
LDH
SP1
Lamin
Mettl16
LDH
SP1
Lamin
Mettl16
Control
B
Total
Cyto
Nuc-S
Nuc-IS
Mettl16
LDH
SP1
Lamin
Cytoplasm
Nucleus-Soluble
Nucleus-Insoluble
100%
75%
50%
25%
0%
Mettl16
LDH
SP1
Lamin

Figure 2.3: Determination of METTL16 cellular localization in HEK293T cells. (A) Extracts from HEK293T cells stably expressing FLAG-METTL16 or an empty vector control were separated into Total, Insoluble Nuclear (Nuc-IS), Cytoplasmic (Cyto), and Soluble Nuclear (Nuc-S) fractions and subjected to Western blot with METTL16 antibody to determine METTL16 cellular localization. Lamin B was used as an insoluble nuclear marker, SP1 as a soluble nuclear marker, and lactate dehydrogenase (LDH) as a cytoplasmic marker. (B) Biochemical cellular fractionation was also used to determine the location of endogenous METTL16 protein in untreated HEK293T cells (representative of three to five experiments).

Using an antibody from a previous study we attempted to use immunohistochemistry to verify METTL16's cellular localization [54]. Initial experiments showed METTL16 staining in both the cytoplasm and nucleus of HEK293T cells (Figure 2.4). To validate antibody specificity, we ran both Western blotting and immunohistochemistry on control and METTL16 siRNA knockdown HEK293T cells. Despite almost complete knockdown of METTL16 protein by siRNA (as confirmed by western blotting) similar staining patterns and intensities were observed in both control and METTL16 siRNA treated samples suggesting that the immunohistochemical staining observed may be non-specific (Figure 2.4). A second antibody gave similar results with fluorescent signal in both the cytoplasm and nucleus of HEK293T cells. However, once again, the signal was not decreased in the immunohistochemistry when METTL16 was depleted with long-term (6 day) siRNA treatment suggesting that the majority of the signal from this antibody is also coming from non-specific binding (Figure 2.5).

As an alternative approach, we again used biochemical fractionation to examine METTL16's localization in two other cell lines in which immunohistochemistry had indicated nuclear localization [54,58]. As shown in Figure 2.6A, in HEK293 cells, METTL16 protein appears to be predominately located in the cytoplasm with almost 90% of the protein in the cytoplasm, while in the HELA cells approximately 55% of METTL16 protein appears cytoplasmic. To determine if this a more widespread observation, we also examined METTL16's localization in a lung fibroblast cell line (CCD34LU) as well as a lung cancer cell line (NCI-H1299) and again found METTL16 to be predominant in the cytoplasm of both cell types (Figure 2.6B). We also examined METTL16's localization in a series of MCF10 breast cancer cells representing different stages of breast cancer progression. MCF10-A's represent immortalized, yet nontumorigenic cells. MCF10- AT1's are transformed but are weakly tumorigenic, while the MCF10-Ca1h line

Figure 2.4

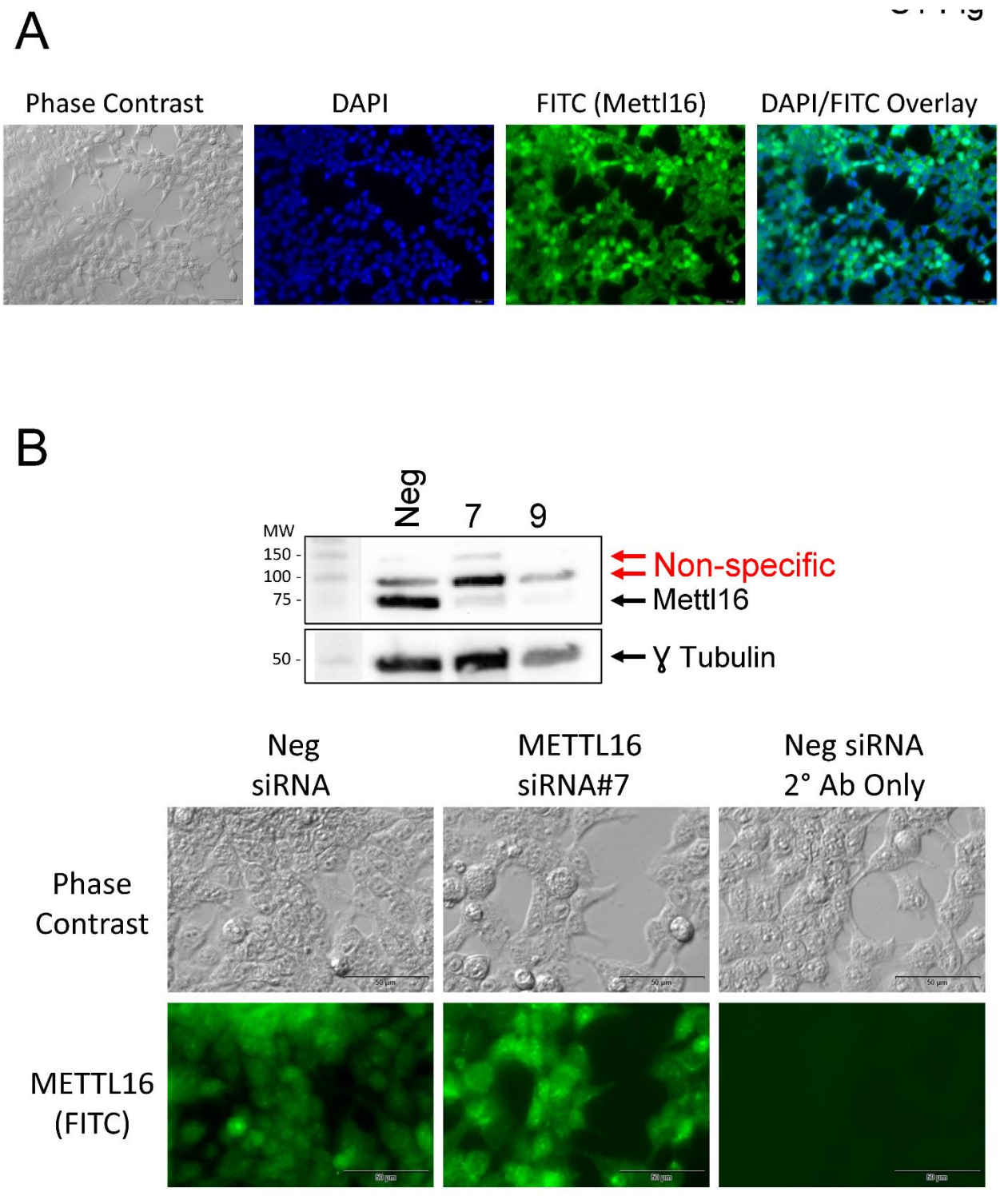
A
Phase Contrast
DAPI
FITC (Mettl16)
DAPI/FITC Overlay
B
Neg
7
9
MW
150 -
100 -
75 -
50 -
Non-specific
Mettl16
γ Tubulin
Neg siRNA
METTL16 siRNA#7
Neg siRNA 2° Ab Only
Phase Contrast
METTL16 (FITC)

Figure 2.4: Validation of HPA020352 METTL16 antibody. (A) Methanol fixed HEK293T cells subjected to immunohistochemistry with METTL16 antibody and DAPI nuclear stain. (B) HEK293T cells were treated for 6 days with either a negative control siRNA (Neg) or METTL16-specific siRNAs. Western blotting indicated substantial METTL16 knockdown (similar to Figure 2.8) with additional non-specific background bands. Immunohistochemistry on methanol fixed cells from the same experiment showed similar staining in both location and intensity despite METTL16 knockdown suggesting non-specific binding.

Figure 2.5

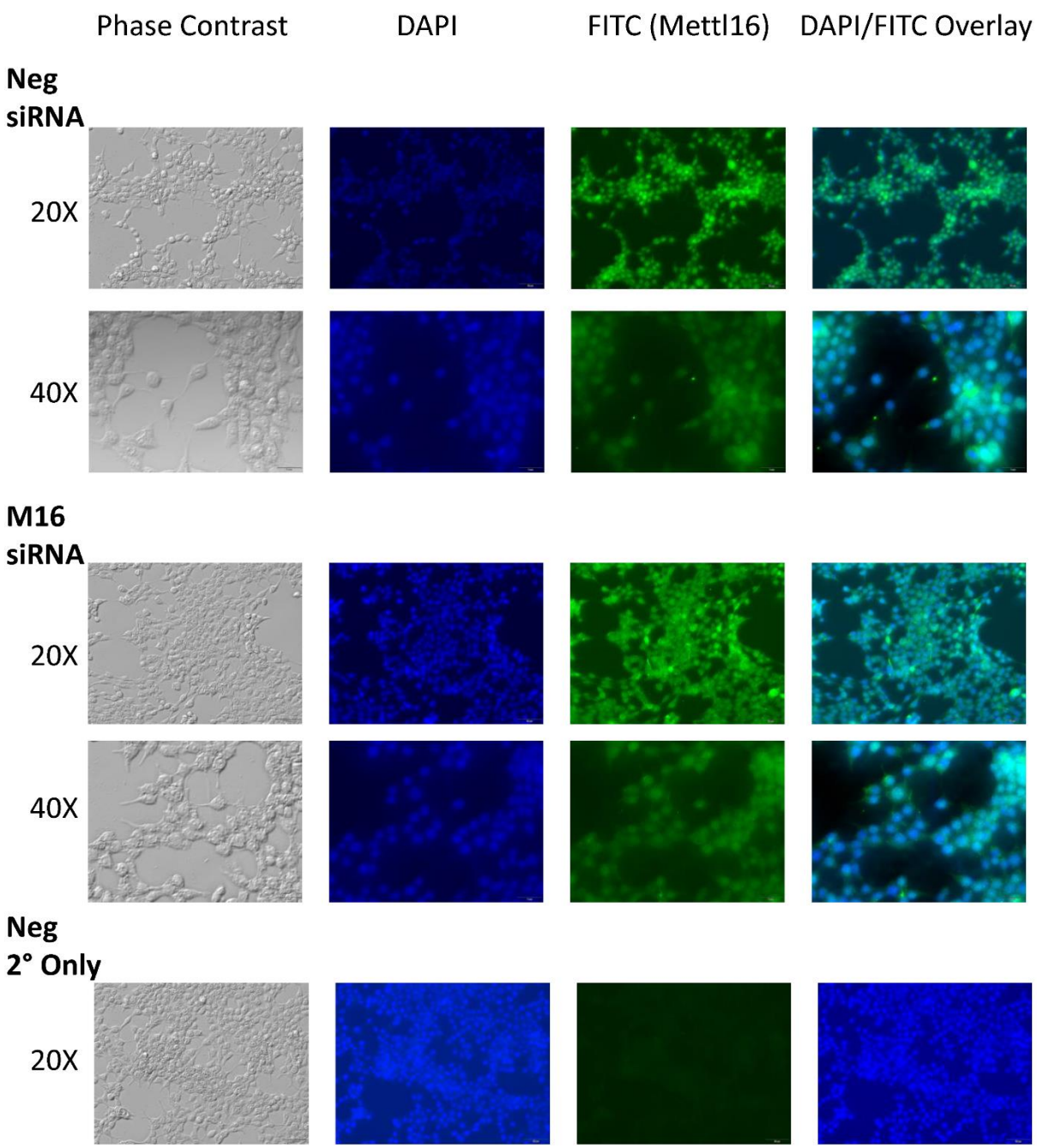
Phase Contrast
DAPI
FITC (Mettl16)
DAPI/FITC Overlay
Neg siRNA
20X
40X
M16 siRNA
20X
40X
Neg 2° Only
20X

Figure 2.5: Immunohistochemistry on second METTL16 antibody. HEK293T cells were treated for 6 days with either a negative control siRNA (Neg) or METTL16-specific siRNAs. Immunohistochemistry on paraformaldehyde fixed cells with PA5-54185 METTL16 antibody showed similar staining in both location and intensity despite METTL16 knockdown suggesting non-specific binding. DAPI was used to visualize the nucleus.

Figure 2.6

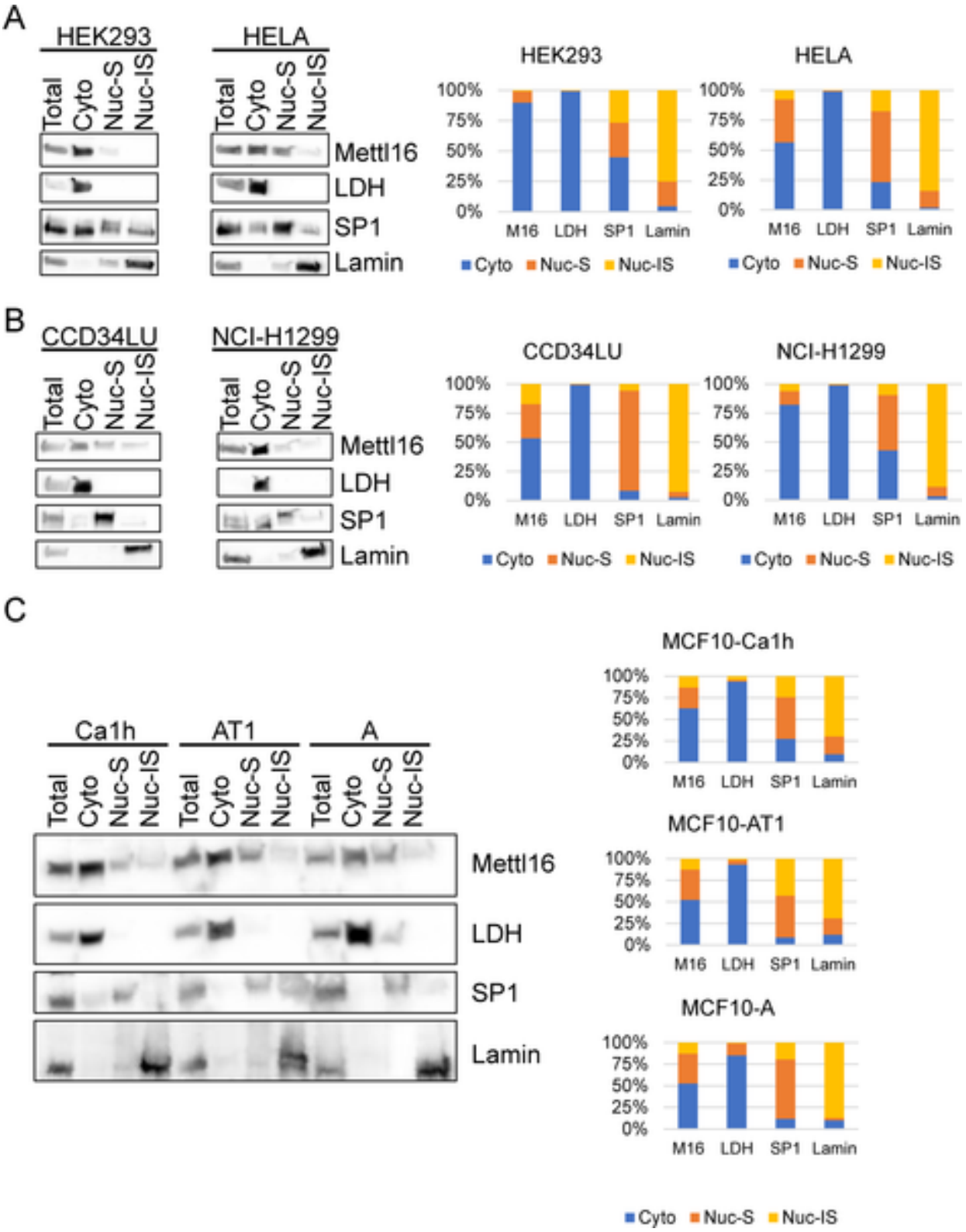
A
HEK293
HELA
Total
Cyto
Nuc-S
Nuc-IS
Mettl16
LDH
SP1
Lamin
HEK293
HELA
100%
75%
50%
25%
0%
M16
LDH
SP1
Lamin
Cyto
Nuc-S
Nuc-IS
B
CCD34LU
NCI-H1299
C
Ca1h
AT1
A
MCF10-Ca1h
MCF10-AT1
MCF10-A

Figure 2.6: Determination of METTL16 cell localization in multiple cell lines. (A) Extracts from HEK293 or HELA cells were separated into Total, Cytoplasmic (Cyto), Soluble Nuclear (Nuc-S), and Insoluble Nuclear (Nuc-IS) fractions and subjected to Western blot with METTL16 antibody to determine METTL16 cellular localization. Lamin B was used as an insoluble nuclear marker, SP1 as a soluble nuclear marker, and lactate dehydrogenase (LDH) as a cytoplasmic marker. (B, C) Biochemical cellular fractionation was also used to determine the location of METTL16 protein in lung cell lines CCD34LU and NCI-H1299 as well as breast cancer cell lines MCF10-Ca1h, MCF10-AT1, and MCF10-A. (representative of two to three experiments). The experiments in this figure were performed by Kristen Carraway.

represents a highly aggressive tumorigenic cell line[154,155]. Again, we saw at least 50% of METTL16 protein located in the cytoplasm of all three of these cell lines (Figure 2.6C), confirming that in addition to its reported nuclear localization, METTL16 protein is found in the cytoplasm of a number of cell types and localization does not appear to be affected by transformation.

Effect of METTL16 knockdown on target expression

We attempted to determine the physiological role of METTL16 by knocking it out using CRISPR, but we were unable to create stable cell lines. This is in line with previous literature reports that suggest that METTL16 is likely an essential gene[56,127]. METTL16 was instead knocked down for an extended period of time using siRNA. In this set of experiments, HEK293T cells were transfected with either a scrambled negative control siRNA or one of two METTL16-specific siRNAs. After 48 hours of siRNA expression, cells were harvested or replated and re-transfected the following day with the same siRNA. Cells were then harvested 6 days after the initial transfection (3 days after the 2nd transfection). Western blotting confirmed that compared to the negative control siRNA, treatment with either METTL16 siRNA resulted in significant knockdown of METTL16 expression at both the RNA (Figure 2.7A) and protein (Figure 2.8) level, with 6 days treatment resulting in almost complete loss of the protein. Real-time PCR was then used to assess the effect of METTL16 knockdown on the expression of METTL16 target RNAs. As shown in Figure 2.7A, 48-hour knockdown of METTL16 caused small changes in expression of a number of RNAs but significantly increased the expression of NT5DC2 mRNA. Interestingly, many of these changes were reduced, lost, or even reversed after 6 days of METTL16 knockdown, and instead we observed decreases in the MALAT1 lncRNA and STUB1 mRNAs (Figure 2.7B) although it was only with the #7 siRNA that showed greater METTL16 knockdown. No changes

Figure 2.7

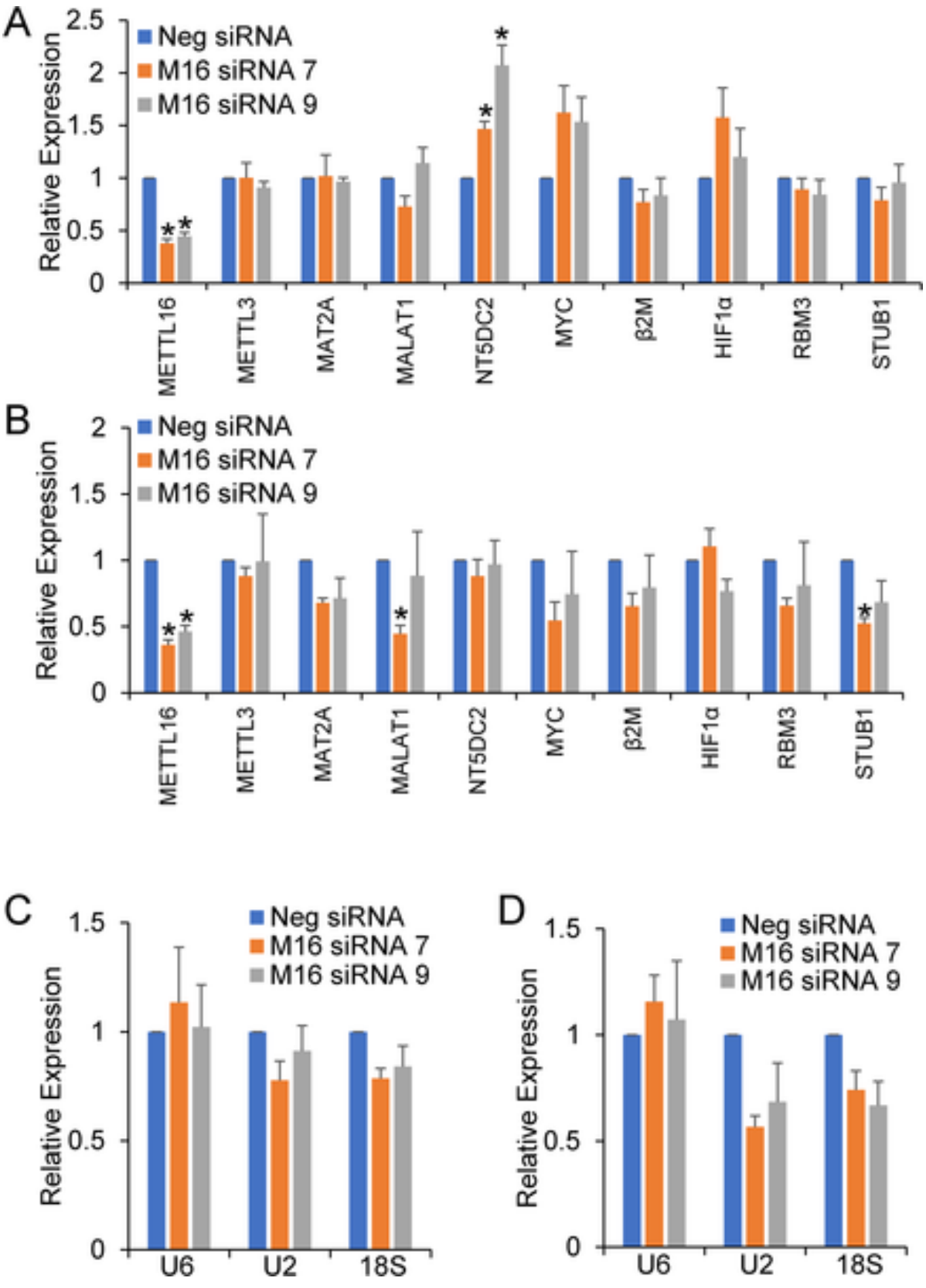
A
Relative Expression
2.5
2
1.5
1
0.5
0
Neg siRNA
M16 siRNA 7
M16 siRNA 9
METTL16
METTL3
MAT2A
MALAT1
NT5DC2
MYC
β2M
HIF1α
RBM3
STUB1
B
Relative Expression
2
1.5
1
0.5
0
Neg siRNA
M16 siRNA 7
M16 siRNA 9
METTL16
METTL3
MAT2A
MALAT1
NT5DC2
MYC
β2M
HIF1α
RBM3
STUB1
C
Relative Expression
1.5
1
0.5
0
Neg siRNA
M16 siRNA 7
M16 siRNA 9
U6
U2
18S
D
Relative Expression
1.5
1
0.5
0
Neg siRNA
M16 siRNA 7
M16 siRNA 9
U6
U2
18S

Figure 2.7: Effect of METTL16 knockdown on mRNA expression. HEK293T cells were treated for 2 days (A, C) or 6 days (B, D) using either a negative control siRNA (Neg) or one of two METTL16-specific (7 & 9) siRNAs. Real-time PCR was used to determine the effect on RNA expression normalized to GAPDH and expressed as relative to the negative siRNA control. (*) $P \leq 0.05$ by one-way ANOVA with post-hoc Tukey HSD test. Error bars represent SEM of five experiments.

Figure 2.8

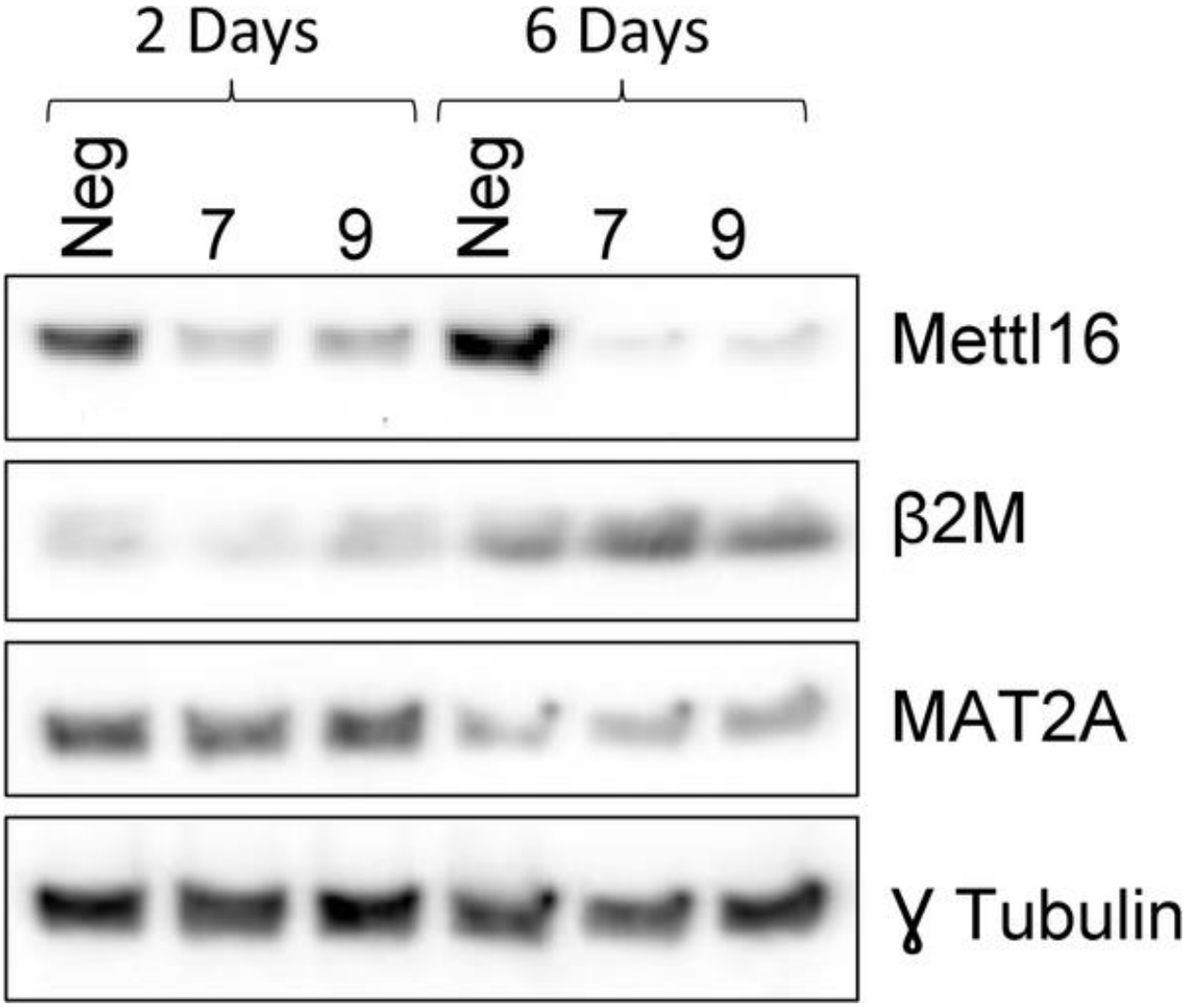

Figure 2.8: Effect of METTL16 knockdown on protein expression. HEK293T cells were treated for 2 days (A) or 6 days (B) using either a negative control siRNA (Neg) or one of two METTL16-specific (7 & 9) siRNAs. Western blotting was used to determine the effect on protein expression (representative of five experiments).

were seen in the expression levels of a number of other coding and noncoding RNAs. Consistent with the real-time PCR results, we saw little to no effect of METTL16 knockdown on the protein expression of any of the targets tested (Figure 2.8).

Discussion

Overall, our work provides new insight into both the targets of METTL16 as well as its potential for the regulation of gene expression while also raising some new questions about METTL16's role in the cell. Through immunoprecipitation we have verified the three most well-defined and researched METTL16 RNA substrates[54,56,58]. While U6 snRNA was the preferred target of FLAG-METTL16, it appears that MAT2A may be the preferred endogenous target in HEK293Ts. We also verified the first identified METTL16 target, lncRNA MALAT1 [54]. Previous reports have found METTL16 bound to ribosomal RNA [58], and our data suggests that 18S rRNA is the preferred target. However, recent studies have identified ZCCHC4 and METTL5 as the 28S and 18S rRNA m6A methyltransferases respectively[71,72]. This raises the question as to whether the rRNAs are indeed specific binding targets of METTL16, and if they are, what role might METTL16 be playing.

While MAT2A was clearly the preferred mRNA binding target of METTL16 in our system, we were also able to confirm a number of other mRNA binding targets including RBM3, STUB1, and NT5DC2 identified in previous studies [56,58]. In addition, our studies have identified several novel mRNAs including β2M, HIF-1α and MYC which also appear to be bound by METTL16. However, our long-term knockdown studies failed to reveal any significant expression changes at either the RNA or protein level of these targets. The question of whether these mRNAs

are regulated in some way by METTL16 methylation or even METTL16 protein binding remains to be determined.

The change in target preference that we saw between exogenous and endogenous METTL16 immunoprecipitations made us question whether expression levels might impact METTL16 cellular localization, and in turn, modulate its binding preferences. Biochemical fractionation of HEK293T cells suggests that a majority of METTL16 protein is localized to the cytoplasm with lesser amounts of protein found in the nucleus. This contradicts previous characterizations of METTL16 as a predominately nuclear m6A methyltransferase[54,56,58,88]. We also observed cytoplasmic METTL16 localization in a number of other cell types representing normal cells as well as different stages of cancer suggesting that this may be a more general finding relevant to all cell types.

Our attempts to verify the biochemical fractionation results with immunohistochemistry were unsuccessful due to non-specific binding of the antibodies tested. This was quite surprising as the antibodies were verified to recognize METTL16 in western blotting as confirmed by loss of signal with long-term siRNA treatment. However, when siRNA knockdown cells were probed for METTL16 by immunohistochemistry, similar signal intensities and localization were seen, suggesting that in immunohistochemistry the antibodies were recognizing other antigens. This explanation is supported by the fact that non-specific bands were also observed in the Western blotting and may be contributing to this erroneous signal. Thus, we feel the immunohistochemistry results are suspect until a specific antibody can be verified.

While it is clear from our fractionation data that METTL16 can be found in the cytoplasm of cells, all of its currently reported activities take place in the nucleus[56,81,88]. Splicing of MAT2A is clearly a nuclear activity, as is U6 snRNA processing. Small amounts of U6 snRNA have been

found in the cytoplasm but it is not clear if this is a widespread phenomenon[156,157]. Finally, to date, the majority of METTL16-mediated methylations have been identified in introns [56], which again suggests a nuclear role for the protein. While we have clearly shown METTL16 protein in the cytoplasm of cells, the role it plays there is unclear. It is interesting that in our study, all of our primers were directed to mature mRNA and do not amplify pre-mRNA, which suggests that METTL16 can bind to mature mRNA, although we did not investigate its methylation of those mRNA.

METTL16 is essential for mammalian life based on our (and others) attempts at creating METTL16 knockout cell lines via CRISPR and knockout studies in mice embryos [56,60]. This observation is also supported by global screens for essential genes that have identified METTL16[127,150–153]. The reason for its essentiality is unclear, but it has been implicated in two major roles in cellular development and survival. It is clear that METTL16's regulation of MAT2A mRNA levels via the SAM synthetase pathway affects developmental events [60]. METTL16 knockout downregulates MAT2A mRNA levels, which likely leads to the production of blastocysts that are not capable of further development. It is also possible that METTL16-mediated m6A methylation of U6 snRNA is important for proper functionality of the spliceosome complex, and the lack of this modification could have global effects on splicing that result in production of incorrect proteins and eventual cell death. It is known that the methylated adenosine (A43) is essential for U6 snRNAs function in yeast [158], however, widespread changes in splicing were not observed in the knockout mouse studies [60], raising the question of whether the methylation of this residue of U6 snRNA impacts splicing in any appreciable way.

Given that METTL16 appears to be essential, conditional knockout/knockdown models will need to be developed to better investigate the effects of METTL16 methylation on mRNA

stability, translation, as well as splicing via U6. Of particular interest will be determining whether there are differences between METTL16-mediated methylation and METTL3-mediated methylation, particularly in the RNA binding proteins which recognize the methylation and/or the functional consequences of methylation. In the future, it will be interesting to create METTL16 variants with localization sequences that force the protein to either the nucleus or cytoplasm. These variants can be used to determine the binding preferences of METTL16 based on its localization, which may explain the differences we have seen in this study.

Materials and methods

Tissue culture

HEK293T, HEK293, HELA, CCD34LU and NCI-H1299 cells were obtained directly from ATCC. MCF10-A, MCF10-AT1, and MCF10-Ca1h were obtained from Barbara Ann Karmanos Cancer Center. Cells were routinely cultured at 37˚C, 5% CO2. HEK293T, HEK293, and HELA cells were maintained in DMEM with 4g/L glucose, 10% FBS, 2 mM L-glutamine, and 1X Pen/Strep. CCD34LU cells were maintained in EMEM with 10% FBS, and 1X Pen/Strep. NCI-H1299 cells were maintained in RPMI-1640 with 4g/L glucose with 10% FBS, 2 mM L-glutamine, and 1X Pen/Strep. MCF10-A, MCF-AT1, and MCF10-Ca1h cells were maintained in a 50/50 mix of DMEM/F12 with 5% horse serum, 1mM CaCl2, and 1X Pen/Strep, 10 μg/ml insulin, 20 ng/ml EGF, 0.5 μg/ml Hydrocortisone, and 0.1 μg/ml cholera enterotoxin.

Knockdown and overexpression of METTL16

For knockdown, HEK293T cells were transfected with 20 μM siRNA (Life Technology Silencer Select) targeting METTL16 (siRNA ID# S35507 or S35509) or Negative Control #1 (Catalog # AM4635) siRNA with Lipofectamine 2000 (Thermo Fisher) according to

manufacturer's directions. For long-term knockdown, cells were transfected and allowed to recover for 48 hours. Cells were lifted, counted and replated for 2nd round of transfection while the remainder of the cells were harvested for RNA and protein. The following day cells were transfected again and allowed to recover for 3 more days before final harvesting (6 days knockdown total). For overexpression, 2 μg of plasmid expressing a FLAG-tagged METTL16 (Origene: RC208648) or GFP were used. Cells were transfected for 72 hours before harvesting to allow for sufficient overexpression of METTL16.

Western blots

Whole-cell lysates were prepared in whole-cell extract buffer (WCEB: 50 mM Tris pH 7.4, 150 mM NaCl, 5 mM EDTA, 0.1%SDS, and complete protease inhibitor [Promega]). After sonication, equal amounts of protein (30–50 μg) were electrophoresed on a mini-PROTEAN any KD acrylamide gel (Bio-Rad Laboratories) and transferred to Hybond ECL nitrocellulose (GE Healthcare). The blot was blocked with 5% non-fat dry milk (LabScientific) in Tris-buffered saline with 0.1% Tween 20 (TBST) for 1 hour at room temperature, followed by primary antibody incubation in blocking buffer overnight at 4˚C. After washing extensively with TBST, blots were incubated for 1–2 hour at room temperature with appropriate HRP-linked secondary antibody (GE Healthcare), washed again with TBST, developed using Bio-Rad Clarity Western ECL Substrate (Bio-Rad Laboratories), and imaged via MYECL Imager (Thermo Scientific). Antibody details including working dilutions can be found below.

RNA extraction

Trizol (Life Technologies) was used for all RNA extractions according to the manufacturer's protocol. For RNA extraction from ribonucleoprotein immunoprecipitations (RIP),

GlycoBlue (Life Technologies) was added as a carrier during the precipitation step. RNA quality and quantity were determined via NanoDrop 1000 (ThermoFisher Scientific).

PCR

Reverse transcription was performed on 1 µg of total RNA in a 20 µl reaction with the iScript cDNA synthesis kit (Bio-Rad Laboratories,170–8891). Quantitative real-time PCR was performed using a Roche Lightcycler 96 with Fast Start Essential DNA Green (Roche Diagnostics Corporation, 06-924-204-001) and primers from Integrated DNA Technologies, Inc. Primer efficiency was verified to be over 95% for all primer sets used. Quantification of mRNA was carried out via ΔΔCT analysis using GAPDH mRNA and the respective control condition for normalization. All real-time PCR primer sets were designed so the products would span at least one intron (>1kb when possible) to prevent detection of the pre-mRNA and/or DNA, and amplification of a single product was confirmed by agarose gel visualization and/or melting curve analysis (See below for sequences).

FLAG immunoprecipitation of METTL16

Beads labeled with FLAG Antibody (Sigma) were washed and resuspended in NT2 buffer (50 mM Tris-HCl (pH 7.4), 150 mM NaCl, 1 mM MgCl2, 0.05% NP40) supplemented with 1 mM DTT, 100 units/ml RNase Out and 20mM EDTA. Cells were harvested in Polysome Lysis Buffer (PLB; (100 mM KCl, 5 mM MgCl2, 10 mM HEPES (pH 7.0), 0.5% NP40, 1 mM DTT, 100 units/ml RNase Out, with Protease inhibitor cocktail)) and equal amounts of lysate were added to each IP reaction and tumbled for 4 hours at 4˚C. After washing 5 times with NT2, beads were resuspended in Trizol for RNA or WCEB with protease inhibitors (PI) for protein. Relative and fold enrichment of RNA in the IP was determined as indicated in the results section.

Immunoprecipitation of endogenous METTL16

Cells were harvested in PLB. Beads labeled with METTL16 Antibody (Bethyl Laboratories) or normal rabbit serum (NRS) were washed and resuspended in NT2 supplemented with 1 mM DTT, 100 units/ml RNase Out and 20mM EDTA. Equal amounts of lysate were added to each IP and tumbled for 4 hours at 4˚C. After washing, beads were lysed in Trizol (RNA) or WCEB (protein). Relative and fold enrichment was determined as indicated in the results section.

Cell fractionation

For total extracts, 10% of the cells were lysed in WCEB with Pierce protease inhibitor cocktail (PI; Thermo Scientific). The remaining cells were resuspended in hypotonic buffer (10 mM NaCl, 10 mM Tris-HCl, pH 7.4, 1.5 mM MgCl2 with PI) and incubated on ice for 5 minutes before freezing at -80˚C. After thawing on ice, lysis was achieved by vortexing for 2–3 seconds and nuclei were pelleted at 1,000 xG for 5 minutes at 4˚C. The supernatant was removed and stored as cytoplasmic fraction. The pellet was then resuspended in the above buffer containing 1% NP40 and 0.5% sodium deoxycholate and centrifuging at 1,000 xG for 5 minutes at 4˚C. The supernatant after centrifugation was designated the soluble nuclear fraction. The remaining insoluble nuclear pellet was sonicated in WCEB with PI. Equal volumes of each fraction were subjected to western blotting as described above. MyImage Analysis (Thermo Scientific) was used to quantify the bands in the cytoplasmic, soluble nuclear and insoluble nuclear fractions. Data were expressed as a percentage of the total protein (summed from the three fractions) found in each fraction.

Immunohistochemistry

HEK293T cells with or without 6 days of siRNA treatment (as described above) were fixed in either ice cold 4% paraformaldehyde or 95% methanol/5% acetic acid for 15mins. Paraformaldehyde-treated cells were permeabilized with 0.1% Triton in PBS for 10 minutes. After washing with PBS, cells were blocked with 1% BSA in PBS at 4˚C for at least 1 hour. Primary

antibody incubation was performed for at least 16 hours in blocking buffer, followed by extensive washing in PBS. Secondary antibody incubation was performed for 1.5 hours in blocking buffer at room temperature in the dark, followed by extensive washing with PBS. Cells were then counterstained with DAPI before being imaged on an Olympus IX73 inverted compound microscope. Images were captured with Olympus cellSens software using default settings. Briefly, a random field of Neg siRNA treated cells were imaged for phase contrast, FITC, and DAPI and the exposure times for the FITC and DAPI stains were then used for subsequent images of the siRNA treated cells to allow for comparison between the two conditions. A secondary antibody-only control was also imaged with this same exposure. All individual images were converted to lossless JPEGs without any modifications from the original .vsi file. The "Combine Channels" option in the cellSens software was used to create the FITC/DAPI overlays. For clearer visualization and background reduction, the overlays were subjected to the "Optimize Contrast" option in the cellSens software.

Statistical analysis

All experiments were performed on at least three separate occasions to generate biological replicates unless otherwise indicated. For the immunoprecipitations, statistical significance was calculated by a two-tailed, paired Student's t-test comparing the METTL16 IP to the GFP or NRS IP. Outliers were identified utilizing the Grubb's test but only one outlier was ever removed for a given RNA target. For the real time analysis of the siRNA knockdown experiments, a one-way ANOVA with post-hoc Tukey HSD test was run for each RNA target comparing all six conditions. For all experiments, a P-value below 0.05 was defined as statistically significant, while a P-value less than 0.1 was considered reportable.

Table 2.1: Antibodies used in this study.

Antibody	Catalog #	Vendor	Dilution
β-2-Microglobulin	12851	Cell Signaling	1:1,000 (WB)
FLAG	MA1-91878	Thermo Fisher	1:1,000 (WB)
Lamin B	SC-6216	Santa Cruz	1:200 (WB)
LDH	SC-133123	Santa Cruz	1:1,000 (WB)
MAT2A	SC-166452	Santa Cruz	1:200 (WB)
Mettl16	A304-192A	Bethyl Labs	1:1,000 (WB)
Mettl16	HPA020352	Millipore Sigma	1:1000 (WB) 1:200 (ICC)
Mettl16	PA5-54185	Invitrogen	1:200 (ICC)
SP1	MA5-27783	Invitrogen	1:1000 (WB)
Ɣ-Tubulin	MA1-850	Thermo Fisher	1:1,000 (WB)

Table 2.2: PCR Primers used in this study.

Gene	Forward (5'-3')	Reverse (5'-3')
18s rRNA	CTGAGAAACGGCTACCACATC	GCCTCGAAAGAGTCCTGTATTG
28s rRNA	GGGTGGTAAACTCCATCTAAGG	GCCCTCTTGAACTCTCTCTTC
5s rRNA	CGTCTGATCTCGGAAGCTAAG	CCTACAGCACCCGGTATTC
β2M	AGATGTCTCGCTCCGTGGCCTTA	TGTCGGATGGATGAAACCCAGACA
GapDH	AAGGTCGGAGTCAACGGATTTGGT	AGCCTTGACGGTGCCATGGAATTT
HIF1α	CCGAATTGATGGGATATGAGCCAG	TTGGCAAGCATCCTGTACTGTCCT
MALAT1	GAATTGCGTCATTTAAAGCCTAGTT	GTTTCATCCTACCACTCCCAATTAAT
MAT2A	CTGCTGTTGACTACCAGAAAGT	GCTACCAGCACGTTACAAGT
METTL3	AGCCTTCTGAACCAACAGTCC	CCGACCTCGAGAGCGAAAT
METTL16	GGCAGAAGGAGGTGAATTAGAG	TTCCCAGCATGCAGCTATAC
Myc	TCCTCGGATTCTCTGCTCTCCT	AGAAGGTGATCCAGACTCTGACCT
NT5DC2	GATGAGAAGGGCTCACTTCAG	CCATTCCGTCAAGCGTAAGA
RBM3	TTCATCACCTTCACCAACCC	ATCTGACGACCATCCAGAGA
STUB1	GGCCAAGCACGACAAGTA	GATCTTGCCACACAGGTAGTC
U1	CCATGATCACGAAGGTGGTTT	ATGCAGTCGAGTTTCCCACAT
U2	TTCTCGGCCTTTTGGCTAAG	CTCCCTGCTCCAAAAATCCA
U4	GCCAATGAGGTTTATCCGAGG	TCAAAAATTGCCAATGCCG
U6	CTCGCTTCGGCAGCACA	AACGCTTCACGAATTTGCGT

Chapter 3:

RNA Methyltransferase METTL16's Protein Domains Have Differential Functional Effects on Cell Processes

The majority of the work presented in this chapter is anticipated to be published as "RNA Methyltransferase METTL16's Protein Domains Have Differential Functional Effects on Cell Processes"

Emily R. Satterwhite[1], Kristen Carraway[1], Ashley Wooten[2], Tonya Zeczycki[1,2], Kyle D. Mansfield[1]

[1]Biochemistry and Molecular Biology Department, Brody School of Medicine, East Carolina University, Greenville NC, 27834

[2]Mass Spectrometry Core Facility, Brody School of Medicine, East Carolina University, Greenville NC, 27834

Abstract

METTL16, a human m6A RNA methyltransferase, is currently known for its modification of U6 and MAT2A RNAs. Several studies have identified additional RNAs to which METTL16 binds, however whether METTL16 modifies these RNAs is still in question. Moreover, a recent study determined that METTL16 contains more than one RNA binding domain, leaving the importance of each individual RNA binding domain unknown. Here we examined the effects of mutating the METTL16 protein in certain domains on overall cell processes. We chose to mutate the N-terminal RNA binding domain, the methyltransferase domain, and the C-terminal RNA binding domain. With these mutants, we identified changes in RNA binding ability, protein and RNA expression, and cell cycle phase occupancy. From the resulting changes in RNA and protein expression, we saw changes in cell cycle, metabolism, intracellular transport, and RNA processing pathways, which varied between the METTL16 mutant lines. We also saw significant effects on the G1 and S phase occupancy times with some but not all the mutants. We have therefore concluded that while METTL16 may or may not m6A-modify all RNAs it binds, it's binding (or lack of) has a significant outcome in a variety of cell processes.

Introduction

Modification of adenosine to methyl-6-adenosine (m6A) in RNA has been extensively studied in multiple species of prokaryotes, eukaryotes, and viruses for several decades[22,159–161]. This modification, which has been shown in mRNA, lncRNA, rRNA, miRNA, snRNA, snoRNA, and tRNA, has been proven to affect the half-life[24,25,162], translation efficiency[2,26,52,92,125,163,164], splicing[124,165,166], storage[167], or (in the case of miRNA) maturation of the RNA[168,169]. These effects are brought about either by interactions with m6A RNA binding proteins or by fine-tuning the thermodynamics of the RNA structure[23,113,137]. Furthermore, m6A modification is one of the most common modifications in cellular RNA and currently considered the most common modification in mRNA [22].

The m6A modification is produced by m6A RNA methyltransferases, colloquially termed "m6A writers". These m6A writers catalyze the transfer of a methyl group from a S-adenosylmethionine molecule to the target adenosine's 6th base position [170]. There are more than 60 known RNA methyltransferases in humans, however most of these have been shown to modify tRNAs and rRNAs [171]. Currently, there are two established human m6A RNA methyltransferases shown to modify mRNA, which are the METTL3/14 complex and METTL16. METTL3/14 is the more studied of the two and is known to modify many mRNAs [162,168,172–175]. RNA substrates for this m6A writer complex need to be in a single-stranded conformation and contain a "DR<u>A</u>CH" consensus sequence (D=A/U/G, R= A/G, H=A/U/C; underlined A is the modified adenosine) [22,42,51,176,177]. Of the few RNAs that have been observed in complex with METTL16, they have all shown a double-stranded conformation and contain a "UAC<u>A</u>GAGAA" consensus sequence (underlined A is the modified adenosine) [56,58]. RNAs modified by the METTL3/14 complex have a wide variety of functions, therefore it is unsurprising that dysregulation of this complex is

frequently observed in multiple diseases including several cancers [52,178–184]. While METTL16 is the lesser studied, its dysregulation has been observed in several cancers as well [185–188].

Proteins known as "m6A readers" have a high affinity for binding RNAs that are m6A modified. After binding to m6A RNAs, these proteins are directly or indirectly responsible for the effects of m6A modification mentioned previously (such as splicing). Currently known m6A readers include YTHDF1/2/3[26,138,139], YTHDC1/2[81,189–191], HNRNPA2B1[140,192], HNRNPC[137], HNRNPG[193], IGF2BP1/2/3[167], and others. The m6A modification can be removed from the RNA by m6A demethylase also known as "m6A erasers", which include ALKBH5[194] and FTO[195,196]. These enzymes transfer the methyl group from the RNA to a 2-oxoglutarate molecule. The balance between adding and removing this modification from cell RNAs is a complex and delicate system that can become upset by dysregulation of any of the enzymes mentioned in this pathway.

As an m6A RNA methyltransferase, METTL16 has gained attention as a potential therapeutic for several diseases associated with cellular m6A dysregulation. It has been shown by several groups to methylate MAT2A mRNA, and U6 snRNA and bind to MALAT1 lncRNA [53,54,56,58,59,81]. Global effects on cellular m6A levels with knockdown or knock out of METTL16 have also been reported [56,186]. Moreover, widespread RNA expression changes have been seen in response to changes in METTL16 protein levels[56]. Despite a number of studies, there unfortunately seems to be little overlap between the m6A and RNA expression datasets. This could be due to different cell types being used, availability of SAM for modification to occur (which is produced by MAT2 enzyme), or a difference in the extent and/or duration of METTL16 knockdown. Furthermore, METTL16 has been implicated in a large number of cancer studies with both oncogenic and tumor-suppressive effects associated with changes in METTL16 expression levels [103,104,106,108,109,185–188,197–204]. For example, the database OncoMX demonstrates that METTL16

RNA has shown significant upregulation in kidney and colorectal cancers, but significant downregulation in uterine, bladder, prostate, breast, and lung cancers[205].

Because METTL16 studies have shown a wide variety of effects due to knockdown, knockout, mutation, or overexpression, we decided to further study the functional effects of individual domains of METTL16 to determine their specific duties. We chose to mutate the N-terminal RNA binding domain, the methyltransferase domain, or the VCR domain using previously published mutations. We then stably expressed the mutated METTL16 in HEK293 cells. The endogenous METTL16 was then removed from these same cells so that the only the mutated version of METTL16 remained. These cells lines were established, confirmed, and analyzed for changes in RNA binding abilities of METTL16, global RNA expression, protein expression, and cell cycle effects.

Results

To observe the responsibilities of each METTL16 protein domain, we created transgenic HEK293 cell lines expressing a METTL16 protein mutated in one of the domains (Figure 3.1A). The mutations included an N-terminal RNA binding domain mutant (described previously by Mendel et al 2018), a methylation mutant (PP185/186AA, described previously by Pendleton et al 2017), a C-terminal RNA binding mutant (in which the VCR linker region was deleted), and a wild-type control. The sequence also contained a silent mutation rendering it resistant to a CRISPR-Cas9 gRNA sequence to be used later, and a Myc-FLAG tag at the C-terminus. These mutations were introduced via site-directed mutagenesis and confirmed with Sanger sequencing. Clonal lines of these cells were produced with antibiotic selection and then colony selection. RNA

Figure 3.1A

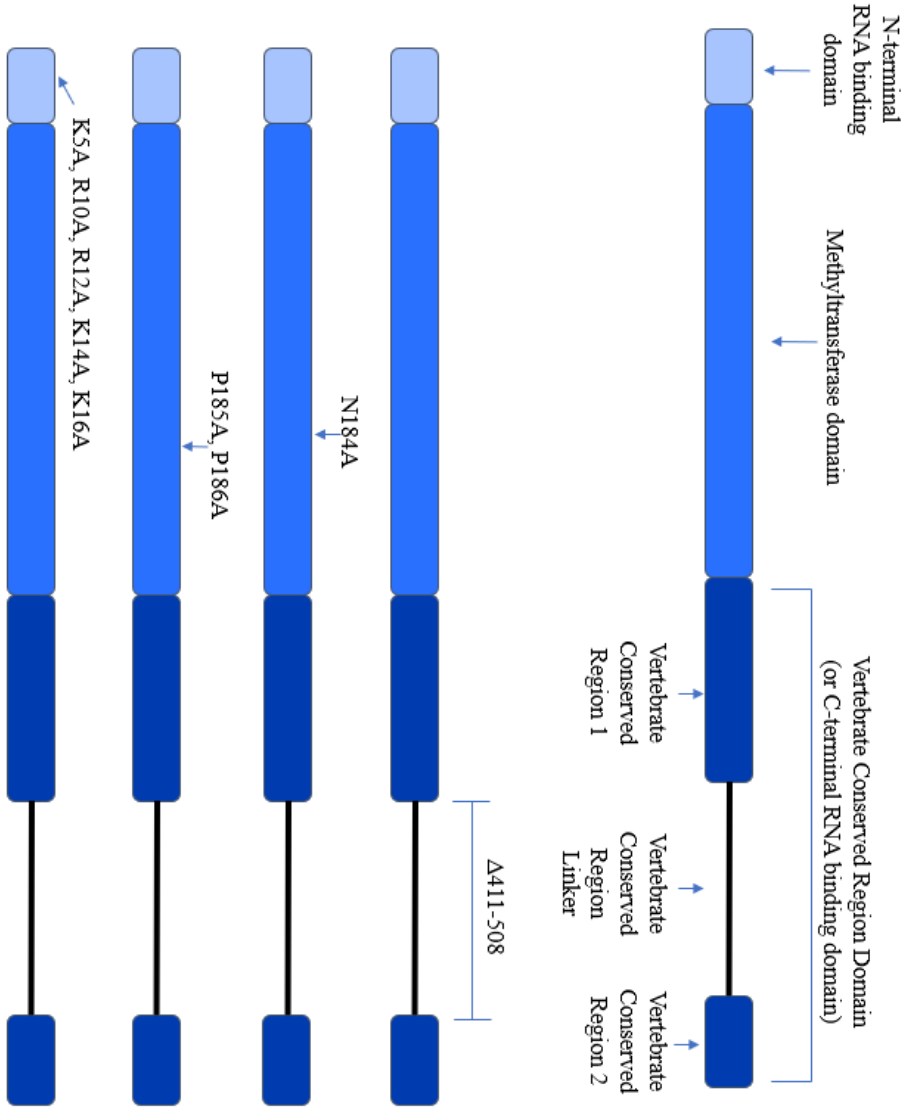
N-terminal RNA binding domain
Methyltransferase domain
Vertebrate Conserved Region Domain (or C-terminal RNA binding domain)
Vertebrate Conserved Region 1
Vertebrate Conserved Region Linker
Vertebrate Conserved Region 2
METTL16 Protein Diagram
Δ411-508
METTL16 C-terminal RNA binding mutant (Δ Linker)
N184A
METTL16 N-terminal RNA binding mutant (N-term)
P185A, P186A
METTL16 Methylation mutant PP185/186AA (PP185/186AA)
K5A, R10A, R12A, K14A, K16A
METTL16 Methylation mutant N184A (N184A)

Figure 3.1B

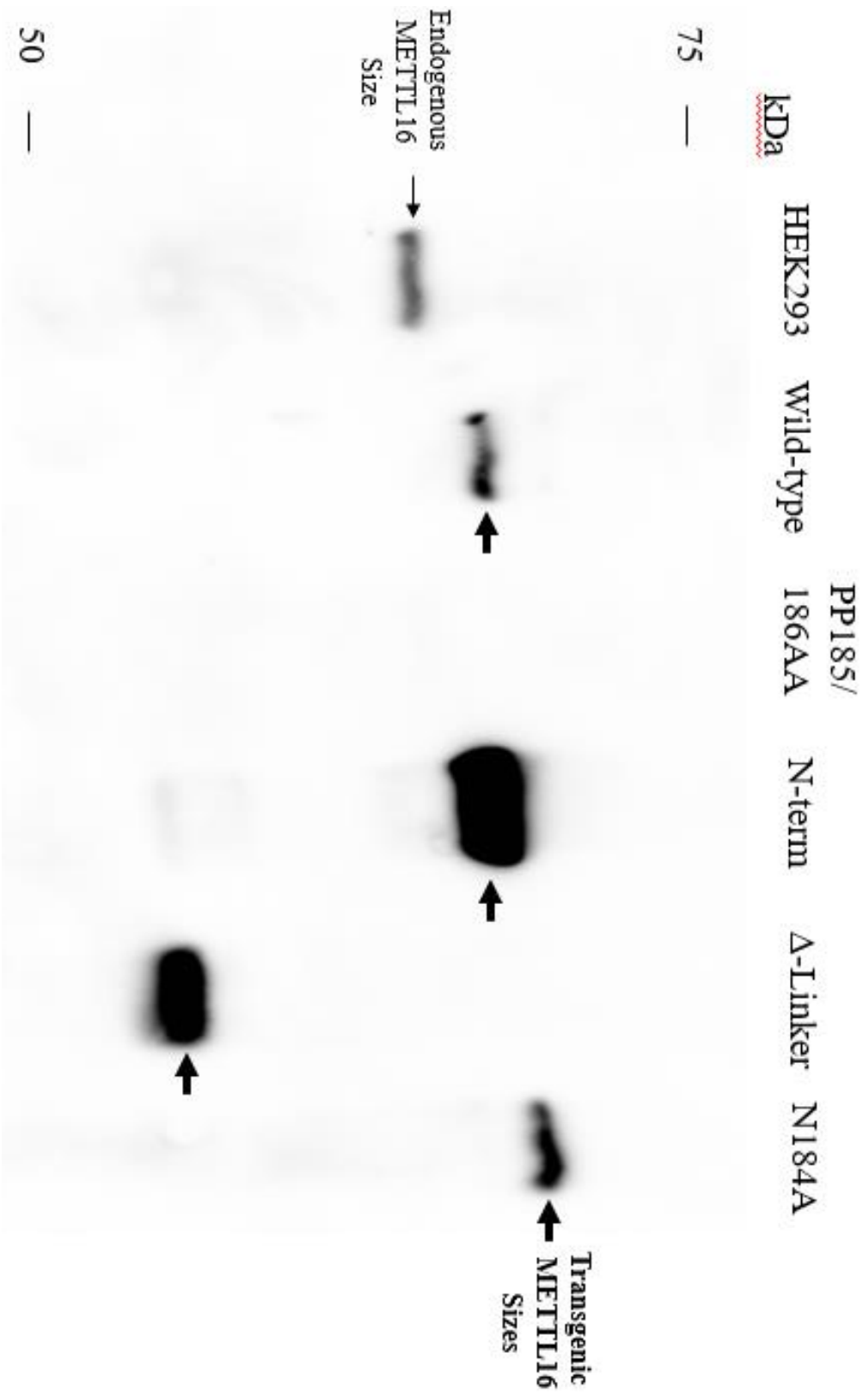
kDa
HEK293
Wild-type
PP185/
186AA
N-term
Δ-Linker
N184A
75
50
Endogenous
METTL16
Size
Transgenic
METTL16
Sizes

Figure 3.1C

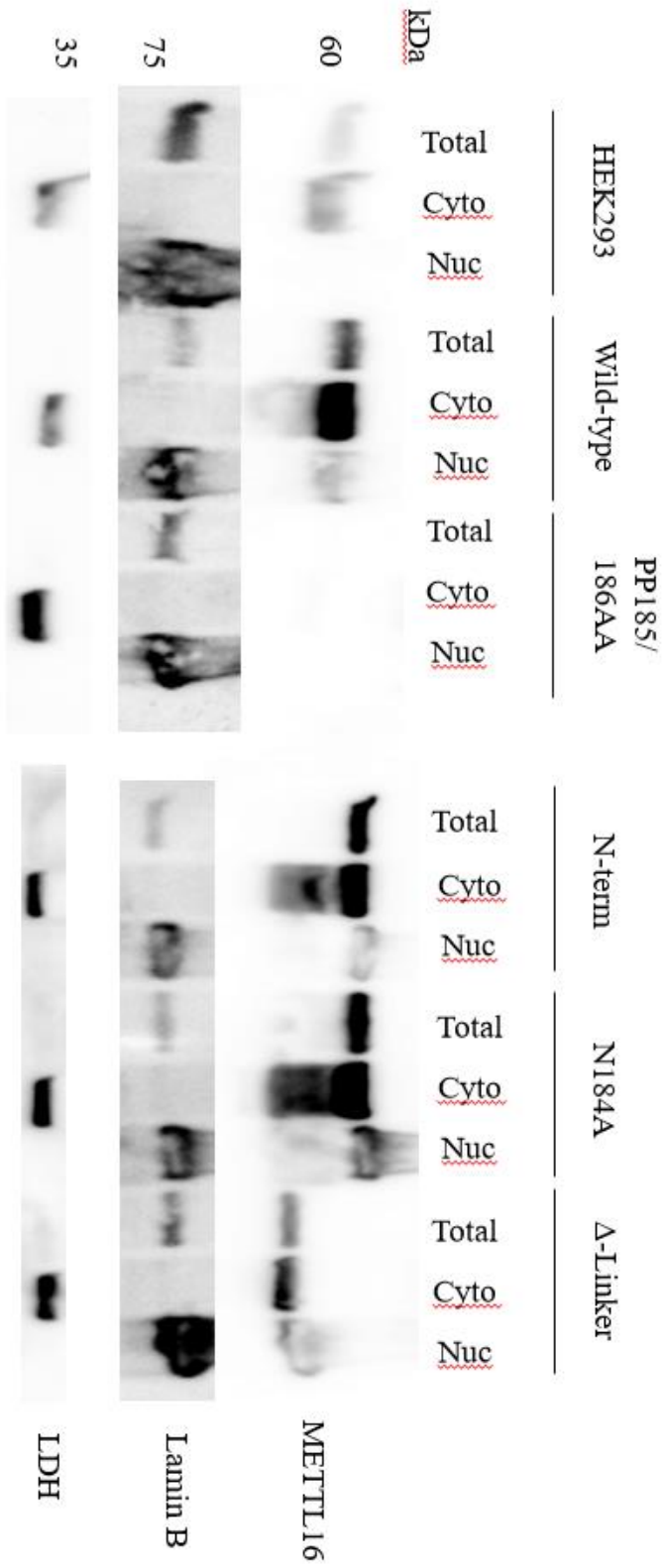
kDa
60
75
35
METTL16
Lamin B
LDH
HEK293
Wild-type
PP185/
186AA
N-term
N184A
Δ-Linker
Total
Cyto
Nuc

Figure 3.1D

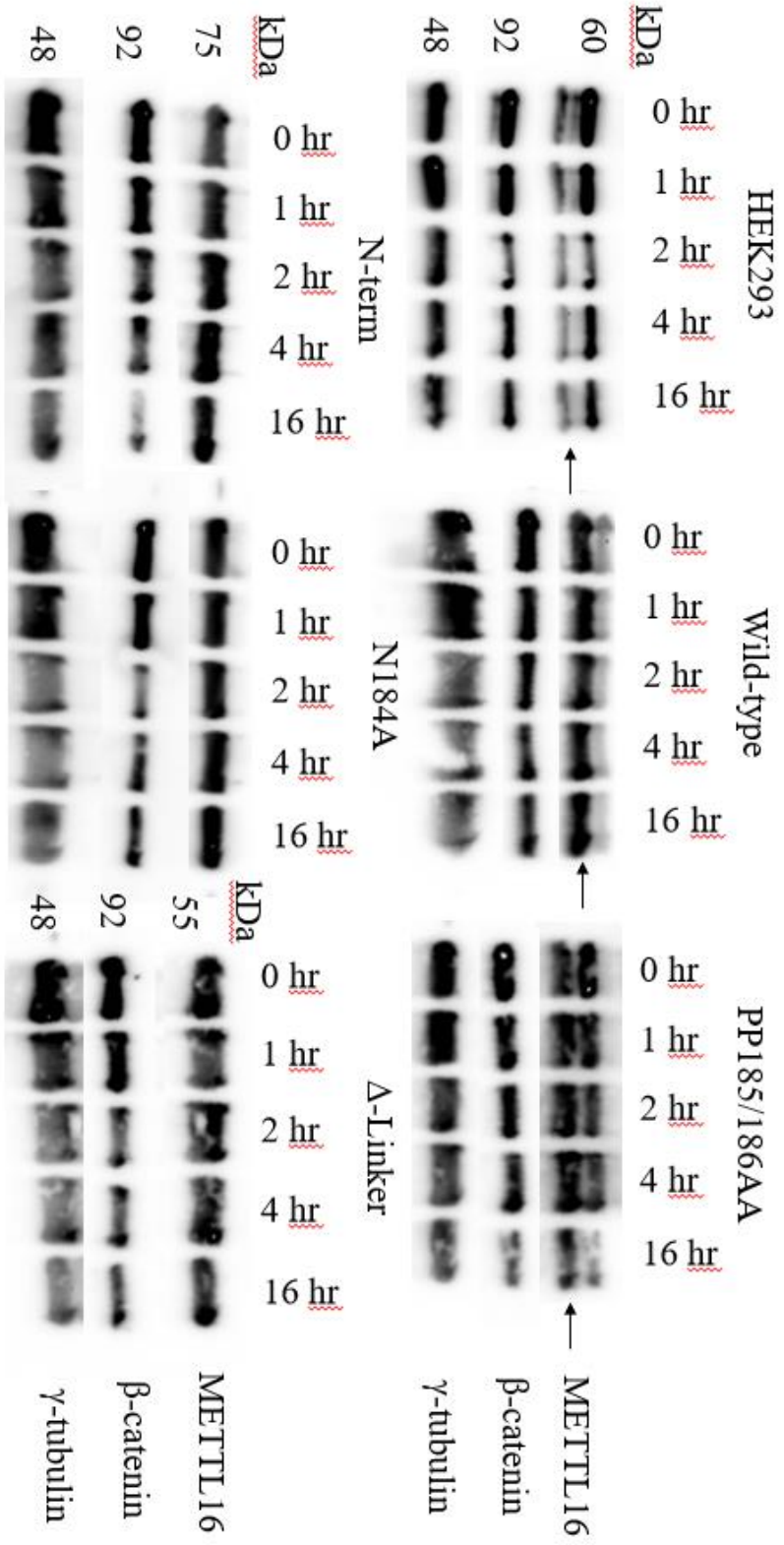
HEK293
Wild-type
PP185/186AA
N-term
N184A
Δ-Linker
kDa
60
92
48
75
55
0 hr
1 hr
2 hr
4 hr
16 hr
METTL16
β-catenin
γ-tubulin

Figure 3.1: Human METTL16 mutants used in this study. (A) Protein diagrams of each METTL16 mutant produced for this study. Sizes of each domain are approximate to actual size. (B) Western blot of HEK293 transgenic METTL16 mutant cell lines with endogenous METTL16 removed via CRISPR-Cas9 using METTL16 antibody. Large separation polyacrylamide gel shows the difference in molecular weight between endogenous and transgenic mutant METTL16 proteins. Mutant PP185/186AA cell line shows no expression of METTL16. (C) Cellular localization of METTL16 in HEK293 and HEK293 transgenic METTL16 mutant cell lines via Western blot after removal of endogenous METTL16 via CRISPR-Cas9. PP185/186AA METTL16 mutant CRISPR clonal line shows no detectable METTL16 protein. Lactate Dehydrogenase (LDH) was used to confirm cytoplasmic content, Lamin B was used to confirm nuclear content. (D) Western blots of HEK293 and each HEK293 METTL16 mutant CRISPR clonal line used in this study subjected to 0, 1, 2, 4, or 16 hours of cycloheximide to determine half-life of endogenous and transgenic mutant METTL16.

binding ability of the mutated METTL16 protein was confirmed with FLAG immunoprecipitation (data not shown). As expected, the N-terminal RNA binding mutant showed very little binding ability, however the methylation mutant (PP185/186AA) also showed stunted RNA binding. We continued with this mutant but also produced a 2nd methylation mutant (N184A, previously described by Doxtader et al 2018) which showed comparable RNA binding ability to the wild-type protein. Interestingly, deletion of the VCR linker region in our C-terminal RNA binding domain mutant resulted in increased RNA binding ability over the wild-type.

After confirming the expression and RNA binding ability of these mutants, we introduced a METTL16 CRISPR-Cas9 construct targeting exon 2, selected for expression via puromycin, and generated clonal lines. Clones were screened for removal of endogenous METTL16 but continued expression of the exogenous METTL16. Due to the Myc-FLAG tag on the exogenous METTL16, separation of the two METTL16 species was achieved with a long gel electrophoresis run and subsequent Western blotting (Figure 3.1B). The Western blot confirms there is no detectable endogenous METTL16 protein expression in any of our METTL16 transgenic cell lines. Of note, during the continued culturing of these mutant cell lines, we noticed the first methylation mutant (PP185/186AA) line eventually lost all detectable METTL16 expression. As mentioned previously, we continued to include this cell line in our experiments, however we interpreted the results of this cell line as if it was a METTL16 null line.

Once exogenous METTL16 expression was verified, we again tested the RNA binding ability of the mutants to ensure CRISPR-Cas9 exposure did not alter the intended METTL16 mutation. For this we used METTL16 immunoprecipitation in comparison to the wild-type exogenous METTL16 line as well as the starting HEK293 line (data not shown). Methylation

ability was shown to be ablated in the PP185/186AA, N184A, and N-terminal RNA binding METTL16 mutants previously[56,59,60] and was not further investigated here.

Previously we had shown that endogenous and exogenous wild-type METTL16 was predominantly cytoplasmic in a number of cell lines [55]. To determine the effect of METTL16 mutation on cellular localization we used biochemical fractionation Western blots. Antibodies for nuclear lamina protein Lamin B and cytoplasmic protein lactate dehydrogenase were used to confirm fractions of cells were pure. As shown in Figure 3.1C, all mutated METTL16 proteins had similar localization as the endogenous METTL16, with most located in the cytoplasm. Thus, it appears that mutating METTL16 in these ways does not affect its cellular distribution. Lastly, we investigated the half-life of the exogenous METTL16 proteins using cycloheximide to block translation (Figure 3.1D). Again, we determined the half-life of the METTL16 protein in these clones closely mimicked the half-life of the HEK293 endogenous METTL16, which was shown to be more than 16 hours. Therefore, we have shown METTL16 to be a long-lived nuclear and cytoplasmic protein, and that these characteristics are not substantially changed when either the methylation or RNA binding activity of the protein is altered.

Given the recent correlations cited between METTL16 expression and cancer progression, we performed an EdU assay with these clonal lines to investigate changes in cell cycle (Figure 3.2). Using this method, we are able to quantify the number of cells in the G1, S, or G2/M phase of the cell cycle (Figure 3.2A). To quantify the effect, the percentage of HEK293 cells in each cell cycle phase was normalized to 1 and then the relative change in each. METTL16 transgenic cell line could be calculated (Figure 3.2B). We found no significant difference in G1, S, or G2 phase occupancy times between the starting HEK293 cell line and the transgenic wild-type METTL16 cell line. However, we determined the cell lines with no detectable METTL16 and the

Figure 3.2

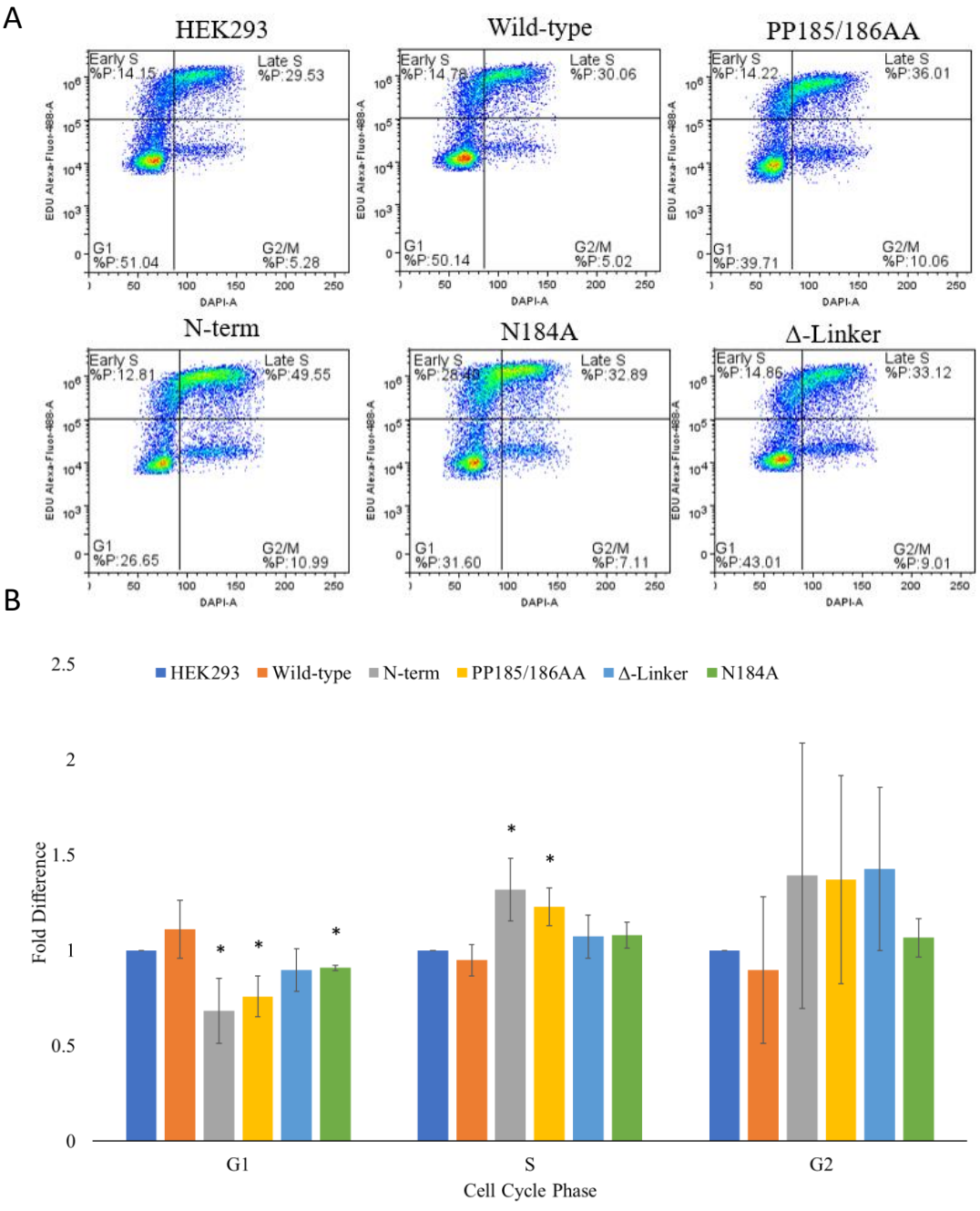
A
HEK293
Early S %P:14.15
Late S %P:29.53
G1 %P:51.04
G2/M %P:5.28
Wild-type
Early S %P:14.78
Late S %P:30.06
G1 %P:50.14
G2/M %P:5.02
PP185/186AA
Early S %P:14.22
Late S %P:36.01
G1 %P:39.71
G2/M %P:10.06
N-term
Early S %P:12.81
Late S %P:49.55
G1 %P:26.65
G2/M %P:10.99
N184A
Early S %P:28.49
Late S %P:32.89
G1 %P:31.60
G2/M %P:7.11
Δ-Linker
Early S %P:14.86
Late S %P:33.12
G1 %P:43.01
G2/M %P:9.01
EDU Alexa-Fluor-488-A
DAPI-A
B
HEK293
Wild-type
N-term
PP185/186AA
Δ-Linker
N184A
Fold Difference
Cell Cycle Phase
G1
S
G2

Figure 3.2: EdU Assays with HEK293 and HEK293 METTL16 mutant CRISPR clonal cell lines used in this study. “Wild-type” is the non-mutated exogenous METTL16 line, “PP185/186AA” is the PP185/186 methylation mutant exogenous METTL16 line, “N-term” is the N-terminal RNA binding mutant exogenous METTL16, “Δ-Linker” is the C-terminal RNA binding mutant exogenous METTL16 line, and “N184A” is the N184A methylation mutant exogenous METTL16 line. (A) Representative flow cytometry plots from each cell line. (B) Analysis of EdU assay results from each cell line. Percentage of HEK293 cells in each phase shown was normalized to 1. Percentage of M16 mutant CRISPR clonal cells were normalized to HEK293. P-value <0.05 indicated with *. Representative of 3-7 experiments.

N-terminal RNA binding mutant METTL16 had a higher occupancy time in the G1 phase and less occupancy time in the S phase compared to the starting cell line as seen in Figure 3.2B. This indicates these two cell lines are proliferating slower than the starting cell line and the wild-type transgenic control. The C-terminal and N184A mutant transgenic lines showed no significant difference in cell cycle phase occupancy. Given that the G2 phase is shorter than G1 and S, and that the assay detects DNA content, we were unable to determine any significant differences during that cell cycle phase using this method.

To further investigate METTL16 mutation-driven changes, RNA sequencing and proteomics analysis was performed. For RNA sequencing, polyA RNA was extracted from the clones and sequenced as unamplified, barcoded cDNA using the Oxford Nanopore MinION Sequencer. Interestingly, mutating the various domains of METTL16 only resulted in significant changes to about 50-400 transcripts compared to the transgenic wild-type cell line (Figure 3.3A). In addition, while some of the gene expression changes were shared amongst the mutants, the majority were unique to a given mutant line (Figure 3.3B). Gene set enrichment analysis also identified unique subsets of genes that were altered by each mutation (Figure 3.3C). As might be expected, the null line (PP185/186AA) showed the greatest effect of all four mutant lines with almost 400 genes altered (Figure 3.3A). The major pathways altered in the null mutant were involved in protein localization, catabolic processes, organelle organization, and mitotic cell cycle (Figure 3.3C) Surprisingly, the methylation mutant (N184A) showed the smallest effect with only 44 genes altered and no significant GO pathways identified. This suggests that METTL16's methylation activity may only be small part of its overall cellular activity. The two RNA binding mutants both had a moderate effect on gene expression but affected vastly different pathways (Figure 3.3C) suggesting that each domain plays a distinct role in METTL16's activity. Expression

Figure 3.3A and 3.3B

A

	N-term (44)	Delta-Linker (186)	PP185/186AA (398)
N184A (145)	16	50	16
N-term (44)		23	5
Delta-Linker (186)			18

B

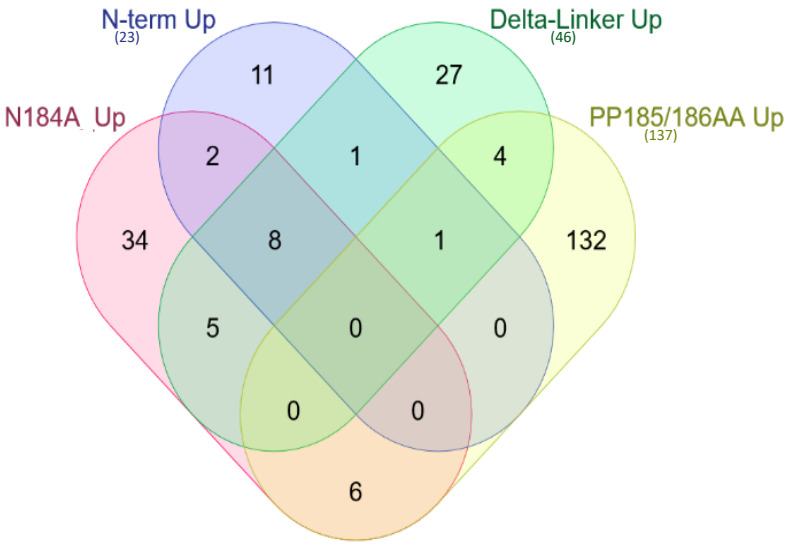

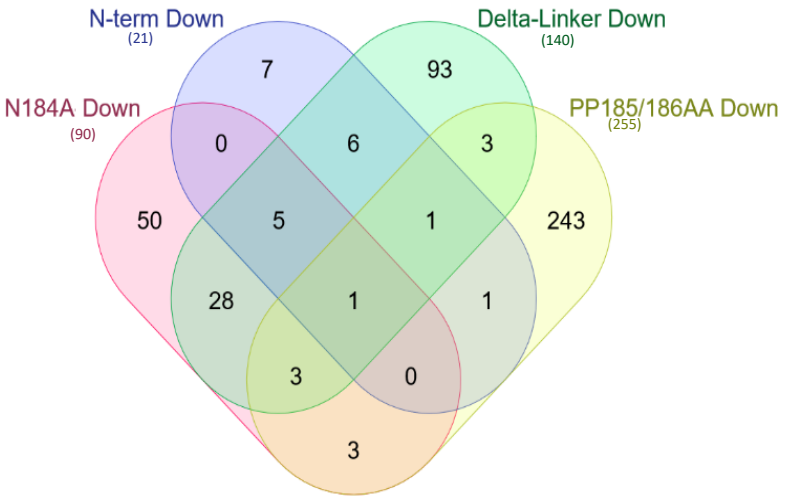

Figure 3.3C

PP185/186AA

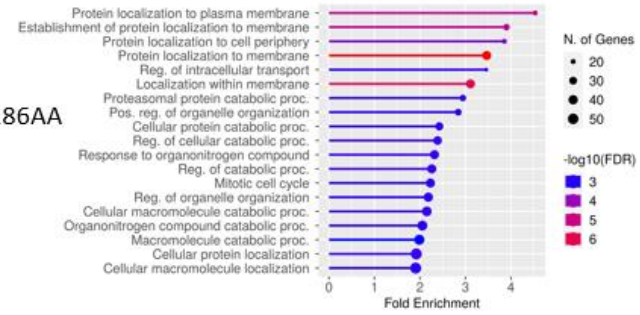

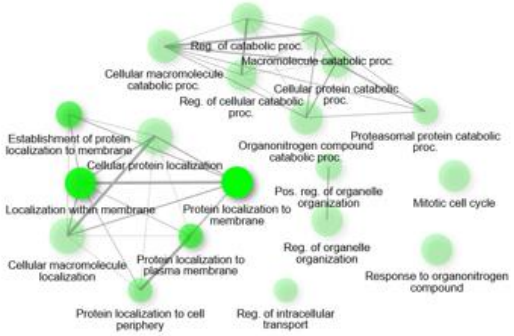

N184A

No Significant Pathways

No Significant Pathways

N-term

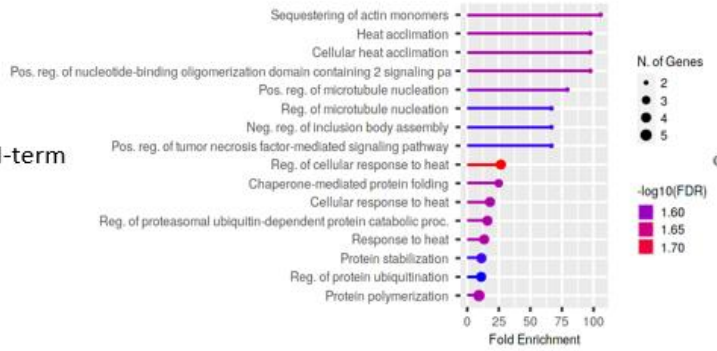

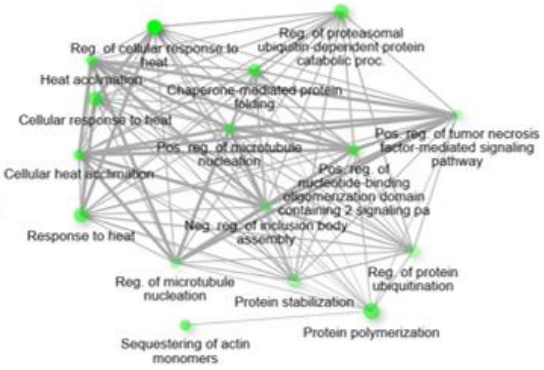

Δ-Linker

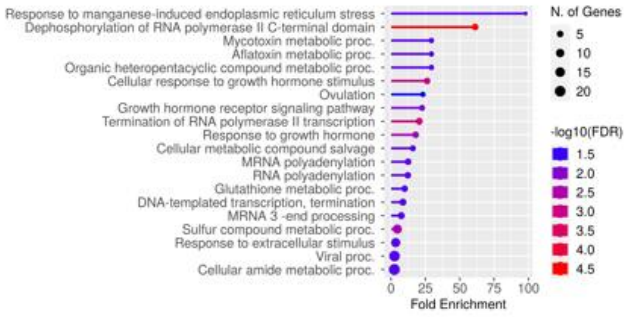

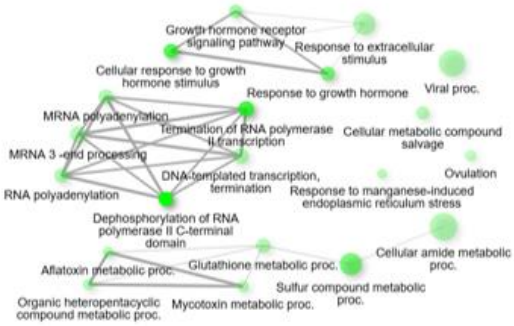

Figure 3.3: RNA sequencing results of METTL16 transgenic cell lines produced in this study. (A) Overlap of all genes significantly different from WT METTL16 line. (B) Overlap of genes significantly increased (left) or decreased (right) as compared to WT METTL16 line. Numbers in (parenthesis) are total number of significant genes in each mutant. (C) Gene set enrichment analysis of the genes significantly different from the WT METTL16 line. Left: Enrichment charts of the significant gene sets ranked by fold enrichment. Right: Network maps of significantly altered pathways. All analysis was performed with ShinyGo 0.76.2 (http://bioinformatics.sdstate.edu/go/).

changes of a select group of mRNAs were confirmed via real-time PCR with results normalized to the wild-type METTL16 transgenic line (Figure 3.4A). The N-terminal and C-terminal RNA binding METTL16 mutant lines generally show the same trend of expression change in those RNAs affected. We did not see RNA expression change in U1 snRNA (our negative control), MAT2A mRNA, or U6 snRNA. There were several RNAs whose expression significantly changed in all 4 METTL16 transgenic lines, but the expression varied among the different lines suggesting differing effects of the various mutants.

To determine whether the mRNA expression changes could be linked to direct interaction with METTL16, we performed FLAG immunoprecipitations followed by real-time PCR normalized to the wild-type METTL16 transgenic line. As the best characterized METTL16 targets, MAT2A mRNA and U6 snRNA were significantly bound by the wild-type transgenic METTL16 as expected (Figure 3.4B), Mutation of the N-terminal RNA binding domain decreased binding to MAT2A mRNA significantly, as did the N184A methylation mutant (Figure 3.4). Intriguingly, the C-terminal RNA binding mutant bound MAT2A mRNA better than the wild-type METTL16. This binding trend seen with MAT2A was also observed amongst most of the probed RNAs shown in Figure 3.4, in which the N-terminal RNA binding METTL16 mutant bound less of the RNA, the N184A methylation METTL16 mutant showed similar binding, and the C-terminal RNA binding METTL16 mutant showed higher binding. In fact, the C-terminal RNA binding METTL16 mutant showed significantly higher binding in most of the RNAs probed. Despite differences in binding to the mRNAs tested, all transgenic lines' METTL16 bound the U6 snRNA in similar amounts (Figure 3.4).

To assess global changes in whole cell protein expression, liquid chromatography tandem mass spectrometry was used. Overall, we identified 200-300 statistically significant altered

Figure 3.4A

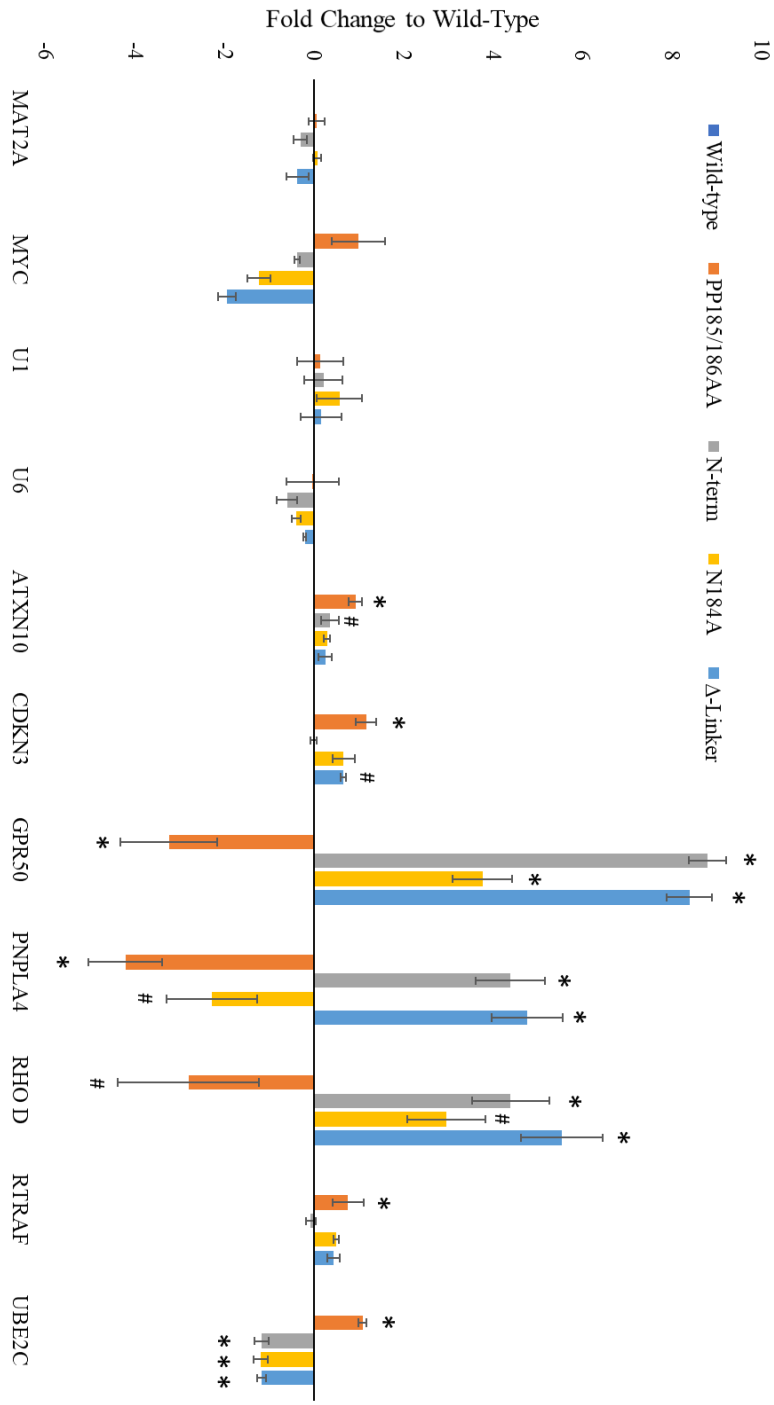
Fold Change to Wild-Type
-6
-4
-2
0
2
4
6
8
10
Wild-type
PP185/186AA
N-term
N184A
Δ-Linker
MAT2A
MYC
U1
U6
ATXN10
CDKN3
GPR50
PNPLA4
RHO D
RTRAF
UBE2C

Figure 3.4B

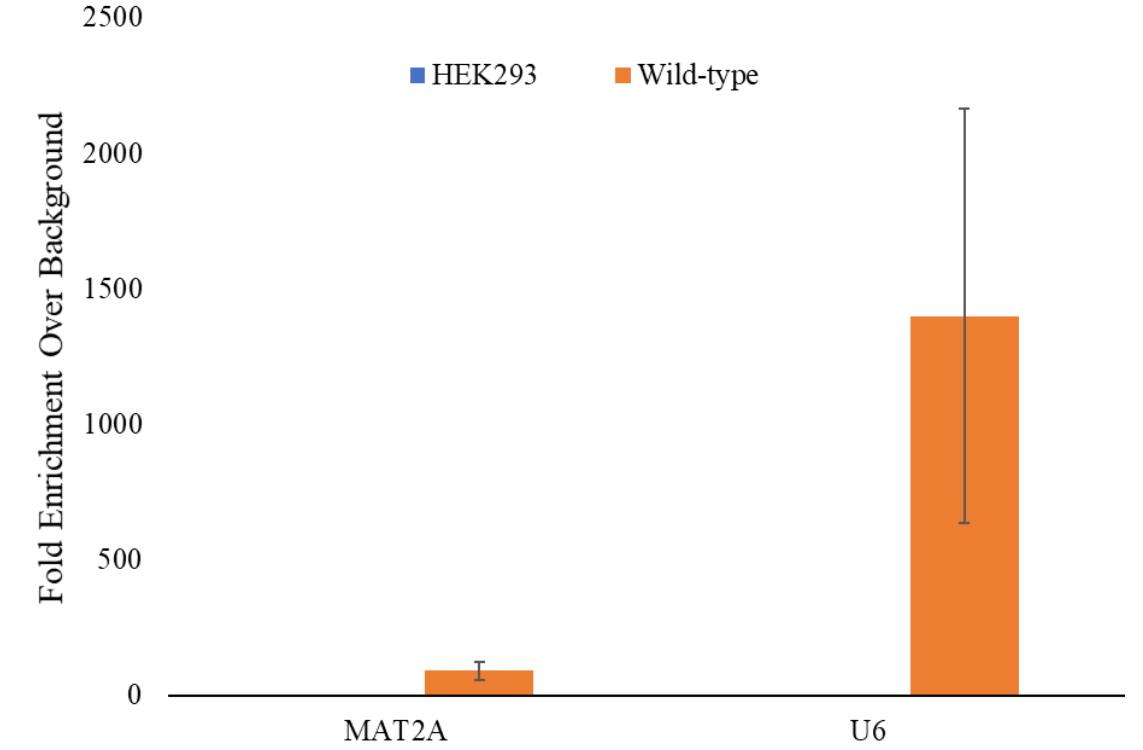
2500
2000
1500
1000
500
0
Fold Enrichment Over Background
HEK293
Wild-type
MAT2A
U6

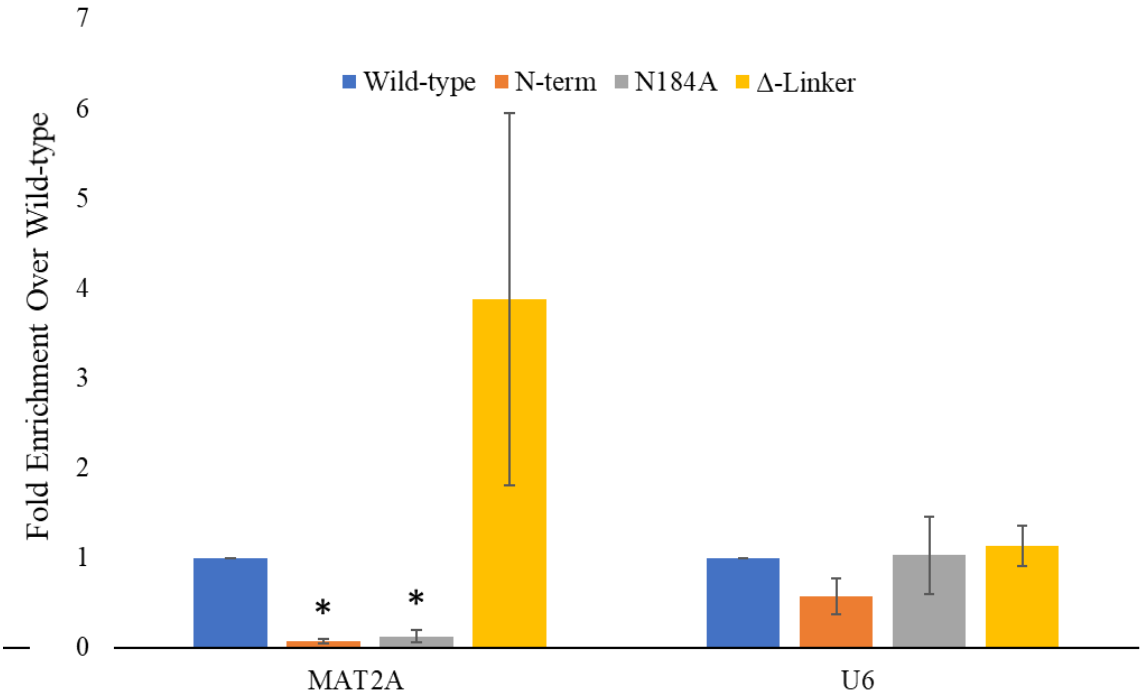
7
6
5
4
3
2
1
0
Fold Enrichment Over Wild-type
Wild-type
N-term
N184A
Δ-Linker
*
*
MAT2A
U6

Figure 3.4C

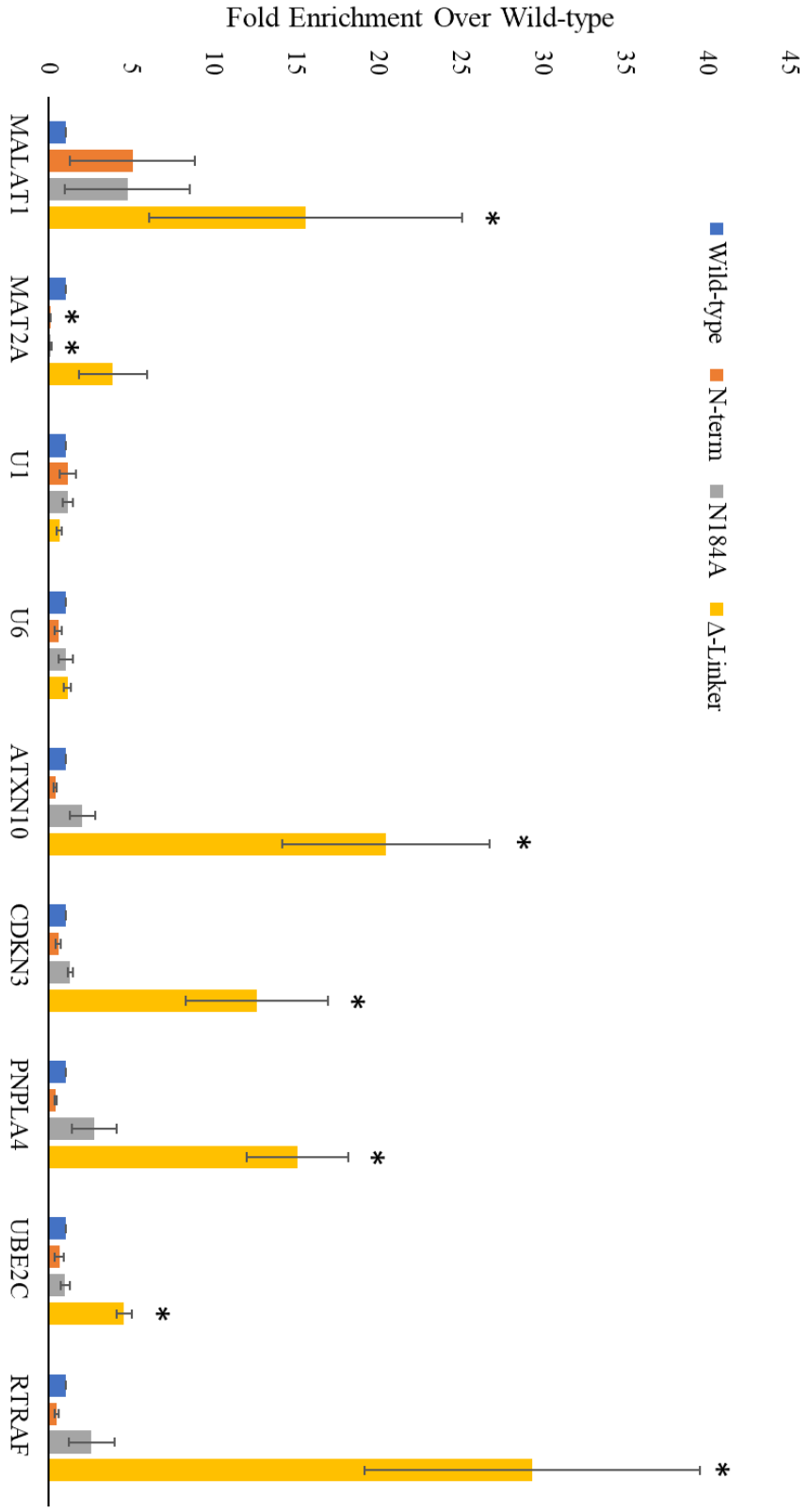
Fold Enrichment Over Wild-type
0
5
10
15
20
25
30
35
40
45
MALAT1
MAT2A
U1
U6
ATXN10
CDKN3
PNPLA4
UBE2C
RTRAF
Wild-type
N-term
N184A
Δ-Linker

Figure 3.4: (A) RNA expression results from HEK293 METTL16 mutant CRISPR clonal lines. RNA expression from real-time PCR analysis of each cell line with all normalized to wild-type transgenic METTL16 line. Representative of 3-4 experiments, error bars display SEM, # indicates $p<0.1$, * indicates $p<0.05$. (B, C) FLAG RNA immunoprecipitation results from each METTL16 mutant CRISPR clonal line used in this study. "Wild-type" is the non-mutated exogenous METTL16 line, "PP185/186AA" is the PP185/186 methylation mutant exogenous METTL16 line, "N-term" is the N-terminal RNA binding mutant exogenous METTL16, "Δ-Linker" is the C-terminal RNA binding mutant exogenous METTL16 line, and "N184A" is the N184A methylation mutant exogenous METTL16 line. Representative of 3 experiments, error bars display SEM, * indicates $p<0.05$.

proteins compared to the wild-type exogenous METTL16 clone, depending on the mutant (Figure 3.5). Volcano plots of all proteins identified with high confidence are displayed in Figure 3.5A, with significant differences in expression between the two cell lines compared located above the dotted horizontal line. As with other experiments in this study, we compared the proteins identified in HEK293 cells against those identified in the wild-type METTL16 transgenic cell line, and the mutant METTL16 transgenic line identified proteins were compared to the wild-type METTL16 transgenic line proteins. With these results, we have listed the top 20 proteins that increased and the top 20 proteins that decreased in expression in Figure 3.5B. We also put all proteins identified with high confidence into Reactome[206] to determine the top ten protein pathways affected by each mutation (Figure 3.5C). Again, similar to the RNA expression changes, about 50% of the significant protein changes seen in each mutant cell line were unique to that cell line with varying amounts of overlap with the others (Figure 3.3C and Figure 3.5), suggesting differing effects of the mutants on METTL16's cellular function.

Figure 3.5A

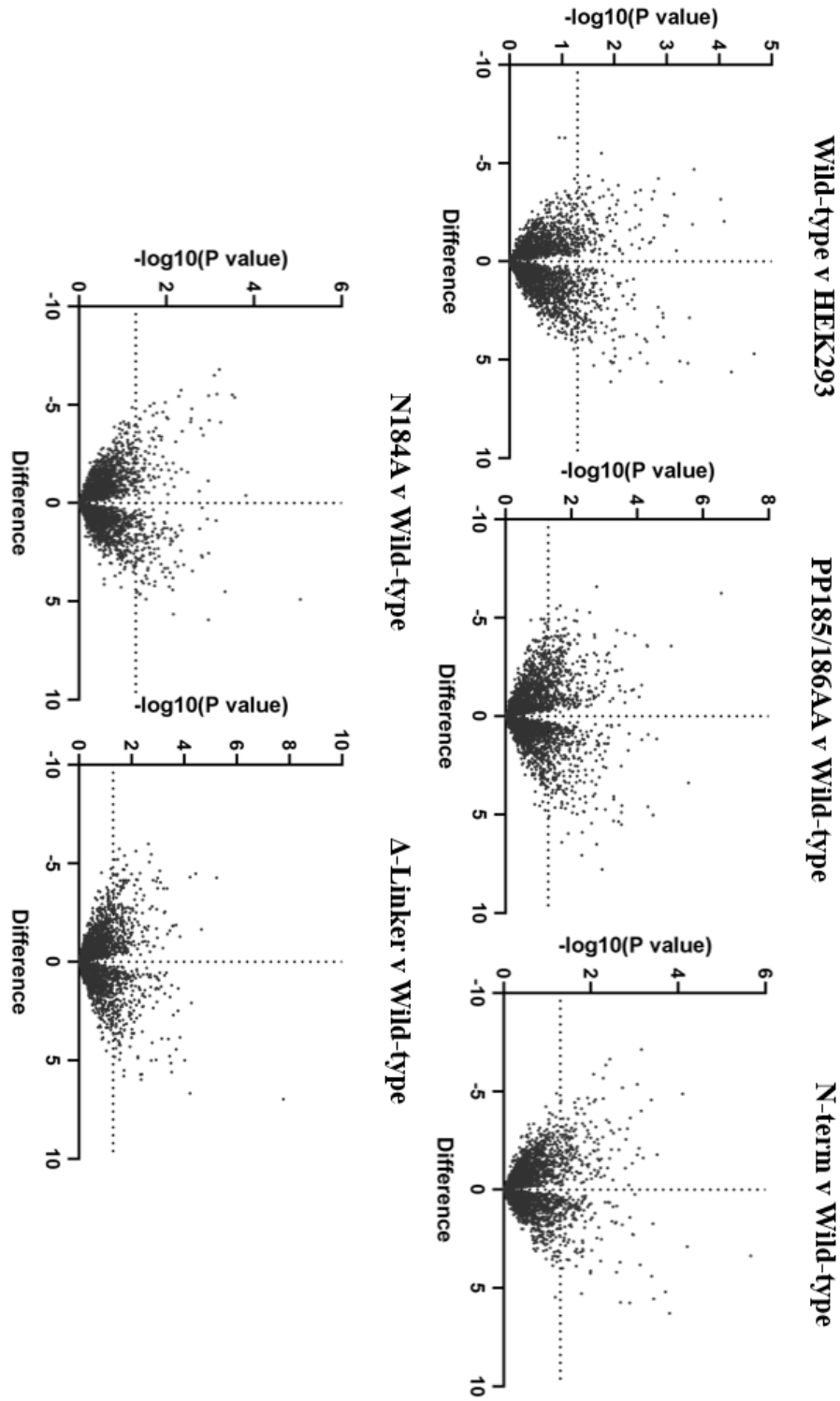
Wild-type v HEK293
PP185/186AA v Wild-type
N-term v Wild-type
N184A v Wild-type
Δ-Linker v Wild-type
-log10(P value)
Difference

Figure 3.5B

Wild-type Up	Wild-type Down	PP185/186AA Up	N-term Up	N184A Up	Δ-Linker Up	PP185/186AA Down	N-term Down	N184A Down	Δ-Linker Down
MARK3	DDX10	TUBB	TTC4	TUBB	ANXA4	SF3B4	SF3B4	SF3B4	MYLK2
SF3B4	WASHC3	ALDH3B1	DDX10	MSI2	CDK16	MYLK2	PEPD	OTUD6B	SF3B4
RAB6B	PRKACB	DDX10	UBE4A	SDHAF3	TUBB	RBM47	TUBAL3	RPS2	DECR1
RBM47	NIBAN2	RAP1B	STXBP3	ATXN10	NUP88	EFHD2	ACOT2	DECR1	OTUD6B
RRP1	ZNF503	RPL30	ZNF503	MACROH2A1	SDHAF3	SEPTIN14	MYH11	ARF4	ANXA2P2
NHP2	RPL3L	TMPO	SMC2	RAB43	SMC2	PRPF38A	ANO6	POTEKP	PEPD
USP30	TTLL12	CDK16	WASHC3	PIR	IMMT	ARF4	POTEKP	POU2F1	EXOC5
TUBAL3	FADS2	CHTOP	PHACTR4	BRD2	RTN4IP1	MTA3	SRSF12	EXOC5	METTL1
PLRG1	NCBP1	PRKACB	SAMD1	SULT1A2	ATP2B2	DHTKD1	TMTC3	ANO6	AURKB
ANO6	SMC2	POLE4	RPL3L	NUP88	ACTBL2	BOLA2-SMG1P6	RMDN1	PCBD1	ARF4
RAB4B	TAGLN3	ATXN10	TWF2	ZNF503	HAGH	AURKB	RAB4B	MICALL1	RAB4B
TRMT10C	PHACTR4	WASHC3	MRPS9	CDK16	RAD21L1	CD109	MYLK2	MARK3	FAM50B
FAH	AGPS	MAPK8IP3	IQGAP3	DNAJC7	RPL30	PDCD2	SNTB2	DMAC1	CELF2
ITCH	TTC33	ATAD3B	RIMOC1	RAP1B	POGLUT2	SRSF12	GFPT2	RAB4B	RMDN1
SEC11A	TUBB8	JMJD6	HSPE1	CAMK2A	RAB12	MAPK13	PAPSS1	PPHLN1	FAM126A
STRN3	ERAL1	AP1M2	HNRNPCL2	SMARCD1	SCAF8	FAM50B	ARF4	PEPD	RAB6B
KIF5A	ITPK1	TTC4	ITPK1	DRAP1	USP9Y	KATNAL2	GATC	MRPL20	CILK1
ANP32C	GNPNAT1	ZMPSTE24	ATP2B2	ZMPSTE24	LDHC	SUN1	STAM2	FAM50B	MARK3
RDH11	MCM3AP	SKA1	TOLLIP	HDGFL3	CALD1	IQGAP3	KIF5A	WNK4	SRSF6
PPHLN1	SIGMAR1	ACACB	DRAP1	ROMO1	PPP3CB	COPE	IAH1	FAM126A	COPE

Figure 3.5C

PP185/186AA	N-term	N184A	Δ-Linker
Reversible hydration of carbon dioxide	Reduction of cytosolic Ca^{2+} levels	Signaling by RAS/RAF/BRAF	ROBO receptors bind AKAP5
Golgi-to-ER retrograde transport	Hemostasis	Oncogenic MAPK signaling	Reduction of cytosolic Ca^{2+} levels
Oncogenic MAPK signaling	Megakaryocyte development and platelet production	Reversible hydration of carbon dioxide	Cell cycle
Mitotic Prometaphase	Protein folding	Signaling by Activin	SUMOylation of DNA replication proteins
Post NMDA receptor activation events	Platelet calcium homeostasis	MAP2K and MAPK activation	DARPP-32 events
Rho GTPase Effectors	Rho GTPase signaling/cycle	M phase	Glycolysis
Mitotic Spindle Formation and Checkpoint	STAT3 nuclear events downstream of ALK signaling	Mitotic cell cycle	M phase
Reduction of cytosolic Ca^{2+} levels	p75NTR negatively regulates cell cycle via SC1	Signaling by NODAL	NS1-mediated effects on host pathways
Resolution of Sister Chromatid Cohesion	Pyrophosphate hydrolysis	L1CAM interactions	Calcineurin activates NFAT
Kinesins	LRRFIP1 activates type I IFN production	Resolution of Sister Chromatid Cohesion	Golgi-to-ER retrograde transport

Figure 3.5: Protein expression results from proteomics analysis of each cell line. "Wild-type" is the non-mutated exogenous METTL16 line, "PP185/186AA" is the PP185/186 methylation mutant exogenous METTL16 line, "N-term" is the N-terminal RNA binding mutant exogenous METTL16, "Δ-Linker" is the C-terminal RNA binding mutant exogenous METTL16 line, and "N184A" is the N184A methylation mutant exogenous METTL16 line. Wild-type expression changes shown are compared to HEK293 protein expression. PP185/186AA, N-term, N184A, and Δ-Linker expression changes shown are compared to wild-type protein expression. (A) Volcano plots displaying comparisons of protein expressions among the cell lines tested. (B) Top 20 protein expression changes in each METTL16 transgenic cell line. Both the top 20 increased and decreased protein expressions for each line are shown. (C) Top 10 pathways affected by METTL16 mutation in each METTL16 transgenic cell line. Generated using Reactome analysis.

Discussion

After our previous published study in 2020 showing METTL16 protein was localized to both the cytoplasm and the nucleus, we hypothesized METTL16, in addition to RNA methylation, had another role related to its RNA binding ability [55]. To investigate this, we conceptualized and produced cell lines with one of the METTL16 protein's domains mutated to observe the impact of the partial loss of function on the cell. Because METTL16 was thought to be essential for all cells at the time of project conception, we opted to first introduce the mutated METTL16 into cells before removing the endogenous METTL16 from the genome to ease the cells into the transition. Given our and others' success in mutating/removing METTL16[58,186], it may be that METTL16 is only essential for certain cell types, such as stem cells, certain embryonic cells, or cells not yet included in METTL16 studies.

From our mutated METTL16 cell lines, we have determined first that METTL16's methylation ability appears to be dispensable for cell survival. Given that m6A methylation is a further fine-tuning of the RNA's processing or half-life, it is probable that there are other modes of regulation in place that are more influential on the RNA affected by METTL16. This is not to say there aren't consequences to removing METTL16's methylation ability. We saw widespread protein expression changes with our METTL16 N184A mutant cell line which suggests that methylation does indeed play a role in METTL16's function, perhaps by regulating translation of a subset of proteins.

Secondly, we determined METTL16's RNA binding ability is reliant on both the N-terminal and C-terminal RNA binding domains. Mutation of the METTL16 N-terminal RNA binding domain resulted in lower relative amounts of immunoprecipitated RNA but did not completely abrogate binding. This mutant was adapted from Mendel et al, who showed that

mutation of the N-terminal RNA binding domain completely abrogated binding to the MAT2A hairpin 1 when the C-terminal domain of METTL16 was not present. Interestingly, when we deleted the linker region between the VCRs of the C-terminal RNA binding domain, it actually increased the RNA binding efficiency of METTL16. Almost every RNA for which we probed in the immunoprecipitation studies showed increased binding to the C-terminal transgenic METTL16 compared to the wild-type transgenic METTL16. We speculate that removal of the linker region between the vertebrate conserved regions in this mutant slowed and/or limited the range of motion of the vertebrate conserved region domain as a whole and therefore allowed for stronger or longer binding. The region deleted is not evolutionarily conserved and is a disordered region[53]. Therefore, it is probable that this disordered region is vital to attenuating the RNA binding that the rest of the domain does. It is interesting to note that METTL16 has been implicated in recruiting RNA to translation machinery[186]. Further studies will determine which of these RNA binding domains (if not both) is responsible for the aid in translation.

Because we suspected METTL16 to bind and/or influence more RNAs than those currently published, we searched for changes in protein and RNA expression in the clonal lines we produced. We determined more extensive changes in protein expressions compared to RNA expressions. This could be because our RNA sequencing analysis did not probe for splicing changes among the RNAs identified. It could also be due to the recently cited role of METTL16 in translation. There were some similarities among the proteins whose expression changed among the clonal lines, however there were even more differences, indicating recruitment to the translation machinery is not the only reason for the noted changes. We chose several RNAs from among the expression changes to search for a direct interaction with METTL16 via RNA immunoprecipitation. Using

U1 snRNA as a negative control and U6 snRNA and MAT2A mRNA as positive controls, we have identified ATXN10, CDKN3, PNPLA4, and RTRAF as potential RNA targets of METTL16.

From our RNA expression and immunoprecipitation studies, we have determined the RNAs affected by METTL16 alteration belong in 1 of 3 groups. Group 1 contains RNAs that bind METTL16 but do not reflect an expression change when METTL16 protein becomes mutated. Among this group is MAT2A mRNA and U6 snRNA. The lack of change in expression is not necessarily indicative of a lack of effect on the RNA; for instance, U6 snRNA expression is not expected to change, and MAT2A mRNA is more likely to show splicing changes, which we did not investigate in this study. Other RNAs that fall into this group are likely to be imperative to cell survival such as the two listed. Group 2 contains RNAs that show expression changes but do not seem to bind METTL16. These RNA expressions are most likely changing as an indirect or secondary effect of true METTL16 target changes. Group 3 contains RNAs that both bind METTL16 and show RNA expression changes. Among this group is ATXN10 and PNPLA4 mRNAs. METTL16 may have more than one direct effect on these RNAs, or it is possible they are both directly and indirectly affected by METTL16. Even though the RNAs of groups 1 and 3 are of the most interest, RNAs in group 2 aid in the cell-wide effects observed by altering METTL16.

Regardless of the exact mechanisms METTL16 uses to produce the changes we have observed, we have shown that it significantly affects the cell cycle timing. Our EdU assay results show our transgenic METTL16 cell lines spend more time in S phase if METTL16 is mutated in certain domains. Furthermore, we determined CDKN3 to be an RNA binding target of METTL16, which is well known to affect the G1/S phase transition of the cell cycle. Future studies will determine the effect this binding has on CDKN3 RNA and subsequent protein expression.

The METTL16 mutant cell lines produced for this publication will provide insight into disease states where METTL16 has been documented as mutated or dysregulated. Most diseases associated with METTL16 are currently listed as due to an over- or under-expression of the protein. There is one documented type of large intestinal cancer which has a mutation (in the methyltransferase domain) that abolishes METTL16's methylation activity[59]. More in-depth analysis of the METTL16 protein in these types of studies may reveal a pattern of mutation correlating with expression. The investigation of mutated METTL16 qualities and cellular outcomes such as this study, will branch the functionality of METTL16 with its consequences in disease.

Materials and Methods

Plasmid Production

METTL16-Myc-FLAG plasmid, METTL16 CRISPR-Cas9 plasmid, and scrambled CRISPR-Cas9 plasmid were purchased from Origene and Genecopoeia. Mutations in the METTL16 plasmid coding sequence were introduced using the Q5 Site-Directed Mutagenesis Kit (New England Biolabs). Plasmids were amplified with transformation of FB5α *E. coli* cells (ThermoFisher) by incubation for 30 seconds at 45°C, then 5 minutes on ice. *E. coli* suspension was then adjusted to 1 mL with SOC Outgrowth Media (New England Biolabs) and incubated for 1 hour at 37°C on a shaker at 250 rpm. Bacterial cells were spun down, resuspended in 50 µL of SOC Outgrowth Media, and spread on a Luria Broth (LB) agar plate (Luria Broth from FisherScientific, Agar from Sigma) containing the appropriate antibiotic for selection. Plates were incubated at 37°C overnight. Colonies were selected from plates after growth, suspended in 3 mL of LB media with appropriate antibiotic and grown for approximately 16 hours at 37°C on a shaker

at 250 rpm. Plasmids were harvested from bacteria using GeneJET Plasmid Miniprep Kit (ThermoFisher) according to manufacturer protocols. Some of the *E. coli* was kept at 4°C for later use. The mini-prepped plasmids were sequenced with Sanger sequencing using primers directed at key sequences in the plasmids. Once verified, the stored *E. coli* cell suspensions were adjusted with another 3 mL LB media and respective antibiotic, grown overnight at 37°C, and then added to 250 mL of LB with antibiotic, which was again grown overnight at 37°C. Plasmids from these cells were harvested using NucleoBond Xtra Midi Kit (Macherey-Nagel) according to manufacturer protocols. When appropriate, a final concentration of 100 µg/mL ampicillin (Sigma) or 100 µg/mL kanamycin (Sigma) was used for selection. Plasmid concentrations were determined with a Nanodrop 2000 spectrophotometer.

Tissue Culture

HEK293 cells were obtained directly from American Type Culture Collection (ATCC). Cells were cultured at 37°C, 5% CO_2, in Dulbecco's Modification of Eagle's Medium 4.5 g/L glucose (Corning) supplemented with 10% fetal bovine serum (Gemini Bio), 2mM L-glutamine (Corning), and 1X Penicillin/Streptomycin (Corning). When appropriate, G418 (Sigma) was used in culture at 0.5mg/mL for selection and 0.25mg/mL for maintenance; puromycin (Sigma) was used in culture at 7.5µg/mL for selection and 3.75µg/mL for maintenance.

Plasmid Transfection

For clone production, cells were plated at $0.5x10^6$/well in a 6 well plate (CytoOne, USA Scientific) the day before transfection. On the day of transfection, 2 µg of plasmid was transfected with Opti-MEM (Gibco) and Lipofectamine 2000 (Invitrogen) according to manufacturer protocols. Plasmid mixture was incubated with cells overnight and media was changed the next day. Antibiotic selection was started 24 hours after initial transfection time. Cell colonies were

selected after approximately 1 week, grown separately, and screened for proper plasmid expression and integration using Western blotting. Cells transfected for transient overexpression were plated in a 10 cm cell culture dish (CytoOne, USA Scientific) with $2.5x10^6$ cells and transfected with 10 µg of plasmid and were harvested one to two days after transfection.

Western Blots

Cells were harvested using 0.05% Trypsin (Corning), quenched with media, and washed with 1X Dulbecco's Phosphate Buffered Saline (DPBS) (Corning), and then lysed with Whole Cell Extract buffer (WCEB) (150 mM NaCl (Mallinckrodt), 10 mM Tris pH=7.6 (Corning), 0.1% SDS (Sigma), 5 mM EDTA (Ambion), 1X protease inhibitors (Pierce, ThermoScientific), incubated on ice for about 5 minutes, and stored at -80°C until use. After thawing on ice, extracts were sonicated, and protein was quantified with BCA kit (ThermoFisher) in triplicate according to manufacturer protocols with Promega GloMax Multi Detection plate reader. Unless otherwise stated, 35 µg of protein was loaded from each sample with 5x loading buffer (250mM Tris-HCl pH=6.8, 10% SDS w/v, 500mM DTT, 750µM Bromophenol Blue sodium salt (Sigma), 50% Glycerol v/v (Sigma), 1% β-Mercaptoethanol (Sigma)) into the Western gel. For mini gels (Bio-Rad, 10% polyacrylamide), gel was electrophoresed at room temperature at 250V for 25 minutes in 1x Tris-Glycine-SDS buffer (Bio-Rad). Protein was transferred to an Amersham Protran 0.2 µm nitrocellulose membrane (GE Healthcare) at room temperature with an ice pack and stir bar at 300mA for 1 hour in 1X Tris-Saline + 20% methanol (Fisher Chemical) buffer. For large separation gels (20 cm), gel was electrophoresed at 4°C at approximately 150V for several hours in 1X Tris-Glycine-SDS buffer (Bio-Rad) until proper separation achieved. Protein was transferred to a nitrocellulose membrane at 4°C at 300mA for 1 hour in 1X Tris-Saline + 20% methanol buffer. After transfer, membranes were handled in the same manner. Membranes were blocked with 5%

nonfat milk (LabScientific) in 1x TBS-T (Tris buffered saline with 0.1% Tween 20 (Sigma)) at room temperature for 1 hour on a shaker, and then incubated in appropriate primary antibody suspended in 5% nonfat milk or 5% bovine serum albumin (Fisher Scientific) in 1X TBS-T (with 0.01% NaN_3 (Sigma-Aldrich)) overnight at 4°C on a shaker (See Supplemental Table 1 for antibody details). The next day, membranes were washed at room temperature on a shaker with 1X TBS-T 3 times with incubations in each wash at least 5 minutes. Membranes were then incubated with 5% nonfat milk in 1x TBS-T with appropriate 1:10000 secondary HRP antibody (GE Healthcare) at room temperature for 1 hour on a shaker. Washes were repeated as described with 1X TBS-T. Western blot was imaged with Clarity Western ECL Substrate kit (Bio-Rad) according to manufacturer protocol using MyECL Imager (ThermoFisher) or iBright CL1500 Imager (Invitrogen).

Cycloheximide Treatment

Cells were lifted with 0.05% Trypsin (Corning), counted with Trypan Blue (Corning), and plated in a 6 well dish the day before treatment at $0.4x10^6$ cells/well. On the day of treatment, all wells were treated with a final concentration of 25 ug/mL of cycloheximide (Sigma) and harvested at the time points specified in WCEB with 1X protease inhibitor. Protein concentration was quantified using BCA kit from ThermoFisher and Western blots were produced as listed in Western blot section.

Cell Biochemical Fractionation

Cells were lifted with 0.05% Trypsin, quenched with media, centrifuged at 1500g for 5 minutes, rinsed with 1mL of 1x DPBS, and centrifuged again after moving 100 µL to a separate tube. DPBS was removed. The 100µL of cells was resuspended in 100 µL of Total Lysis Buffer (TLB) (50mM Tris pH=8 (Sigma), 150mM NaCl, 0.1% SDS, 1% NP40 (Fluka Analytical), 0.5%

sodium deoxycholate (Sigma-Aldrich)) + protease inhibitors and the 900 µL of cells was resuspended in 100 µL of Hypotonic Lysis Buffer (HLB) (10mM Tris pH=8, 10mM NaCl, 1.5mM $MgCl_2$ (Sigma)) + protease inhibitors. Both were frozen at -80°C overnight to further the lysis. The HLB cells were then thawed on ice, vortexed for a few seconds to lyse, and centrifuged at 1500g for 5 minutes. The resulting supernatant was the cytoplasmic fraction which was moved to a separate tube. The pellet was the nuclear fraction and was resuspended in 100 µL of TLB + protease inhibitors. Nuclear and total fractions were sonicated to break up DNA, and equal amounts were loaded for Western blotting after addition of loading buffer. Western blots were produced as listed in Western blot section.

RNA Extraction

Cells were collected and then lysed with 1 mL TRIzol (Ambion). RNA was isolated according to manufacturer protocols and kept on ice thereafter. RNA concentrations were determined with a Qubit 4 Fluorometer (Invitrogen) and stored in RNase-free H_2O at -80°C until use.

Immunoprecipitations

A confluent 10 cm cell culture dish was harvested by gently rinsing the cells off with 1 mL 1X DPBS. Cells were spun down and resuspended in 125-250 µL of Polysome Lysis Buffer (100mM KCl (Sigma), 5mM $MgCl_2$, 10mM HEPES pH=7 (Sigma), 1mM DTT (Thermo Scientific), 10% digitonin (Wako), 1x protease inhibitors (Pierce), 100 U/mL RNaseOut (Invitrogen)). Suspension was spun down at 15000g for 15 minutes at 4°C. This separates organelles, membranes, and DNA from the aqueous fraction of the cells. For each IP, 100 µL of supernatant was used, along with 50 µL of washed IP bead slurry, 10 µL of 100mM DTT, and 40 µL of 0.5M EDTA, brought to 1 mL in NT2 buffer (50mM Tris pH=7, 150mM NaCl, 1mM $MgCl_2$,

0.05% NP40). IP tubes were incubated at 4°C for at least 4 hours on a shaker. IP input and supernatant samples were taken after incubation but before washing, final IP samples were taken after 5 washes with NT2 buffer to confirm protein attachment. 1 mL of TRIzol was added directly to washed beads and RNA was isolated according to manufacturer protocols. 10% of the amount of PLB supernatant used in IP was used to quantify RNA input and was isolated with TRIzol as well. Anti-FLAG-labeled IP beads were purchased from Sigma.

Polymerase Chain Reaction

Reverse transcription PCR was accomplished with a Bio-Rad T100 thermal cycler. For RNA directly isolated from cells, 100 ng polyA RNA was adjusted to 10 µL with H_2O and used with iSCRIPT cDNA synthesis kit (Bio-Rad) and incubated the thermal cycler according to manufacturer protocols. For RNA resulting from immunoprecipitations, 80% was used in cDNA synthesis to ensure equal amounts were used.

Real-time PCR was performed using cDNA described above, primers from Integrated DNA Technologies (See Supplemental Table 2 for primer details), and Roche LightCycler products including FastStart DNA Green, multiwell clear plates, and the LightCycler 96 machine. cDNA was diluted 5x with H_2O when directly isolated from cells and 2x with H_2O when resulting from immunoprecipitations.

RNA Sequencing

Cells from a confluent 10 cm dish were harvested with 0.05% Trypsin, quenched with media, and washed with 1x DPBS before resuspension in 1 mL TRIzol. After RNA isolation according to manufacturer protocols, the RNA was reprecipitated in 3M sodium acetate (Sigma) and 100% 2-propanol overnight at -20°C. The next day, reprecipitation was completed, RNA was suspended in H_2O, and was quantified using Qubit 4 Fluorimeter. PolyA RNA was isolated from

100 µg of this RNA using the Poly(A)Purist MAG Kit (Invitrogen) according to manufacturer protocols. PolyA RNA was quantified with the Qubit 4 Fluorimeter. 200 ng of each cell line's polyA RNA was used in the Direct cDNA Native Barcoding Nanopore protocol in preparation for sequencing using the MinION Nanopore Sequencer. Protocol was performed to manufacturer's recommendations. Sequences were basecalled using the high accuracy basecalling setting. Passed reads were then processed using the Galaxy platform. Sequences were mapped using MinMap2 to Human Hg38 genome with the Oxford Nanopore read to reference mapping option enabled (minimap2 -x map-ont --q-occ-frac 0.01 -t 6 -a). Reads were quantified using featureCounts and differential expression determined with DESeq2.

Liquid Chromatography-MS/MS

Once cell lines were established and expressions verified, cells were lifted with 1 mL Accutase (Innovative Cell Technologies) and counted using 0.4% Trypan Blue stain. Five replicates of $2x10^6$ cells were harvested and washed several times with 1x DPBS and stored at -80°C until protein isolation and digestion.

Protein samples for label-free proteomics analysis included five independent biological replicates from five independent cell culture experiments for each group (n=5). Cell pellets were thawed and after thorough washing, cells were resuspended in equal volumes of cold lysis buffer (8 M urea, 40 mM Tris-HCl, 40 mM NaCl, 2 mM MgCl2 pH=8.0, 1X HALT Protease Inhibitor) and subjected to 3 freeze-thaw cycles prior to sonication (Branson sonifier, 30% amplitude, 15 sec, 4 ◦C). The lysate was clarified via centrifugation (10000 g, 10 min, 4 °C) and total protein content was determined by BCA assay (Pierce BCA Assay Kit). Equal amounts of proteins (1 mg/mL) were reduced (5mM DTT, 30 min, 32 ◦C) and alkylated with iodoacetamide (15 mM IAM, 30 min, room temperature in the dark). Unreacted iodoacetamide was quenched with an

additional 15 mM DTT. Samples were diluted to 1.5 M urea using a buffer containing 40 mM Tris (pH=8.0), 30 mM NaCl and 1 mM CaCl2 and then digested with MS grade Trypsin overnight (1:50, trypsin:total protein) at 37 °C. After digestion, the samples were acidified with 0.1% formic acid and subjected to desalting via solid-phase extraction (C18 SEP-PAK columns; Waters) Soluble peptides were eluted using acetonitrile + formic acid (25%-50%, 0.1%) washes, lyophilized overnight and resuspended in 0.1% formic acid. Peptide concentrations were determined by coulometric assays (Pierce Quantitative Peptide Assay) and adjusted to 0.25 mg/mL with 0.1% formic acid. Digested samples were analyzed by nanoLC-MS/MS using an UltiMate 3000 RSLCnano system (ThermoFisher) coupled to a Q Exactive Plus Hybrid Orbitrap mass Spectrometer (ThermoFisher) via nanoelectrospray ionization as previously described [207]. Peptides were separated using an effective linear gradient of 10-40% acetonitrile (0.1% formic acid) over 120 min. For data dependent acquisition, MS spectra were acquired in positive mode. MS1 were performed at a resolution of 70,000 with an AGC target of $2x10^6$ ions and a maximum injection time of 100 ms. Data dependent acquisition was used to collect MS2 spectra on the top 15 most abundant precursor ions with a charge >1 and an isolation window of 1.5 m/z, fixed first mass of 140 m/z, and a normalized collision energy for MS2 scans was 27. MS2 spectra were acquired at 17,500 resolution, maximum injection time of 50 ms, and AGC target of $1x10^5$.

Proteomics Data Analysis

Proteome Discover 2.5 was used for processing of raw data files and protein identification. Defaults search parameters included Met oxidation (+15.99492 Da) as a variable modification and Cys carbiomidomethylation (+57.02146 Da) as a fixed modification. Data were search against the Uniprot Homo Sapiens reference proteome (UP000005640) which contained additional sequences for the Wild-type, PP185/186AA, N-terminal, and Δ-Linker METTL16 mutants, and CRISPR

proteins. Precursor ion m/z tolerance was ±10 ppm and fragment ion m/z tolerance: ±0.6 Da with three missed cleavages allowed. The search results were filtered by a 1% false discovery rate (FDR) at the peptide-level. Strict parsimony was used to group peptides to proteins. Label free quantification was carried out using MS1 precursor intensity. Intensities were normalized to both the average intensities and the distribution width of the intensities within the sample. Relative abundances for low sampling proteins were determined via imputation [208]. Assuming a normally distributed population and unequal variance between the control and experimental values, we used a Welch's two sample two-tailed t-test in GraphPad Prism and considered all proteins with a p-value ≤ 0.05 to be statistically significant.

EdU Flow Cytometry Assay

Once cell lines were established and expressions verified, cells were plated at $0.5x10^6$ cells in a 10cm dish and allowed to attach overnight. The next day, 10 µL of 10mM EdU (Click-iT Plus EdU Alexa Fluor 488 Flow Cytometry Assay Kit, Invitrogen) was added to each culture and incubated at 37°C for 1 hour, after which media was replaced with fresh and were incubated for another 3 hours. Cells were then lifted with 1 mL 0.05% Trypsin, quenched with media, collected, and washed once with 1% BSA (Fisher Bioreagents) in 1x DPBS. Cells were then fixed and stained using the Click-iT kit contents and DAPI (Invitrogen) according to manufacturer protocols. Cells were analyzed for fluorescence with the Cytek Aurora Flow Cytometer using SpectroFlo and FlowLogic software for analysis.

Table 3.1: Antibodies used in this study

Product	**Vendor**	**Catalog #**	**Dilution**
Anti-Lactate Dehydrogenase	Santa Cruz Biotechnology	sc-133123	1:250 (WB)
Anti-Lamin B	Santa Cruz Biotechnology	sc-6216	1:200 (WB)
Anti-METTL16	Bethyl Laboratories	A304-192A	1:2000 (WB)

Table 3.2: PCR primers used to produce mutations in METTL16 sequence-containing plasmid

METTL16 Mutant	Site-Directed Mutagenesis Forward Sequence	Site-Directed Mutagenesis Reverse Sequence
CRISPR-Resistant	caacctcaacGGAAGAGTGAGCCTTAATTTTAAAG	atttgcacgtgCTGCTTAAAATCTGGATATTTG
N-terminal RNA binding	aatgcatacgcggacgcaCCTCCTGACTTTGCATATCTG	tgctgcatgcattgatgcACTCAGAGCCATGGCGAT
PP185/186AA Methylation	CATGTGCAACgcagccTTTTTTGCCAATC	CAAAAGTCATAGATTATCTCAGATTC
N184A Methylation	TTGCATGTGCcgcCCTCCCTTTTTTG	AAGTCATAGATTATCTCAGATTCTTC
Δ-Linker	GGAGTGGCCGGACAGTAC	CTTTTTCTCTTCCAAGGCCTGAATG

Table 3.3: Plasmids and guide RNA sequences used in this study

Plasmid	**gRNA sequence**	**Catalog #**
Scrambled CRISPR	GGCTTCGCGCCGTAGTCTTA	CS-CCPCTR01-CG12-01-10
METTL16 CRISPR	CATGTTCAGATAAATCTGAA	CS-HCP218894-CG12-3-10-A
METTL16 ORF	-	RC208648

Table 3.4: Real-time PCR primers used in this study

Gene	Forward (5'-3')	Reverse (5'-3')
ATXN10	GATACGATTGGTGTTGCTGTTG	GTCTATTGTTTGGGTGCATGC
CCND1	CATCTACACCGACAACTCCATC	CGGATGATCTGTTTGTTCTCCT
CDKN3	CCCAAACCTTCTGGATCTCTAC	TATGGAGGACTTGGGAGATCT
GPR50	GAATACCCACCGGCTCTAATC	TCTTCGTGGTCAGTCTCTCT
MALAT1	GAATTGCGTCATTTAAAGCCTAGTT	GTTTCATCCTACCACTCCCAATTAAT
MAT2A	CTGCTGTTGACTACCAGAAAGT	GCTACCAGCACGTTACAAGT
MYC	GCTGCTTAGACGCTGGATTT	GAGTCGTAGTCGAGGTCATAGTT
PNPLA4	CGTTGGTTGCTTCTGTTCTG	GACTAAGAAGTGGGATGGAGTC
RHO D	GCAGGGCAAGATGACTATGA	CAAGAAGGTACCCATCATCGT
RTRAF	ACAGGATGCAGTTGCTAAGG	TAGCTCTCTGAGCTCCTCTATG
U1	CCATGATCACGAAGGTGGTTT	ATGCAGTCGAGTTTCCCACAT
U6	CTCGCTTCGGCAGCACA	AACGCTTCACGAATTTGCGT
UBE2C	GCAGTTGCAGTCGTGTTCTC	TACAGCAGGAGCTGATGACC

Chapter 4:

Discussion: Widespread Effects of METTL16 on Cells

The work shown in this dissertation furthers the currently limited knowledge of METTL16's function in and essentiality to human cells, both through and beyond m6A RNA modification. As m6A has gained appreciation for its role in fine-tuning RNA (and subsequently protein) expression, a number of diseases have been associated with its aberration[17,20,31,164,180,182,209]. Attenuation or correction of m6A levels in affected cells is the goal of many potential therapies for these diseases. The association has led to a large interest in the enzymes and conditions that influence the modification process. While one of the known human m6A mRNA methyltransferases (METTL3/14) has been extensively studied, the other (METTL16) has not been investigated except within the last few years. In aiding the investigation into METTL16's function, this project has proven METTL16 effects changes in cellular pathways within and outside of m6A RNA modification.

METTL16 Localization in Human Cells

mRNA is produced in the nucleus of the cell with transcription machinery, however before it is sent to the cytoplasm for translation, it undergoes several changes known as post-transcriptional modifications. Post-transcriptional modifications include processes such as polyadenylation, splicing, 5' capping, and m6A modification. It follows that all the cellular machinery needed for these processes would be located in the nucleus. When METTL16 was first investigated, it was indeed found in the nucleus by several groups. In our 2020 study of METTL16, we used plasmids and siRNA to overexpress and knockdown METTL16 expression in human cells to observe changes in RNA binding and expression. When we received some interesting results, we utilized biochemical cell fractionation and immunocytochemistry to confirm METTL16

protein was still nuclear, and we unexpectedly saw METTL16 in both in the nucleus and cytoplasm. Even though it has never been proven that m6A modification does not occur in the cytoplasm, all other post-transcriptional modification machinery (as mentioned previously) has only been observed in the nucleus. Among the interesting results mentioned, we found METTL16 significantly bound several ribosomal RNAs. Ribosomal RNA is also known to contain m6A modification[68,210], however the majority of rRNA is found in the cytoplasm in the ribosome complex. These together was our first definitive evidence that METTL16 has a cellular role outside of the nucleus, and probably outside of m6A modification. Furthermore, it was this discovery that enabled the m6A methyltransferase community to widen their scope of potential METTL16 functions. In fact, only two years later, a study confirmed our localization findings and showed METTL16 recruiting RNA to the cytoplasmic ribosomal machinery[186]. It further demonstrated that this translation promotion accounts for some of the oncogenic effects presented in hepatocellular carcinoma cases. While it demonstrated the methyltransferase domain of METTL16 was crucial for the translation role, the RNA binding domains were not included in their mutagenic studies. Therefore, it is possible that other responsibilities of METTL16 in the cytoplasm or nucleus have yet to be discovered.

Aberrant Expression of Human METTL16

There are several reports stating that METTL16 protein expression is correlated with a poor cancer prognosis[103,105,106,108,109,199,203,211,212]. It seems that whether the poor prognosis is associated with high or low expression of METTL16 is dependent on the tissue type afflicted. Right before this dissertation was completed, one study demonstrated METTL16 protein could be

phosphorylated by ATM, which in turn displaces RNA bound in METTL16's N-terminal RNA binding domain[213]. This led to higher occurrence of homologous recombination in response to DNA damage, which is favorable in cancerous cells, since they are known for having chromosomal instability leading to widespread gene mutations. While this may explain one of METTL16's tumor-suppressive roles, it does not explain the oncogenic role(s). Taken with other hints of METTL16's cancer relations, this has attracted research into METTL16's potential oncogenic/tumor-suppressive effect on the cell. In chapter three, it was shown the N-terminal and PP185/186AA (our null model) mutations of METTL16 significantly affected cell cycle occupancy, meaning METTL16 is involved in the cell cycle process. We also found several RNAs bound to METTL16 which have a role in cell cycle progression, such as CDKN3, MAT2A, and RTRAF. Because RTRAF is involved in regulating transcription, aberrant expression could encourage cell growth beyond what is needed by the organism. MAT2A dysregulation could supplement the growth by producing more methionine for protein production and RNA regulation. Furthermore, excessive CDKN3 could contribute to bypassing the G1/S checkpoint, all of which could result in unrestricted cell replication, allowing mutations in DNA to occur and accumulation of cells. Together, our results begin to elucidate how METTL16 could contribute to cancer formation and progression.

We also saw several RNAs which bound METTL16 or showed expression level changes with METTL16's aberration that are involved in other pathways such as calcium signaling, intracellular trafficking including cytoskeletal reorganization, and metabolism. In preparation of this dissertation, a study published results showing they also saw changes in intracellular trafficking upon METTL16 knockout[214]. The changes seen in a multitude of pathways reveals the potential for METTL16 to be involved in promoting multiple diseases. Regulation of calcium

storage and levels in cells affects stress response, neuronal and muscular signaling, and energy production. The most notable diseases associated with calcium signaling are neurodegenerative diseases such as Alzheimer's and Parkinson's diseases. Intracellular trafficking (which includes membrane localization, protein localization, and organelle trafficking) dysregulation can also result in neurological disorders such as anxiety, schizophrenia, and parkinsonism[215]. Metabolic disorders often result in early cell death either from toxic buildup of unprocessed molecules or lack of proper nutrients for cell function. From our results, we propose further studies into these types of diseases take METTL16's effect on cells into account.

There are several explanations for the widespread changes observed in RNA and protein expression when METTL16 is mutated, and it is possible that more than one explanation is accurate. U6 snRNA was the first RNA determined to be m6A modified by METTL16[112], and subsequent studies have shown that this modification fine-tunes the splicing of mRNAs directed by U6[124,132]. If U6 RNA does not become methylated, or even only some but not all become methylated, the splicing outcome directed by U6 will be skewed. Since U6 directs splicing in a plethora of RNAs, this change in processing could have extensive effects on cellular mRNA and the resulting proteins that are produced. It is my expectation, however, that a global change in splicing would result in more changes in expression than we see with our proteomics and RNA sequencing results. Adversely, it is known that expression of U6 is essential for cell survival[130], but it is not yet proven that the m6A modification in U6 is part of that essentiality, although splicing changes have been seen when it is lacking[60]. Furthermore, our mutations of METTL16 did not reflect significant changes in binding to U6, even when RNA binding was affected with every other RNA tested. This suggests that METTL16 binds to U6 in an additional m6A-independent way. Whether or not this is the case, we can safely predict changes in splicing due to the

METTL16-driven U6 snRNA modification which could underly some of the expression changes we observed.

Another explanation for the expression changes due to METTL16 mutation is the effect on MAT2A. MAT2A mRNA is m6A-modified by METTL16 which partially regulates the protein expression of MAT2[56,81], the enzyme responsible for producing the methyl-donating molecule (SAM) used in almost all cellular methylation reactions[216]. It follows that changes in the regulation of this RNA could result in a change in accessibility of SAM for methylation reactions, including m6A methylation. This would not only affect m6A modification, but almost all other methylation reactions needed to maintain cell functions and homeostasis. Once again, it is my expectation that affecting MAT2A levels enough to induce large-scale methylation changes would result in more expression changes than we see, and perhaps even cell death. MAT2A expression is regulated by other methods in addition to METTL16[96]. This is illustrated by the lack of change in MAT2 protein expression (via proteomics analysis) when METTL16 was mutated.

Because METTL16 was shown to recruit RNA to translation machinery in the cytoplasm[186], another potential reason for the widespread expression changes with METTL16 mutation may be due to the attenuation or lack of this recruitment. As mentioned previously, METTL16 knockout was shown to attenuate proliferation, invasion, and translation efficiency in hepatocellular carcinoma[186]. However, in a previous chapter, it was mentioned that either upregulation or downregulation of METTL16 could correlate with oncogenicity depending on the tissue-type afflicted[103,105–107,109,185–188,198,200–203,211,212]. The cell line utilized in this study is an embryonic human kidney cell line with neuronal properties. While the lack/attenuation of RNA recruitment for translation may be the reason for the widespread expression changes seen, it is

interesting to note that we saw widespread changes between the different METTL16 mutants. From the RNA sequencing and proteomics data, we observed prominent cell cycle changes in the PP185/186AA null and N184A models, but not much in the N-terminal mutant and Δ-Linker models. We saw cell trafficking changes in the PP185/186AA null, N184A, and Δ-Linker models, but not in the N-terminal mutant. Furthermore, we saw Ras/MAPK signaling changes in the PP185/186AA null and N184A models, but not in the N-terminal mutant or Δ-Linker models. All of this points to effects on the cell being dependent on the type of mutation in METTL16. If recruitment to the translation machinery was the main cause, we would most likely see similarities between the RNA-binding mutants, which is not what the results show. Some of the changes could be a secondary cellular response to functionally losing one of METTL16's protein domains. Luckily, there does seem to be overlap in the overall processes affected by METTL16 between the hepatocellular carcinoma and the embryonic kidney cells. Three mRNA targets of METTL16 (CDKN3, RTRAF, and MAT2A) have been associated with liver cancer[205], and METTL16's protein expression itself is correlated with the cancer prognosis[106,186,197]. More studies with a variety of cell types would help bridge the different reactions the cell has to METTL16 loss/mutation, and correlation of those changes to the genetic profile of the cancer seen in that specific cell type, is key to fully understanding METTL16's impact in cancer and other diseases.

Regardless of the mechanism(s) by which it is acting, the studies in this document solidify the implication of METTL16 in a variety of diseases. Cellular pathways compiled from the proteomics of other aberrant-METTL16-expressing cell studies has correlated well with those in chapter three. The most implicated pathways include cell cycle, intracellular transport/microtubule organization, RNA processing and metabolism, and catabolic metabolism. Cell cycle and catabolic metabolism pathways are prominently disrupted in cancerous cells, potentially explaining why

METTL16 seems to significantly contribute to the prognosis of a variety of cancers. However, there are many other diseases that utilize these pathways, ranging from neurodegenerative diseases and cardiomyopathies to developmental and circadian rhythm disorders. As METTL16 has been successfully removed from embryonic kidney cell cultures[186], it is likely that other dysregulations would need to occur with aberrant METTL16 expression for these diseases to present. Still, now that several studies have come to these same conclusions, METTL16 can be explored in diseases in these pathways as a potential therapeutic alongside others.

RNA Binding Targets of Human METTL16

Before the discovery of METTL16's recruitment of RNA to ribosomes, METTL16 was considered only to be an m6A RNA methyltransferase, and only a few RNAs seemed to be targets. With each study about METTL16 published, it seemed almost any RNA could bind METTL16 (to at least a small extent), some of which were never shown to contain an m6A modification[55,58]. Furthermore, correlation among datasets showing RNAs bound to METTL16 and RNA expression changes with METTL16 knockdown/knockout showed very little overlap. Right before the translation discovery, the structure of the C-terminal of the human METTL16 protein was finally solved and identified as a second RNA binding domain[53]. Since the translation discovery, the focus on METTL16 has shifted to involvement with protein synthesis, but the requirements of the RNA to be bound and recruited by METTL16 has not been thoroughly investigated. It is our belief that both RNA binding domains restrict the RNAs that METTL16 can bind. From x-ray crystallography, it has been shown that the N-terminal RNA binding domain forms a groove that can accommodate a double stranded RNA form, most likely in a hairpin since the groove is not

open-ended[59]. From both homology and crystallography, it has been determined that the C-terminal RNA binding domain forms a clamp-like structure which is also predicted to bind double-stranded RNA[53]. While most RNAs adopt a secondary structure with stems and hairpins, it is clear from our studies that METTL16 does not bind all RNAs. Therefore, while the association with translation is exciting, continued studies into the specific RNAs bound (or the requirements set by METTL16's structure for RNA binding) are crucial.

Chapters two and three of this dissertation have identified RNAs that both do and do not show significant binding to METTL16, which not only implicates METTL16's role in the RNAs' associated pathways but contribute to the evidence needed to understand METTL16 RNA binding. Immunoprecipitation with the mutated METTL16 proteins in chapter three illustrates a binding pattern. Compared to the wild-type transgenic METTL16, the N184A methylation mutant only showed a significant decrease in binding to MAT2A RNA. In contrast, a previous study showed a longer binding time to MAT2A when METTL16 was unable to methylate it[56]. The previous study was performed in live cells, whereas our immunoprecipitations were not, however all cell contents (including SAM) were available to METTL16 in the immunoprecipitation experiment. It is possible that our mutation changed the protein structure of METTL16, however we saw no significant difference in binding to any other RNA target, including U6, which argues against this explanation. It is also possible that, out of the RNAs we found bound, METTL16 only methylates U6 and MAT2A. Because the VCR region shows structural homology to TUT1[53], which uridylates U6[83], it could be that the C-terminal RNA binding domain binds well enough to U6 to overcome the N184A mutation's effect on binding in the methyltransferase region. Further studies are needed to confirm these potential explanations.

The PP185/186AA transgenic METTL16 methylation mutant unfortunately could not be used in the RNA immunoprecipitation studies since we could not maintain its expression in cells. We were able to produce the cell line and confirm the expression of the protein, however subsequent culturing continually led to loss of detection. Although another study published this METTL16 mutant as showing no changes in RNA binding[56], we believe the lack of function of this protein in vitro led to the rapid loss of its expression. This, however, became an opportunity for us to observe cells without METTL16 expression, given that our previous attempts at its removal from the genome were unsuccessful. Therefore, while we were unable to obtain RNA binding information on this mutant METTL16, we arguably received a better opportunity since we were able to produce another METTL16 methylation mutant (N184A) while maintaining this line as an extreme aberration of METTL16 expression.

The C-terminal RNA binding transgenic METTL16 mutant bound almost every RNA we probed significantly better than the wild-type transgenic METTL16. This gain of function was surprising, because we postulated the disordered region (the linker region) that we deleted was necessary for the dynamic motion of RNA binding and unbinding. It seems that rather than prohibiting RNA binding, we prohibited dynamic motion that would have otherwise restricted close contact with the RNA. The linker region of the protein shows low conservation in sequence and size, solidifying the evidence of its lack of function in aiding RNA binding. It is important to note that we observed better binding with this mutant to RNAs that do not seem to even be METTL16 targets. The RNA sequencing and proteomics results from the cell line containing this METTL16 mutant were studied as the effect of METTL16 binding too well on cell processes. One result of this comparison revealed only the Δ-Linker mutant seemed to significantly affect protein expression of RNA transcription/processing and glucose metabolism pathways. In contrast, both

the Δ-Linker and PP185/186AA models reflected cell cycle and calcium signaling pathway protein changes. Comparing the results from the Δ-Linker mutant to those in our PP185/186AA mutant, which we regard as a METTL16 null line, gives an accurate spectrum of consequences from METTL16 not binding RNA to binding too much.

Regardless of METTL16 mutation, we identified several new RNA binding targets of METTL16, including HIF1a, MYC, NT5DC2, ATXN10, CDKN3, PNPLA4, and RTRAF. We have significantly expanded the number of RNAs known to interact with METTL16 from three (MAT2A, MALAT1, and U6) to ten. It is our hope that these studies have revealed METTL16's versatility from the once restricted guidelines once set upon it.

Future Directions

Further mutations in the METTL16 protein will help determine which RNA binding domain is responsible for binding which RNA. Our current evidence leads us to believe that certain RNAs are bound better by one domain over the other. It would be interesting to see the effect of RNA binding when the C-terminal RNA binding domain is mutated to a true loss-of-function. Furthermore, mutating both RNA binding domains would serve as a control to confirm 1) no other region of METTL16 is responsible for RNA binding, and 2) a negative control for RNAs that use one or both known RNA binding domains.

Future studies are needed to prove whether the RNAs bound to METTL16 are methylated by METTL16 as well. Since it has been determined METTL16 recruits RNA to other ribosomal proteins[186], it is very likely that not all RNAs bound will contain an m6A deposited by METTL16.

RNAs bound to another protein which complexes with METTL16 could be mistaken as an RNA target in immunoprecipitations. It is also important in these studies to eliminate detection of m6A-modified RNAs which were modified by a methyltransferase other than METTL16. Since METTL16 does not have a definitive consensus sequence, the RNAs bound to METTL16 should first be isolated. These RNAs could be identified at this stage, *in vitro* synthesized, and then subjected to a methylation reaction with only the METTL16 methyltransferase available. Methylation reactions with METTL16 are still in their infancy since only 2 RNAs have been verified as targets for m6A methylation which currently restricts the knowledge of preferred conditions for all elements to optimally react. Using the current METTL16 methylation studies will provide a starting guide.

Conclusions

Overall, the results from this dissertation have provided progress and revealed discrepancies in the m6A and METTL16 field. We have shown widespread effects on human cells when METTL16 was mutated. These included cancer-promoting effects, with which METTL16 has been thoroughly associated, however we also saw effects on pathways not yet associated with METTL16 involvement. Pathways affected include cell cycle progression, metabolism, intracellular transport and microtubule organization, and RNA processing. More in-depth experiments verified binding of known RNA targets of METTL16 but also identified new RNA targets. In the infancy of METTL16 research, it was assumed that METTL16 was only localized to the nucleus and could only interact with a limited number of RNAs that fell into a strict consensus sequence and secondary structure group. Not only has this project revealed METTL16

is located throughout the cell, but it has also consistently shown interaction of METTL16 with a variety of RNAs, relieving the stringent requirements previously set.

References

1. Boo SH, Kim YK. The emerging role of RNA modifications in the regulation of mRNA stability. *Exp Mol Med*. 2020;52(3):400-408. doi:10.1038/s12276-020-0407-z
2. Peer E, Moshitch-Moshkovitz S, Rechavi G, Dominissini D. The Epitranscriptome in Translation Regulation. *Cold Spring Harb Perspect Biol* . 2019;11(8). doi:10.1101/cshperspect.a032623
3. Roundtree IA, Evans ME, Pan T, He C. Dynamic RNA Modifications in Gene Expression Regulation. *Cell*. 2017;169(7):1187-1200. doi:https://doi.org/10.1016/j.cell.2017.05.045
4. Zhao BS, Roundtree IA, He C. Post-transcriptional gene regulation by mRNA modifications. *Nat Rev Mol Cell Biol*. 2017;18(1):31-42. doi:10.1038/nrm.2016.132
5. Roundtree IA, He C. RNA epigenetics--chemical messages for posttranscriptional gene regulation. *Curr Opin Chem Biol*. 2016;30:46-51. doi:10.1016/j.cbpa.2015.10.024
6. Boccaletto P, Machnicka MA, Purta E, et al. MODOMICS: a database of RNA modification pathways. 2017 update. *Nucleic Acids Res*. 2018;46(D1):D303-D307. doi:10.1093/nar/gkx1030
7. Boccaletto P, Bagiński B. MODOMICS: An Operational Guide to the Use of the RNA Modification Pathways Database. *Methods Mol Biol*. 2021;2284:481-505. doi:10.1007/978-1-0716-1307-8_26
8. Cantara WA, Crain PF, Rozenski J, et al. The RNA Modification Database, RNAMDB: 2011 update. *Nucleic Acids Res*. 2011;39(Database issue):D195-201. doi:10.1093/nar/gkq1028
9. Wiener D, Schwartz S. How many tRNAs are out there? *Mol Cell*. 2021;81(8):1595-1597. doi:10.1016/j.molcel.2021.03.021
10. Ge J, Yu Y-T. RNA pseudouridylation: new insights into an old modification. *Trends Biochem Sci*. 2013;38(4):210-218. doi:10.1016/j.tibs.2013.01.002
11. Grosjean H. *Fine-Tuning of RNA Functions by Modification and Editing*. Vol 24. Volume 24. Springer; 2005. doi:https://doi.org/10.1007/b95147
12. Sloan KE, Warda AS, Sharma S, Entian K-D, Lafontaine DLJ, Bohnsack MT. Tuning the ribosome: The influence of rRNA modification on eukaryotic ribosome biogenesis and function. *RNA Biol*. 2017;14(9):1138-1152. doi:10.1080/15476286.2016.1259781
13. Chujo T, Tomizawa K. Human transfer RNA modopathies: diseases caused by aberrations in transfer RNA modifications. *FEBS J*. 2021;288(24):7096-7122. doi:10.1111/febs.15736
14. Suzuki T. The expanding world of tRNA modifications and their disease relevance. *Nat Rev Mol Cell Biol*. 2021;22(6):375-392. doi:10.1038/s41580-021-00342-0
15. Jonkhout N, Tran J, Smith MA, Schonrock N, Mattick JS, Novoa EM. The RNA modification landscape in human disease. *RNA* . 2017;23(12):1754-1769. doi:10.1261/rna.063503.117
16. Nachtergaele S, He C. The emerging biology of RNA post-transcriptional modifications. *RNA Biol*. 2017;14(2):156-163. doi:10.1080/15476286.2016.1267096
17. Jiang X, Liu B, Nie Z, et al. The role of m6A modification in the biological functions and

diseases. *Signal Transduct Target Ther*. 2021;6(1):74. doi:10.1038/s41392-020-00450-x

18. Shi H, Wei J, He C. Where, When, and How: Context-Dependent Functions of RNA Methylation Writers, Readers, and Erasers. *Mol Cell*. 2019;74(4):640-650. doi:10.1016/j.molcel.2019.04.025

19. Zaccara S, Ries RJ, Jaffrey SR. Reading, writing and erasing mRNA methylation. *Nat Rev Mol Cell Biol*. 2019;20(10):608-624. doi:10.1038/s41580-019-0168-5

20. He PC, He C. m6A RNA methylation: from mechanisms to therapeutic potential. *EMBO J*. 2021;40(3):e105977. doi:https://doi.org/10.15252/embj.2020105977

21. Desrosiers R, Friderici K, Rottman F. Identification of Methylated Nucleosides in Messenger RNA from Novikoff Hepatoma Cells. *Proc Natl Acad Sci*. 1974;71(10):3971-3975. doi:10.1073/pnas.71.10.3971

22. Yue Y, Liu J, He C. RNA N6-methyladenosine methylation in post-transcriptional gene expression regulation. *Genes Dev* . 2015;29(13):1343-1355. doi:10.1101/gad.262766.115

23. Du H, Zhao Y, He J, et al. YTHDF2 destabilizes m6A-containing RNA through direct recruitment of the CCR4–NOT deadenylase complex. *Nat Commun*. 2016;7(1):12626. doi:10.1038/ncomms12626

24. Fry NJ, Law BA, Ilkayeva OR, Holley CL, Mansfield KD. N6-methyladenosine is required for the hypoxic stabilization of specific mRNAs. *RNA* . 2017;23(9):1444-1455. doi:10.1261/rna.061044.117

25. Wang X, Lu Z, Gomez A, et al. N6-methyladenosine-dependent regulation of messenger RNA stability. *Nature*. 2014;505(7481):117-120. doi:10.1038/nature12730

26. Wang X, Zhao BS, Roundtree IA, et al. N6-methyladenosine Modulates Messenger RNA Translation Efficiency. *Cell*. 2015;161(6):1388-1399. doi:https://doi.org/10.1016/j.cell.2015.05.014

27. Li A, Chen Y-S, Ping X-L, et al. Cytoplasmic m6A reader YTHDF3 promotes mRNA translation. *Cell Res*. 2017;27(3):444-447. doi:10.1038/cr.2017.10

28. Geula S, Moshitch-Moshkovitz S, Dominissini D, et al. m6A mRNA methylation facilitates resolution of naïve pluripotency toward differentiation. *Science (80-).* 2015;347(6225):1002-1006. doi:10.1126/science.1261417

29. Wang Y, Li Y, Toth JI, Petroski MD, Zhang Z, Zhao JC. N6-methyladenosine modification destabilizes developmental regulators in embryonic stem cells. *Nat Cell Biol*. 2014;16(2):191-198. doi:10.1038/ncb2902

30. Zhao BS, He C. Fate by RNA methylation: m6A steers stem cell pluripotency. *Genome Biol*. 2015;16(1):43. doi:10.1186/s13059-015-0609-1

31. Fustin J-M, Doi M, Yamaguchi Y, et al. RNA-Methylation-Dependent RNA Processing Controls the Speed of the Circadian Clock. *Cell*. 2013;155(4):793-806. doi:10.1016/j.cell.2013.10.026

32. Shi H, Zhang X, Weng Y, et al. m6A facilitates hippocampus-dependent learning and memory through YTHDF1. *Nature*. 2018;563(7730):249-253. doi:10.1038/s41586-018-0666-1

33. Lan Q, Liu PY, Haase J, Bell JL, Hüttelmaier S, Liu T. The Critical Role of RNA m(6)A

Methylation in Cancer. *Cancer Res*. 2019;79(7):1285-1292. doi:10.1158/0008-5472.CAN-18-2965

34. Ke S, Pandya-Jones A, Saito Y, et al. m6A mRNA modifications are deposited in nascent pre-mRNA and are not required for splicing but do specify cytoplasmic turnover. *Genes Dev* . 2017;31(10):990-1006. doi:10.1101/gad.301036.117

35. Liu J, Yue Y, Han D, et al. A METTL3-METTL14 complex mediates mammalian nuclear RNA N6 adenosine methylation. *Nat Chem Biol*. 2014;10(2):93-95. doi:10.1038/nchembio.1432.A

36. Agarwala SD, Blitzblau HG, Hochwagen A, Fink GR. RNA Methylation by the MIS Complex Regulates a Cell Fate Decision in Yeast. *PLOS Genet*. 2012;8(6):e1002732. https://doi.org/10.1371/journal.pgen.1002732

37. Ping X-L, Sun B-F, Wang L, et al. Mammalian WTAP is a regulatory subunit of the RNA N6-methyladenosine methyltransferase. *Cell Res*. 2014;24(2):177-189. doi:10.1038/cr.2014.3

38. Lee M, Kim B, Kim VN. Emerging roles of RNA modification: m(6)A and U-tail. *Cell*. 2014;158(5):980-987. doi:10.1016/j.cell.2014.08.005

39. Patil DP, Chen C-K, Pickering BF, et al. m6A RNA methylation promotes XIST-mediated transcriptional repression. *Nature*. 2016;537(7620):369-373. doi:10.1038/nature19342

40. Schwartz S, Mumbach MR, Jovanovic M, et al. Perturbation of m6A writers reveals two distinct classes of mRNA methylation at internal and 5' sites. *Cell Rep*. 2014;8(1):284-296. doi:10.1016/j.celrep.2014.05.048

41. Li Y, Wang X, Li C, Hu S, Yu J, Song S. Transcriptome-wide N6-methyladenosine profiling of rice callus and leaf reveals the presence of tissue-specific competitors involved in selective mRNA modification. *RNA Biol*. 2014;11(9):1180-1188. doi:10.4161/rna.36281

42. Meyer KD, Saletore Y, Zumbo P, Elemento O, Mason CE, Jaffrey SR. Comprehensive analysis of mRNA methylation reveals enrichment in 3' UTRs and near stop codons. *Cell*. 2012;149(7):1635-1646. doi:10.1016/j.cell.2012.05.003

43. Luo G-Z, MacQueen A, Zheng G, et al. Unique features of the m6A methylome in Arabidopsis thaliana. *Nat Commun*. 2014;5:5630. doi:10.1038/ncomms6630

44. Chen T, Hao Y-J, Zhang Y, et al. m(6)A RNA methylation is regulated by microRNAs and promotes reprogramming to pluripotency. *Cell Stem Cell*. 2015;16(3):289-301. doi:10.1016/j.stem.2015.01.016

45. Wang P, Doxtader KA, Nam Y. Structural Basis for Cooperative Function of Mettl3 and Mettl14 Methyltransferases. *Mol Cell*. 2016;63(2):306-317. doi:https://doi.org/10.1016/j.molcel.2016.05.041

46. Huang H, Weng H, Zhou K, et al. Histone H3 trimethylation at lysine 36 guides m(6)A RNA modification co-transcriptionally. *Nature*. 2019;567(7748):414-419. doi:10.1038/s41586-019-1016-7

47. Śledź P, Jinek M. Structural insights into the molecular mechanism of the m(6)A writer complex. *Elife*. 2016;5. doi:10.7554/eLife.18434

48. Wang X, Feng J, Xue Y, et al. Structural basis of N(6)-adenosine methylation by the

METTL3-METTL14 complex. *Nature*. 2016;534(7608):575-578. doi:10.1038/nature18298

49. Bokar JA, Shambaugh ME, Polayes D, Matera AG, Rottman FM. Purification and cDNA cloning of the AdoMet-binding subunit of the human mRNA (N6-adenosine)-methyltransferase. Published online 1997:1233-1247.

50. Gokhale NS, McIntyre ABR, McFadden MJ, et al. N6-Methyladenosine in Flaviviridae Viral RNA Genomes Regulates Infection. *Cell Host Microbe*. 2016;20(5):654-665. doi:https://doi.org/10.1016/j.chom.2016.09.015

51. Harper JE, Miceli SM, Roberts RJ, Manley JL. Sequence specificity of the human mRNA N6-adenosine methylase in vitro. *Nucleic Acids Res*. 1990;18(19):5735-5741. doi:10.1093/nar/18.19.5735

52. Lin S, Choe J, Du P, Triboulet R, Gregory RI. The m(6)A Methyltransferase METTL3 Promotes Translation in Human Cancer Cells. *Mol Cell*. 2016;62(3):335-345. doi:10.1016/j.molcel.2016.03.021

53. Aoyama T, Yamashita S, Tomita K. Mechanistic insights into m6A modification of U6 snRNA by human METTL16. *Nucleic Acids Res*. Published online 2020:1-12. doi:10.1093/nar/gkaa227

54. Brown JA, Kinzig CG, Degregorio SJ, Steitz JA. Methyltransferase-like protein 16 binds the 3'-terminal triple helix of MALAT1 long noncoding RNA. *Proc Natl Acad Sci U S A*. 2016;113(49):14013-14018. doi:10.1073/pnas.1614759113

55. Nance DJ, Satterwhite ER, Bhaskar B, Misra S, Carraway KR, Mansfield KD. Characterization of METTL16 as a cytoplasmic RNA binding protein. *PLoS One*. 2020;15(1):1-18. doi:10.1371/journal.pone.0227647

56. Pendleton KE, Chen B, Liu K, et al. The U6 snRNA m6A Methyltransferase METTL16 Regulates SAM Synthetase Intron Retention. *Cell*. 2017;169(5):824-835.e14. doi:10.1016/j.cell.2017.05.003

57. Ruszkowska A. Mettl16, methyltransferase-like protein 16: Current insights into structure and function. *Int J Mol Sci*. 2021;22(4):1-21. doi:10.3390/ijms22042176

58. Warda AS, Kretschmer J, Hackert P, et al. Human METTL16 is a N 6 -methyladenosine (m 6 A) methyltransferase that targets pre-mRNAs and various non-coding RNAs. *EMBO Rep*. 2017;18(11):2004-2014. doi:10.15252/embr.201744940

59. Doxtader KA, Wang P, Scarborough AM, Seo D, Conrad NK, Nam Y. Structural Basis for Regulation of METTL16, an S-Adenosylmethionine Homeostasis Factor. *Mol Cell*. 2018;71(6):1001-1011.e4. doi:10.1016/j.molcel.2018.07.025

60. Mendel M, Chen KM, Homolka D, et al. Methylation of Structured RNA by the m6A Writer METTL16 Is Essential for Mouse Embryonic Development. *Mol Cell*. 2018;71(6):986-1000.e11. doi:10.1016/j.molcel.2018.08.004

61. Ruszkowska A, Ruszkowski M, Dauter Z, Brown JA. Structural insights into the RNA methyltransferase domain of METTL16. *Sci Rep*. 2018;8(1):1-13. doi:10.1038/s41598-018-23608-8

62. Baltz AG, Munschauer M, Schwanhäusser B, et al. The mRNA-bound proteome and its

global occupancy profile on protein-coding transcripts. *Mol Cell*. 2012;46(5):674-690. doi:10.1016/j.molcel.2012.05.021

63. Brannan KW, Jin W, Huelga SC, et al. SONAR Discovers RNA-Binding Proteins from Analysis of Large-Scale Protein-Protein Interactomes. *Mol Cell*. 2016;64(2):282-293. doi:10.1016/j.molcel.2016.09.003

64. Castello A, Fischer B, Eichelbaum K, et al. Insights into RNA biology from an atlas of mammalian mRNA-binding proteins. *Cell*. 2012;149(6):1393-1406. doi:10.1016/j.cell.2012.04.031

65. Kwon J, Jo Y-J, Namgoong S, Kim N-H. Functional roles of hnRNPA2/B1 regulated by METTL3 in mammalian embryonic development. *Sci Rep*. 2019;9(1):8640. doi:10.1038/s41598-019-44714-1

66. Conrad T, Albrecht A-S, de Melo Costa VR, Sauer S, Meierhofer D, Ørom UA. Serial interactome capture of the human cell nucleus. *Nat Commun*. 2016;7(1):11212. doi:10.1038/ncomms11212

67. Berulava T, Rahmann S, Rademacher K, Klein-Hitpass L, Horsthemke B. N6-Adenosine Methylation in MiRNAs. *PLoS One*. 2015;10(2):e0118438. https://doi.org/10.1371/journal.pone.0118438

68. Iwanami Y, Brown GM. Methylated bases of ribosomal ribonucleic acid from HeLa cells. *Arch Biochem Biophys*. 1968;126(1):8-15. doi:https://doi.org/10.1016/0003-9861(68)90553-5

69. Reddy R, Ro-Choi TS, Henning D, Shibata H, Choi YC, Busch H. Modified Nucleosides of Nuclear and Nucleolar Low Molecular Weight Ribonucleic Acid. *J Biol Chem*. 1972;247(22):7245-7250. doi:10.1016/S0021-9258(19)44620-6

70. Zhou KI, Parisien M, Dai Q, et al. N6-Methyladenosine Modification in a Long Noncoding RNA Hairpin Predisposes Its Conformation to Protein Binding. *J Mol Biol*. 2016;428(5, Part A):822-833. doi:https://doi.org/10.1016/j.jmb.2015.08.021

71. van Tran N, Ernst FGM, Hawley BR, et al. The human 18S rRNA m6A methyltransferase METTL5 is stabilized by TRMT112. *Nucleic Acids Res*. 2019;47(15):7719-7733. doi:10.1093/nar/gkz619

72. Ma H, Wang X, Cai J, et al. N6-Methyladenosine methyltransferase ZCCHC4 mediates ribosomal RNA methylation. *Nat Chem Biol*. 2019;15(1):88-94. doi:10.1038/s41589-018-0184-3

73. Pinto R, Vågbø CB, Jakobsson ME, et al. The human methyltransferase ZCCHC4 catalyses N6-methyladenosine modification of 28S ribosomal RNA. *Nucleic Acids Res*. 2020;48(2):830-846. doi:10.1093/nar/gkz1147

74. Ren W, Lu J, Huang M, et al. Structure and regulation of ZCCHC4 in m6A-methylation of 28S rRNA. *Nat Commun*. 2019;10(1):5042. doi:10.1038/s41467-019-12923-x

75. Dinman JD, Wickner RB. 5 S rRNA is involved in fidelity of translational reading frame. *Genetics*. 1995;141(1):95-105. doi:10.1093/genetics/141.1.95

76. Piekna-Przybylska D, Przybylski P, Baudin-Baillieu A, Rousset J-P, Fournier MJ. Ribosome Performance Is Enhanced by a Rich Cluster of Pseudouridines in the A-site

Finger Region of the Large Subunit * . *J Biol Chem*. 2008;283(38):26026-26036. doi:10.1074/jbc.M803049200

77. Qin D, Liu Q, Devaraj A, Fredrick K. Role of helix 44 of 16S rRNA in the fidelity of translation initiation. *RNA* . 2012;18(3):485-495. doi:10.1261/rna.031203.111

78. Liu S, Zhuo L, Wang J, et al. METTL3 plays multiple functions in biological processes. *Am J Cancer Res*. 2020;10(6):1631-1646. http://www.ncbi.nlm.nih.gov/pubmed/32642280%0Ahttp://www.pubmedcentral.nih.gov/articlerender.fcgi?artid=PMC7339281

79. Gouy M, Guindon S, Gascuel O. SeaView version 4: A multiplatform graphical user interface for sequence alignment and phylogenetic tree building. *Mol Biol Evol*. 2010;27(2):221-224. doi:10.1093/molbev/msp259

80. Sergiev P V, Serebryakova M V, Bogdanov AA, Dontsova OA. The ybiN Gene of Escherichia coli Encodes Adenine-N6 Methyltransferase Specific for Modification of A1618 of 23 S Ribosomal RNA, a Methylated Residue Located Close to the Ribosomal Exit Tunnel. *J Mol Biol*. 2008;375(1):291-300. doi:https://doi.org/10.1016/j.jmb.2007.10.051

81. Shima H, Matsumoto M, Ishigami Y, et al. S-Adenosylmethionine Synthesis Is Regulated by Selective N6-Adenosine Methylation and mRNA Degradation Involving METTL16 and YTHDC1. *Cell Rep*. 2017;21(12):3354-3363. doi:10.1016/j.celrep.2017.11.092

82. Lence T, Paolantoni C, Worpenberg L, Roignant JY. Mechanistic insights into m 6 A RNA enzymes. *Biochim Biophys Acta - Gene Regul Mech*. 2019;1862(3):222-229. doi:10.1016/j.bbagrm.2018.10.014

83. Trippe R, Sandrock B, Benecke BJ. A highly specific terminal uridylyl transferase modifies the 3'-end of U6 small nuclear RNA. *Nucleic Acids Res*. 1998;26(13):3119-3126. doi:10.1093/nar/26.13.3119

84. Paung YT, Seeliger MA. KA1 Domains: Unity in Mechanistic Diversity. *Structure*. 2018;26(8):1045-1047. doi:10.1016/j.str.2018.07.002

85. Marx A, Nugoor C, Panneerselvam S, Mandelkow E. Structure and function of polarity-inducing kinase family MARK/Par-1 within the branch of AMPK/Snf1-related kinases. *FASEB J*. 2010;24(6):1637-1648. doi:10.1096/fj.09-148064

86. Moravcevic K, Mendrola JM, Schmitz KR, et al. Kinase associated-1 domains drive MARK/PAR1 kinases to membrane targets by binding acidic phospholipids. *Cell*. 2010;143(6):966-977. doi:10.1016/j.cell.2010.11.028

87. Nguyen Ba AN, Pogoutse A, Provart N, Moses AM. NLStradamus: a simple Hidden Markov Model for nuclear localization signal prediction. *BMC Bioinformatics*. 2009;10:202. doi:10.1186/1471-2105-10-202

88. Dorsett M, Schedl T. A Role for Dynein in the Inhibition of Germ Cell Proliferative Fate. *Mol Cell Biol*. 2009;29(22):6128 LP - 6139. doi:10.1128/MCB.00815-09

89. Amodio N, Raimondi L, Juli G, et al. MALAT1: A druggable long non-coding RNA for targeted anti-cancer approaches. *J Hematol Oncol*. 2018;11(1):1-19. doi:10.1186/s13045-018-0606-4

90. Hutchinson JN, Ensminger AW, Clemson CM, Lynch CR, Lawrence JB, Chess A. A screen for nuclear transcripts identifies two linked noncoding RNAs associated with SC35 splicing domains. *BMC Genomics*. 2007;8:1-16. doi:10.1186/1471-2164-8-39

91. Arun G, Aggarwal D, Spector DL. MALAT1 long non-coding RNA: Functional implications. *Non-coding RNA*. 2020;6(2):1-17. doi:10.3390/NCRNA6020022

92. Jin D, Guo J, Wu Y, et al. m6A mRNA methylation initiated by METTL3 directly promotes YAP translation and increases YAP activity by regulating the MALAT1-miR-1914-3p-YAP axis to induce NSCLC drug resistance and metastasis. *J Hematol Oncol*. 2019;12(1):135. doi:10.1186/s13045-019-0830-6

93. Linder B, Grozhik A V, Olarerin-george AO, Meydan C, Mason CE, Jaffrey SR. Single-nucleotide resolution mapping of m6A and m6Am throughout the transcriptome. *Nat Methods*. 2015;12(8):767-772. doi:10.1038/nmeth.3453.Single-nucleotide

94. Brown JA, Valenstein ML, Yario TA, Tycowski KT, Steitz JA. Formation of triple-helical structures by the 3′-end sequences of MALAT1 and MENβ noncoding RNAs. *Proc Natl Acad Sci*. 2012;109(47):19202 LP - 19207. doi:10.1073/pnas.1217338109

95. Cantoni GL, Durell J. Activation of methionine for transmethylation II. The methionine-activating enzyme: studies on the mechanism of the reaction. *J Biol Chem*. 1957;(225):1033-1048.

96. Halim A-B, LeGros L, Geller A, Kotb M. Expression and Functional Interaction of the Catalytic and Regulatory Subunits of Human Methionine Adenosyltransferase in Mammalian Cells*. *J Biol Chem*. 1999;274(42):29720-29725. doi:https://doi.org/10.1074/jbc.274.42.29720

97. Lo TF, Tsai WC, Chen ST. MicroRNA-21-3p, a Berberine-Induced miRNA, Directly Down-Regulates Human Methionine Adenosyltransferases 2A and 2B and Inhibits Hepatoma Cell Growth. *PLoS One*. 2013;8(9). doi:10.1371/journal.pone.0075628

98. Simile MM, Peitta G, Tomasi ML, et al. MicroRNA-203 impacts on the growth, aggressiveness and prognosis of hepatocellular carcinoma by targeting MAT2A and MAT2B genes. *Oncotarget*. 2019;10(29):2835-2854. doi:10.18632/oncotarget.26838

99. Scarborough AM, Flaherty JN, Hunter O V., et al. SAM homeostasis is regulated by CFIm-mediated splicing of MAT2A. *Elife*. 2021;10:1-38. doi:10.7554/eLife.64930

100. Parker BJ, Moltke I, Roth A, et al. New families of human regulatory RNA structures identified by comparative analysis of vertebrate genomes. *Genome Res*. 2011;21(11):1929-1943. doi:10.1101/gr.112516.110

101. Martínez-Chantar ML, Latasa MU, Varela-Rey M, et al. L-methionine availability regulates expression of the methionine adenosyltransferase 2A gene in human hepatocarcinoma cells. Role of S-adenosylmethionine. *J Biol Chem*. 2003;278(22):19885-19890. doi:10.1074/jbc.M211554200

102. Koh CWQ, Goh YT, Goh WSS. Atlas of quantitative single-base-resolution N 6-methyl-adenine methylomes. *Nat Commun*. 2019;10(1). doi:10.1038/s41467-019-13561-z

103. Hou M, Guo X, Chen Y, Cong L, Pan C. A Prognostic Molecular Signature of N^6-Methyladenosine Methylation Regulators for Soft-Tissue Sarcoma from The Cancer Genome Atlas Database. *Med Sci Monit*. 2020;26:e928400. doi:10.12659/MSM.928400

104. Li K, Luo H, Luo H, Zhu X. Clinical and prognostic pan-cancer analysis of m6A RNA methylation regulators in four types of endocrine system tumors. *Aging (Albany NY)*. 2020;12(23):23931-23944. doi:10.18632/aging.104064

105. Liu X, Liu L, Dong Z, et al. Expression patterns and prognostic value of m(6)A-related genes in colorectal cancer. *Am J Transl Res*. 2019;11(7):3972-3991.

106. Wang P, Wang X, Zheng L, Zhuang C. Gene Signatures and Prognostic Values of m6A Regulators in Hepatocellular Carcinoma. *Front Genet*. 2020;11(October):1-11. doi:10.3389/fgene.2020.540186

107. Wang S, Fan X, Zhu J, et al. The differentiation of colorectal cancer is closely relevant to m6A modification. *Biochem Biophys Res Commun*. 2021;546:65-73. doi:https://doi.org/10.1016/j.bbrc.2021.02.001

108. Yeon SY, Jo YS, Choi EJ, Kim MS, Yoo NJ, Lee SH. Frameshift Mutations in Repeat Sequences of ANK3, HACD4, TCP10L, TP53BP1, MFN1, LCMT2, RNMT, TRMT6, METTL8 and METTL16 Genes in Colon Cancers. *Pathol Oncol Res*. 2018;24(3):617-622. doi:10.1007/s12253-017-0287-2

109. Zhang B, Gu Y, Jiang G. Expression and Prognostic Characteristics of m(6) A RNA Methylation Regulators in Breast Cancer. *Front Genet*. 2020;11:604597. doi:10.3389/fgene.2020.604597

110. Kalev P, Hyer ML, Gross S, et al. MAT2A Inhibition Blocks the Growth of MTAP-Deleted Cancer Cells by Reducing PRMT5-Dependent mRNA Splicing and Inducing DNA Damage. *Cancer Cell*. 2021;39(2):209-224.e11. doi:10.1016/j.ccell.2020.12.010

111. Jabs S, Biton A, Bécavin C, et al. Impact of the gut microbiota on the m6A epitranscriptome of mouse cecum and liver. *Nat Commun*. 2020;11(1):1-16. doi:10.1038/s41467-020-15126-x

112. Epstein P, Reddy R, Henning D, Busch H. The nucleotide sequence of nuclear U6 (4.7 S) RNA. *J Biol Chem*. 1980;255(18):8901-8906. doi:10.1016/s0021-9258(18)43587-9

113. Roost C, Lynch SR, Batista PJ, Qu K, Chang HY, Kool ET. Structure and thermodynamics of N6-methyladenosine in RNA: A spring-loaded base modification. *J Am Chem Soc*. 2015;137(5):2107-2115. doi:10.1021/ja513080v

114. Svobodová Kovaříková A, Stixová L, Kovařík A, et al. N6-Adenosine Methylation in RNA and a Reduced m3G/TMG Level in Non-Coding RNAs Appear at Microirradiation-Induced DNA Lesions. *Cells*. 2020;9(2):360. doi:10.3390/cells9020360

115. Xiang Y, Laurent B, Hsu C, et al. m6A RNA methylation regulates the UV-induced DNA damage response. *Nature*. 2017;543(7646):573-576. doi:10.1038/nature21671.m

116. Mikutis S, Gu M, Sendinc E, et al. MeCLICK-Seq, a Substrate-Hijacking and RNA Degradation Strategy for the Study of RNA Methylation. *ACS Cent Sci*. Published online 2020. doi:10.1021/acscentsci.0c01094

117. Ascano M, Hafner M, Cekan P, Gerstberger S, Tuschl T. Identification of RNA-protein interaction networks using PAR-CLIP. *Wiley Interdiscip Rev RNA*. 2012;3(2):159-177. doi:10.1002/wrna.1103

118. Hafner M, Katsantoni M, Köster T, et al. CLIP and complementary methods. *Nat Rev Methods Prim*. 2021;1(1):20. doi:10.1038/s43586-021-00018-1

119. Mukherjee N, Corcoran DL, Nusbaum JD, et al. Integrative regulatory mapping indicates that the RNA-binding protein HuR couples pre-mRNA processing and mRNA stability. *Mol Cell*. 2011;43(3):327-339. doi:10.1016/j.molcel.2011.06.007

120. Wheeler EC, Van Nostrand EL, Yeo GW. Advances and challenges in the detection of transcriptome-wide protein–RNA interactions. *WIREs RNA*. 2018;9(1):e1436. doi:https://doi.org/10.1002/wrna.1436

121. Song Y, Xu Q, Wei Z, et al. Predict Epitranscriptome Targets and Regulatory Functions of N6-Methyladenosine (m6A) Writers and Erasers. *Evol Bioinforma*. 2019;15. doi:10.1177/1176934319871290

122. Dorsett M, Westlund B, Schedl T. METT-10, A Putative Methyltransferase, Inhibits Germ Cell Proliferative Fate in Caenorhabditis elegans. *Genetics*. 2009;183(1):233-247. doi:10.1534/genetics.109.105270

123. Li S, Armstrong CM, Bertin N, et al. A Map of the Interactome Network of the Metazoan C. elegans. *Science (80-)*. 2004;303(5657):540-543. doi:10.1126/science.1091403

124. Mendel M, Delaney K, Pandey RR, et al. Splice site m(6)A methylation prevents binding of U2AF35 to inhibit RNA splicing. *Cell*. 2021;184(12):3125-3142.e25. doi:10.1016/j.cell.2021.03.062

125. Barbieri I, Tzelepis K, Pandolfini L, et al. Promoter-bound METTL3 maintains myeloid leukaemia by m6A-dependent translation control. *Nature*. 2017;552(7683):126-131. doi:10.1038/nature24678

126. Guzzardo PM, Rashkova C, dos Santos RL, Tehrani R, Collin P, Bürckstümmer T. A small cassette enables conditional gene inactivation by CRISPR/Cas9. *Sci Rep*. 2017;7(1):16770. doi:10.1038/s41598-017-16931-z

127. Wang T, Birsoy K, Hughes NW, et al. Identification and characterization of essential genes in the human genome. *Science (80-)*. 2015;350(6264):1096-1101. doi:10.1126/science.aac7041

128. Tomasi ML, Tomasi I, Ramani K, et al. S-adenosyl methionine regulates ubiquitin-conjugating enzyme 9 protein expression and sumoylation in murine liver and human cancers. *Hepatology*. 2012;56(3):982-993. doi:https://doi.org/10.1002/hep.25701

129. Vázquez–Chantada M, Fernández–Ramos D, Embade N, et al. HuR/Methyl-HuR and AUF1 Regulate the MAT Expressed During Liver Proliferation, Differentiation, and Carcinogenesis. *Gastroenterology*. 2010;138(5):1943-1953.e3. doi:https://doi.org/10.1053/j.gastro.2010.01.032

130. Brow DA, Guthrie C. Spliceosomal RNA U6 is remarkably conserved from yeast to mammals. *Nature*. 1988;334(6179):213-218. doi:10.1038/334213a0

131. Watts BR, Wittmann S, Wery M, et al. Histone deacetylation promotes transcriptional silencing at facultative heterochromatin. *Nucleic Acids Res*. 2018;46(11):5426-5440. doi:10.1093/nar/gky232

132. Ishigami Y, Ohira T, Isokawa Y, Suzuki Y, Suzuki T. A single m6A modification in U6

snRNA diversifies exon sequence at the 5' splice site. *Nat Commun*. 2021;12(1):3244. doi:10.1038/s41467-021-23457-6

133. Liu N, Parisien M, Dai Q, Zheng G, He C, Pan T. Probing N6-methyladenosine RNA modification status at single nucleotide resolution in mRNA and long noncoding RNA. *Rna*. 2013;19(12):1848-1856. doi:10.1261/rna.041178.113

134. Oerum S, Catala M, Atdjian C, et al. Bisubstrate analogues as structural tools to investigate m 6 A methyltransferase active sites. *RNA Biol*. 2019;16(6):798-808. doi:10.1080/15476286.2019.1589360

135. Ovcharenko A, Weissenboeck FP, Rentmeister A. Tag-Free Internal RNA Labeling and Photocaging Based on mRNA Methyltransferases. *Angew Chemie Int Ed*. 2021;60(8):4098-4103. doi:https://doi.org/10.1002/anie.202013936

136. Xiang S, Gao M, Cao J, et al. Precise identification of an RNA methyltransferase's substrate modification site. *Chem Commun*. 2021;57(20):2499-2502. doi:10.1039/D0CC08260K

137. Liu N, Dai Q, Zheng G, He C, Parisien M, Pan T. N6 -methyladenosine-dependent RNA structural switches regulate RNA-protein interactions. *Nature*. 2015;518(7540):560-564. doi:10.1038/nature14234

138. Wang X, Lu Z, Gomez A, et al. N 6-methyladenosine-dependent regulation of messenger RNA stability. *Nature*. 2014;505(7481):117-120. doi:10.1038/nature12730

139. Shi H, Wang X, Lu Z, et al. YTHDF3 facilitates translation and decay of N6-methyladenosine-modified RNA. *Cell Res*. 2017;27(3):315-328. doi:10.1038/cr.2017.15

140. Alarcón CR, Goodarzi H, Lee H, Liu X, Tavazoie S, Tavazoie SF. HNRNPA2B1 Is a Mediator of m^6A-Dependent Nuclear RNA Processing Events. *Cell*. 2015;162(6):1299-1308. doi:10.1016/j.cell.2015.08.011

141. Liu K, Ding Y, Ye W, et al. Structural and Functional Characterization of the Proteins Responsible for N(6)-Methyladenosine Modification and Recognition. *Curr Protein Pept Sci*. 2016;17(4):306-318.

142. Zhang X, Jia G. RNA epigenetic modification: N6-methyladenosine. *Yi chuan = Hered*. 2016;38(4):275-288. doi:10.16288/j.yczz.16-049

143. Cui Q, Shi H, Ye P, et al. m(6)A RNA Methylation Regulates the Self-Renewal and Tumorigenesis of Glioblastoma Stem Cells. *Cell Rep*. 2017;18(11):2622-2634. doi:10.1016/j.celrep.2017.02.059

144. Fry NJ, Law BA, Ilkayeva OR, Carraway KR, Holley CL, Mansfield KD. N(6)-methyladenosine contributes to cellular phenotype in a genetically-defined model of breast cancer progression. *Oncotarget*. 2018;9(58):31231-31243. doi:10.18632/oncotarget.25782

145. Jaffrey SR, Kharas MG. Emerging links between m(6)A and misregulated mRNA methylation in cancer. *Genome Med*. 2017;9(1):2. doi:10.1186/s13073-016-0395-8

146. Zhang C, Samanta D, Lu H, et al. Hypoxia induces the breast cancer stem cell phenotype by HIF-dependent and ALKBH5-mediated m^6A-demethylation of NANOG mRNA. *Proc Natl Acad Sci U S A*. 2016;113(14):E2047-56. doi:10.1073/pnas.1602883113

147. Zhang C, Zhi WI, Lu H, et al. Hypoxia-inducible factors regulate pluripotency factor expression by ZNF217- and ALKBH5-mediated modulation of RNA methylation in breast

cancer cells. *Oncotarget*. 2016;7(40):64527-64542. doi:10.18632/oncotarget.11743

148. Aguilo F, Zhang F, Sancho A, et al. Coordination of m(6)A mRNA Methylation and Gene Transcription by ZFP217 Regulates Pluripotency and Reprogramming. *Cell Stem Cell*. 2015;17(6):689-704. doi:10.1016/j.stem.2015.09.005

149. Wu Y, Zhang S, Yuan Q. N(6)-Methyladenosine Methyltransferases and Demethylases: New Regulators of Stem Cell Pluripotency and Differentiation. *Stem Cells Dev*. 2016;25(14):1050-1059. doi:10.1089/scd.2016.0062

150. Bertomeu T, Coulombe-Huntington J, Chatr-Aryamontri A, et al. A High-Resolution Genome-Wide CRISPR/Cas9 Viability Screen Reveals Structural Features and Contextual Diversity of the Human Cell-Essential Proteome. *Mol Cell Biol*. 2018;38(1). doi:10.1128/MCB.00302-17

151. Blomen VA, Májek P, Jae LT, et al. Gene essentiality and synthetic lethality in haploid human cells. *Science*. 2015;350(6264):1092-1096. doi:10.1126/science.aac7557

152. Hart T, Chandrashekhar M, Aregger M, et al. High-Resolution CRISPR Screens Reveal Fitness Genes and Genotype-Specific Cancer Liabilities. *Cell*. 2015;163(6):1515-1526. doi:10.1016/j.cell.2015.11.015

153. Silva JM, Marran K, Parker JS, et al. Profiling essential genes in human mammary cells by multiplex RNAi screening. *Science*. 2008;319(5863):617-620. doi:10.1126/science.1149185

154. Pauley RJ, Soule HD, Tait L, et al. The MCF10 family of spontaneously immortalized human breast epithelial cell lines: models of neoplastic progression. *Eur J cancer Prev Off J Eur Cancer Prev Organ*. 1993;2 Suppl 3:67-76.

155. Dawson PJ, Wolman SR, Tait L, Heppner GH, Miller FR. MCF10AT: a model for the evolution of cancer from proliferative breast disease. *Am J Pathol*. 1996;148(1):313-319.

156. Fury MG, Zieve GW. U6 snRNA maturation and stability. *Exp Cell Res*. 1996;228(1):160-163. doi:10.1006/excr.1996.0311

157. Zieve GW, Sauterer RA, Feeney RJ. Newly synthesized small nuclear RNAs appear transiently in the cytoplasm. *J Mol Biol*. 1988;199(2):259-267. doi:10.1016/0022-2836(88)90312-9

158. Madhani HD, Bordonné R, Guthrie C. Multiple roles for U6 snRNA in the splicing pathway. *Genes Dev*. 1990;4(12B):2264-2277. doi:10.1101/gad.4.12b.2264

159. Schwartz S, Agarwala SD, Mumbach MR, et al. High-resolution mapping reveals a conserved, widespread, dynamic mRNA methylation program in yeast meiosis. *Cell*. 2013;155(6):1409-1421. doi:10.1016/j.cell.2013.10.047

160. Ma Z, Gao X, Shuai Y, Xing X, Ji J. The m6A epitranscriptome opens a new charter in immune system logic. *Epigenetics*. 2021;16(8):819-837. doi:10.1080/15592294.2020.1827722

161. Deng X, Chen K, Luo G-Z, et al. Widespread occurrence of N6-methyladenosine in bacterial mRNA. *Nucleic Acids Res*. 2015;43(13):6557-6567. doi:10.1093/nar/gkv596

162. Wu Z, Shi Y, Lu M, et al. METTL3 counteracts premature aging via m6A-dependent stabilization of MIS12 mRNA. *Nucleic Acids Res*. 2020;48(19):11083-11096.

doi:10.1093/nar/gkaa816

163. Yang Y, Fan X, Mao M, et al. Extensive translation of circular RNAs driven by N 6 -methyladenosine. *Cell Res*. 2017;27(5):626-641. doi:10.1038/cr.2017.31

164. Lin X, Chai G, Wu Y, et al. RNA m 6 A methylation regulates the epithelial mesenchymal transition of cancer cells and translation of Snail. *Nat Commun*. 2019;10(1). doi:10.1038/s41467-019-09865-9

165. Zhao X, Yang Y, Sun B-F, et al. FTO-dependent demethylation of N6-methyladenosine regulates mRNA splicing and is required for adipogenesis. *Cell Res*. 2014;24(12):1403-1419. doi:10.1038/cr.2014.151

166. Kasowitz SD, Ma J, Anderson SJ, et al. Nuclear m6A reader YTHDC1 regulates alternative polyadenylation and splicing during mouse oocyte development. *PLoS Genet*. 2018;14(5):e1007412. doi:10.1371/journal.pgen.1007412

167. Huang H, Weng H, Sun W, et al. Recognition of RNA N(6)-methyladenosine by IGF2BP proteins enhances mRNA stability and translation. *Nat Cell Biol*. 2018;20(3):285-295. doi:10.1038/s41556-018-0045-z

168. Han J, Wang J-Z, Yang X, et al. METTL3 promote tumor proliferation of bladder cancer by accelerating pri-miR221/222 maturation in m6A-dependent manner. *Mol Cancer*. 2019;18(1):110. doi:10.1186/s12943-019-1036-9

169. Alarcon CR, Lee H, Goodarzi H, Halberg N, Tavazoie SF. N6-methyl-adenosine (m6A) marks primary microRNAs for processing. *Nature*. 2015;176(3):482-485. doi:doi:10.1038/nature14281

170. Halim AB, LeGros L, Geller A, Kotb M. Expression and functional interaction of the catalytic and regulatory subunits of human methionine adenosyltransferase in mammalian cells. *J Biol Chem*. 1999;274(42):29720-29725. doi:10.1074/jbc.274.42.29720

171. Schapira M. Structural Chemistry of Human RNA Methyltransferases. *ACS Chem Biol*. 2016;11(3):575-582. doi:10.1021/acschembio.5b00781

172. Song H, Feng X, Zhang H, et al. METTL3 and ALKBH5 oppositely regulate m(6)A modification of TFEB mRNA, which dictates the fate of hypoxia/reoxygenation-treated cardiomyocytes. *Autophagy*. 2019;15(8):1419-1437. doi:10.1080/15548627.2019.1586246

173. Chen H, Gao S, Liu W, et al. RNA N(6)-Methyladenosine Methyltransferase METTL3 Facilitates Colorectal Cancer by Activating the m(6)A-GLUT1-mTORC1 Axis and Is a Therapeutic Target. *Gastroenterology*. 2021;160(4):1284-1300.e16. doi:10.1053/j.gastro.2020.11.013

174. Wang Q, Chen C, Ding Q, et al. METTL3-mediated m(6)A modification of HDGF mRNA promotes gastric cancer progression and has prognostic significance. *Gut*. 2020;69(7):1193-1205. doi:10.1136/gutjnl-2019-319639

175. Dominissini D, Moshitch-Moshkovitz S, Schwartz S, et al. Topology of the human and mouse m6A RNA methylomes revealed by m6A-seq. *Nature*. 2012;485(7397):201-206. doi:10.1038/nature11112

176. Pan T. N6-methyl-adenosine modification in messenger and long non-coding RNA. *Trends Biochem Sci*. 2013;38(4):204-209. doi:10.1016/j.tibs.2012.12.006

177. Ke S, Alemu EA, Mertens C, et al. A majority of m6A residues are in the last exons, allowing the potential for 3' UTR regulation. *Genes Dev*. 2015;29(19):2037-2053. doi:10.1101/gad.269415.115

178. Lee H, Bao S, Qian Y, et al. Stage-specific requirement for Mettl3-dependent m(6)A mRNA methylation during haematopoietic stem cell differentiation. *Nat Cell Biol*. 2019;21(6):700-709. doi:10.1038/s41556-019-0318-1

179. Wang H, Hu X, Huang M, et al. Mettl3-mediated mRNA m(6)A methylation promotes dendritic cell activation. *Nat Commun*. 2019;10(1):1898. doi:10.1038/s41467-019-09903-6

180. Dorn LE, Lasman L, Chen J, et al. The N(6)-Methyladenosine mRNA Methylase METTL3 Controls Cardiac Homeostasis and Hypertrophy. *Circulation*. 2019;139(4):533-545. doi:10.1161/CIRCULATIONAHA.118.036146

181. Kobayashi M, Ohsugi M, Sasako T, et al. The RNA Methyltransferase Complex of WTAP, METTL3, and METTL14 Regulates Mitotic Clonal Expansion in Adipogenesis. *Mol Cell Biol*. 2018;38(16). doi:10.1128/MCB.00116-18

182. Xie W, Ma LL, Xu YQ, Wang BH, Li SM. METTL3 inhibits hepatic insulin sensitivity via N6-methyladenosine modification of Fasn mRNA and promoting fatty acid metabolism. *Biochem Biophys Res Commun*. 2019;518(1):120-126. doi:10.1016/j.bbrc.2019.08.018

183. Wanna-Udom S, Terashima M, Lyu H, et al. The m6A methyltransferase METTL3 contributes to Transforming Growth Factor-beta-induced epithelial-mesenchymal transition of lung cancer cells through the regulation of JUNB. *Biochem Biophys Res Commun*. 2020;524(1):150-155. doi:10.1016/j.bbrc.2020.01.042

184. Liu Q, Li M, Jiang L, Jiang R, Fu B. METTL3 promotes experimental osteoarthritis development by regulating inflammatory response and apoptosis in chondrocyte. *Biochem Biophys Res Commun*. 2019;516(1):22-27. doi:10.1016/j.bbrc.2019.05.168

185. Wang X-K, Zhang Y-W, Wang C-M, et al. METTL16 promotes cell proliferation by up-regulating cyclin D1 expression in gastric cancer. *J Cell Mol Med*. 2021;25(14):6602-6617. doi:10.1111/jcmm.16664

186. Su R, Dong L, Li Y, et al. METTL16 exerts an m(6)A-independent function to facilitate translation and tumorigenesis. *Nat Cell Biol*. 2022;24(2):205-216. doi:10.1038/s41556-021-00835-2

187. Zhao H, Xu Y, Xie Y, et al. m6A Regulators Is Differently Expressed and Correlated With Immune Response of Esophageal Cancer. *Front cell Dev Biol*. 2021;9:650023. doi:10.3389/fcell.2021.650023

188. Zhang Y, Yang Y. Effects of m6A RNA methylation regulators on endometrial cancer. *J Clin Lab Anal*. 2021;35(9):e23942. doi:10.1002/jcla.23942

189. Roundtree IA, Luo G-Z, Zhang Z, et al. YTHDC1 mediates nuclear export of N6-methyladenosine methylated mRNAs. *Elife*. 2017;6:e31311.

190. Xiao W, Adhikari S, Dahal U, et al. Nuclear m6A reader YTHDC1 regulates mRNA splicing. *Mol Cell*. 2016;61(4):507-519.

191. Hsu PJ, Zhu Y, Ma H, et al. Ythdc2 is an N6-methyladenosine binding protein that regulates mammalian spermatogenesis. *Cell Res*. 2017;27(9):1115-1127.

192. Wu B, Su S, Patil DP, et al. Molecular basis for the specific and multivariant recognitions of RNA substrates by human hnRNP A2/B1. *Nat Commun*. 2018;9(1):1-12.

193. Liu N, Zhou KI, Parisien M, Dai Q, Diatchenko L, Pan T. N6-methyladenosine alters RNA structure to regulate binding of a low-complexity protein. *Nucleic Acids Res*. 2017;45(10):6051-6063.

194. Zheng G, Dahl JA, Niu Y, et al. ALKBH5 is a mammalian RNA demethylase that impacts RNA metabolism and mouse fertility. *Mol Cell*. 2013;49(1):18-29.

195. Fu Y, Jia G, Pang X, et al. FTO-mediated formation of N6-hydroxymethyladenosine and N6-formyladenosine in mammalian RNA. *Nat Commun*. 2013;4(1):1-8.

196. Jia G, Fu YE, Zhao XU, et al. N6-methyladenosine in nuclear RNA is a major substrate of the obesity-associated FTO. *Nat Chem Biol*. 2011;7(12):885-887.

197. Dai Y-Z, Liu Y, Li J, et al. METTL16 promotes hepatocellular carcinoma progression through downregulating RAB11B-AS1 in an m(6)A-dependent manner. *Cell Mol Biol Lett*. 2022;27(1):41. doi:10.1186/s11658-022-00342-8

198. Cong P, Wu T, Huang X, et al. Identification of the Role and Clinical Prognostic Value of Target Genes of m6A RNA Methylation Regulators in Glioma. *Front cell Dev Biol*. 2021;9:709022. doi:10.3389/fcell.2021.709022

199. Zhang C, Ding Z, Luo H. The Prognostic Role of m6A-Related Genes in Paediatric Neuroblastoma Patients. *Comput Math Methods Med*. 2022;2022:8354932. doi:10.1155/2022/8354932

200. Zheng B, Wang J, Zhao G, et al. A new m6A methylation-related gene signature for prognostic value in patient with urothelial carcinoma of the bladder. *Biosci Rep*. 2021;41(4). doi:10.1042/BSR20204456

201. Zou Z, Zhou S, Liang G, et al. The pan-cancer analysis of the two types of uterine cancer uncovered clinical and prognostic associations with m6A RNA methylation regulators. *Mol Omi*. 2021;17(3):438-453. doi:10.1039/d0mo00113a

202. Liu J, Zhou Z, Ma L, et al. Effects of RNA methylation N6-methyladenosine regulators on malignant progression and prognosis of melanoma. *Cancer Cell Int*. 2021;21(1):453. doi:10.1186/s12935-021-02163-9

203. Zhao Z, Wan J, Guo M, et al. Expression and prognostic significance of m6A-related genes in TP53-mutant non-small-cell lung cancer. *J Clin Lab Anal*. 2022;36(1):e24118. doi:10.1002/jcla.24118

204. Liu X, Liu L, Dong Z, et al. Expression patterns and prognostic value of m(6)A-related genes in colorectal cancer. *Am J Transl Res*. 2019;11(7):3972-3991.

205. Dingerdissen HM, Bastian F, Vijay-Shanker K, et al. OncoMX: A Knowledgebase for Exploring Cancer Biomarkers in the Context of Related Cancer and Healthy Data. *JCO Clin Cancer Informatics*. 2020;(4):210-220. doi:10.1200/CCI.19.00117

206. Fabregat A, Sidiropoulos K, Viteri G, et al. Reactome pathway analysis: a high-performance in-memory approach. *BMC Bioinformatics*. 2017;18(1):142. doi:10.1186/s12859-017-1559-2

207. McLaughlin KL, Nelson MAM, Coalson HS, et al. Bioenergetic Phenotyping of DEN-

Induced Hepatocellular Carcinoma Reveals a Link Between Adenylate Kinase Isoform Expression and Reduced Complex I-Supported Respiration . *Front Oncol* . 2022;12. https://www.frontiersin.org/articles/10.3389/fonc.2022.919880

208. Aguilan JT, Kulej K, Sidoli S. Guide for protein fold change and p-value calculation for non-experts in proteomics. *Mol Omi*. 2020;16(6):573-582. doi:10.1039/D0MO00087F

209. Chen XY, Zhang J, Zhu JS. The role of m6A RNA methylation in human cancer. *Mol Cancer*. 2019;18(1):1-9. doi:10.1186/s12943-019-1033-z

210. Greenberg H, Penman S. Methylation and processing of ribosomal RNA in HeLa cells. *J Mol Biol*. 1966;21(3):527-535. doi:https://doi.org/10.1016/0022-2836(66)90025-8

211. Li K, Luo H, Luo H, Zhu X. Clinical and prognostic pan-cancer analysis of m6A RNA methylation regulators in four types of endocrine system tumors. *Aging (Albany NY)*. 2020;12(23):23931-23944. doi:10.18632/aging.104064

212. Zheng J, Guo J, Wang Y, Zheng Y, Zhang K, Tong J. Bioinformatic Analyses of the Ferroptosis-Related lncRNAs Signature for Ovarian Cancer. *Front Mol Biosci*. 2021;8:735871. doi:10.3389/fmolb.2021.735871

213. Zeng X, Zhao F, Cui G, et al. METTL16 antagonizes MRE11-mediated DNA end resection and confers synthetic lethality to PARP inhibition in pancreatic ductal adenocarcinoma. *Nat cancer*. 2022;3(9):1088-1104. doi:10.1038/s43018-022-00429-3

214. Lu L, Zheng D, Qu J, et al. METTL16 predicts a favorable outcome and primes antitumor immunity in pancreatic ductal adenocarcinoma. *Front cell Dev Biol*. 2022;10:759020. doi:10.3389/fcell.2022.759020

215. Aridor M, Hannan LA. Traffic Jam: A Compendium of Human Diseases that Affect Intracellular Transport Processes. *Traffic*. 2000;1(11):836-851. doi:https://doi.org/10.1034/j.1600-0854.2000.011104.x

216. Mato JM, Corrales FJ, Lu SC, Avila MA. S-Adenosylmethionine: a control switch that regulates liver function. *FASEB J*. 2002;16(1):15-26. doi:10.1096/fj.01-0401rev